PNL-5460 Vol. 1
UC-11

5 D

MELSAR: A Mesoscale Air Quality Model for Complex Terrain

VOLUME I—Overview, Technical Description and User's Guide

K. J. Allwine
C. D. Whiteman

April 1985

Prepared for
the U.S. Environmental Protection Agency
under a Related Services Agreement
with the U.S. Department of Energy
Contract DE-AC06-76RLO 1830

Pacific Northwest Laboratory
Operated for the U.S. Department of Energy
by Battelle Memorial Institute

Battelle

PNL-5460 Vol.

DISCLAIMER

PACIFIC NORTHWEST LABORATORY
operated by
BATTELLE
for the
UNITED STATES DEPARTMENT OF ENERGY
under Contract DE-AC06-76RLO 7830

PNL-5460 Vol. 1
UC-11

MELSAR: A MESOSCALE AIR QUALITY MODEL FOR COMPLEX TERRAIN

Volume 1 - Overview, Technical Description and User's Guide

K. J. Allwine
C. D. Whiteman

April 1985

Prepared for
the U.S. Environmental Protection Agency
under a Related Services Agreement
with the U.S. Department of Energy
Contract DE-AC06-76RLO 1830
Interagency Agreement AD-89-F-2-097-0

Project Officer: Alan H. Huber
Meteorology and Assessment Division
Atmospheric Sciences Research Laboratory
Research Triangle Park, NC 27711

Pacific Northwest Laboratory
Richland, Washington 99352

DISCLAIMER

The research described in this report has been funded wholly or in part by the United States Environmental Protection Agency through Interagency Agreement AD-89-F-2-097-0 to the Pacific Northwest Laboratory, This document has been reviewed in accordance with U.S. Environmental Protection Agency policy and approved for publication. Mention of trade names or commercial products does not constitute endorsement or recommendation for use.

PREFACE

This final report is submitted as part of the Green River Ambient Model Assessment (GRAMA) program conducted at the U.S. Department of Energy's Pacific Northwest Laboratory for the U.S. Environmental Protection Agency. The GRAMA program has, as its ultimate goal, the development of validated air quality models that can be applied to the complex terrain of the Green River Formation of western Colorado, eastern Utah, and southern Wyoming. The Green River Formation is a geologic formation containing large reserves of oil shale, coal, and other natural resources. Development of these resources may lead to a degradation of the air quality of the region. Air quality models are needed immediately for planning and regulatory purposes to assess the magnitude of these regional impacts. This report documents one of the models being developed for this purpose within GRAMA--specifically a model to predict short averaging time ($\leq$24 hr) pollutant concentrations resulting from the mesoscale transport of pollutant releases from multiple sources. MELSAR has not undergone any rigorous operational testing, sensitivity analyses, or validation studies. Testing and evaluation of the model are needed to gain a measure of confidence in the model's performance.

This report consists of two volumes. Volume 1 contains the model overview, technical description, and user's guide, and Volume 2 contains the Appendices which include listings of the FORTRAN code.

ABSTRACT

MELSAR, a mesoscale air quality model, was developed for predicting air pollutant concentrations resulting from releases from multiple sources. The model is a Lagrangian puff model for application in complex terrain, principally at long source-to-receptor transport distances (tens to hundreds of kilometers) and short pollutant averaging times (1 to 24 hr). Terrain influences are treated explicitly by using a three-dimensional mass-consistent flow model, accounting for the influences of terrain roughness on diffusion, using terrain-following plume trajectories with optional corrections for the plume ascending hills, and using a parameterized treatment of pollutant sources located in valleys. The model handles releases from both point and area sources and makes the conservative assumption that the pollutants released are inert and nondepositing. MELSAR is developed for application in a region covering western Colorado, eastern Utah, and southern Wyoming. However, the computer code itself is not site-specific and could conceivably be applied anywhere provided the proper inputs are developed and the parameterizations within MELSAR are applicable to the region to be modeled.

EXECUTIVE SUMMARY

Pacific Northwest Laboratory has developed a mesoscale air quality model for the U.S. Environmental Protection Agency (EPA) under their Green River Ambient Model Assessment (GRAMA) program. This program was initiated in response to the need for air quality assessment tools applicable in the Green River Oil Shale Formation region of western Colorado, eastern Utah, and southern Wyoming. This region has the potential for large-scale growth because vast energy resources, especially oil shale, are located in the region.

The model, MELSAR (MEsoscale Location Specific Air Resources), is a Lagrangian puff model to be applied at long source-to-receptor distances (tens to hundreds of kilometers) and short concentration averaging times (1 to 24 hr). These distances and averaging times are important in estimating the pollutant concentrations at the Prevention of Significant Deterioration (PSD) Class I areas in the region.

MELSAR is designed for application in a specific 500- by 450-km complex terrain region of the Green River Oil Shale Formation. It can compute concentrations for up to 20 sources and two pollutants at a time. The influences of the terrain on pollutant transport and diffusion are treated explicitly in MELSAR. The transport winds are computed from measured upper-air and surface weather data using a mass-consistent three-dimensional flow model. Steering of the winds around major terrain features during stable atmospheric conditions is accounted for, and the effects of terrain roughness on pollutant diffusion are treated. In addition, sources located in valleys are given special treatment. Pollutants trapped in valley drainage flows during nighttime are ventilated to the regional winds during the morning transition period. The pollutants trapped in the valley are treated as a line source at sunrise.

MELSAR has not undergone any rigorous operational testing, sensitivity analyses, or evaluation studies. Three major steps are required before MELSAR is ready for general use in the'region of western Colorado, Eastern Utah, and southern Wyoming: 1) operational and sensitivity testing, 2) testing and upgrading, if necessary, of specific algorithms using the limited tracer data sets available for the region, and 3) conducting a regional-scale tracer experiment to provide a data set for further testing and validation of MELSAR. MELSAR is a highly modularized computer code, which facilitates upgrades and additions to the code. The addition of chemistry and deposition to MELSAR would be straightforward, and would enable MELSAR to be used as a tool for estimating contributions to acid deposition.

CONTENTS

FIGURES

TABLES

ACKNOWLEDGMENTS

Mr. Alan Huber, the EPA Project Officer, and Mr. Rich Fisher, EPA Region VIII meteorologist, are thanked for their support and encouragement of the work. Mr. Huber and Mr. Fisher have both provided a number of useful suggestions regarding the development of the model and the desired features of the model that will prove useful to the user. These suggestions have resulted in improvements to the model code.

The authors' colleagues at PNL contributed suggestions and criticisms as the work progressed that led to significant improvements in the model's design and in the clarity of the text. Drs. Thomas W. Horst and J. Christopher Doran are especially thanked for their help in that regard. The able programming assistance of Mr. Roger L. Schreck of Pacific Northwest Laboratory is also greatly appreciated.

The work was funded by the Energy Air Division, Office of Environmental Processes and Effects Research, Office of Research and Development, U.S. Environmental Protection Agency under Interagency Agreement No. AD-89-F-2-097-0 with the U.S. Department of Energy.

SECTION 1.0

INTRODUCTION

The MELSAR (MEsoscale Location Specific Air Resources) model was developed for application in the complex terrain region of the Green River Oil Shale Formation of Colorado, Utah, and Wyoming shown in Figure 1-1. Its purpose is to aid in assessing the air pollution potential from development of the extensive oil shale reserves and other industrial, mining, manufacturing, or power production development within this region. MELSAR was developed for the U.S. Environmental Protection Agency (EPA) under their Green River Ambient Modeling Assessment (GRAMA) program. The GRAMA program was conducted by Pacific Northwest Laboratory, which is operated by the Battelle Memorial Institute for the U.S. Department of Energy.

This report consists of two volumes: Volume 1 contains the computer model overview, technical description and users guide, and Volume 2 contains the Appendices which include listings of the FORTRAN code. The purpose of this volume is to document the technical foundation of the computer model, MELSAR, provide instruction for its use, and describe its applications and limitations. Section 1.0 gives an overview of the MELSAR model consisting of its background and developrnent, features and limitations, and a description of the model's operation including data requirements. Section 1.0 is intended to provide the decision maker, atmospheric scientist, meteorologist, or engineer with enough information to decide if the model is applicable to their problem. It is also intended to provide the model user with an introduction to the model. Section 2.0 gives the technical details of the model, and Section 3.0 gives the detailed instructions for setting up and executing MELSAR.

1.1 Background

Several studies (Latimer and Doyle 1981; Kronenberger et al. 1981; and Anderson et al. 1980) have indicated that the Prevention of Significant Deterioration (PSD) Class I regulations may be an important factor in limiting development of the vast energy reserves in the Green River Oil Shale Formation. This is because several protected (PSD Class I) areas are present within the region. EPA Region 8, realizing the need for an assessment model to address these regionwide issues, initiated the GRAMA program.

FIGURE 1-1

GREEN RIVER OIL SHALE FORMATION AND OTHER OIL SHALE DEPOSITS
IN THE UNITED STATES (DUNCAN AND SWANSON 1965)

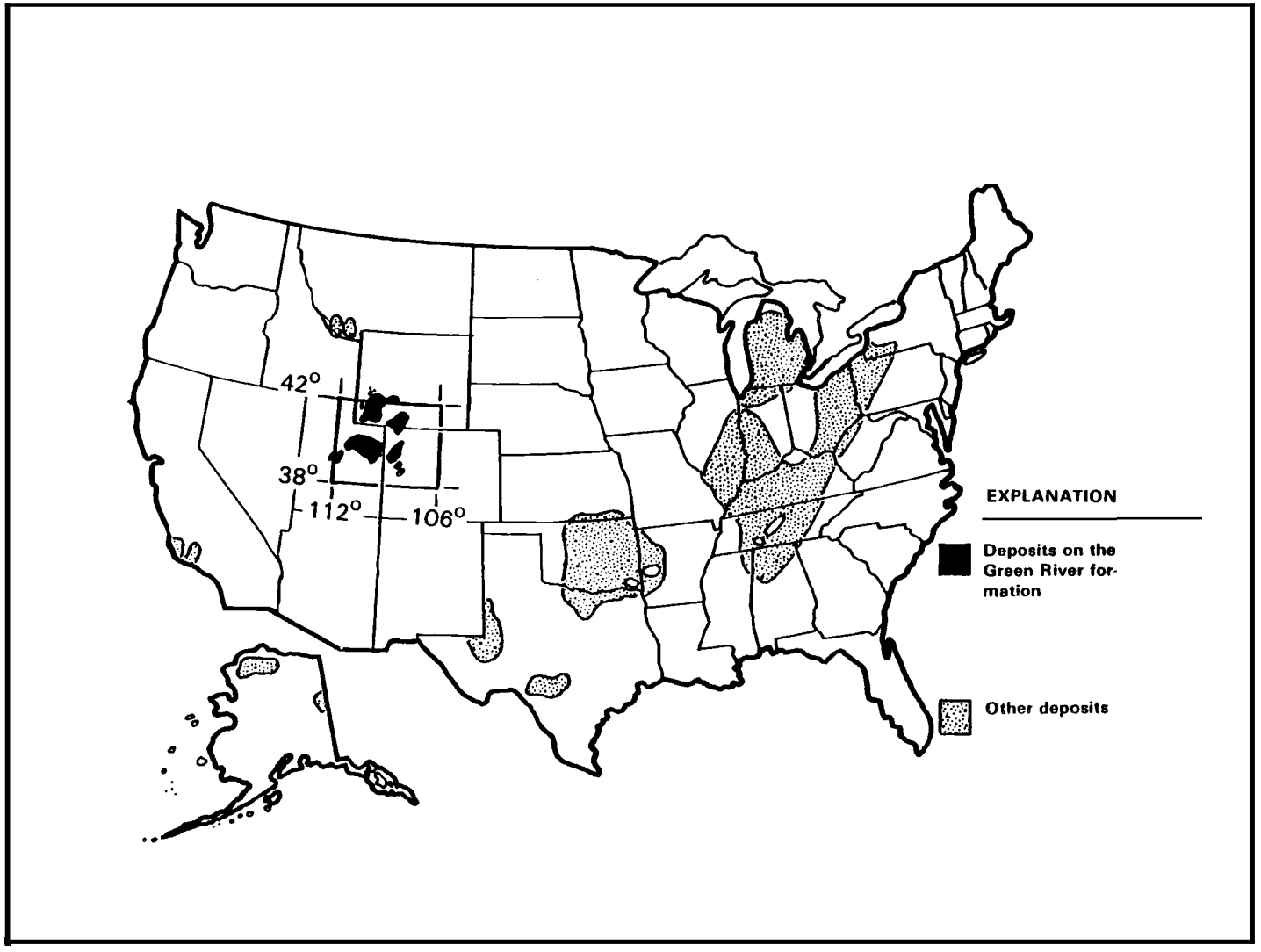

The development of the MELSAR model is one product of the GRAMA program. It is primarily designed to estimate 3-hr and 24-hr average SO_2 and total suspended particulates (TSP) concentrations, from multiple source releases, at the PSD Class I areas. The transport distances from the major source areas in this region to the PSD Class I areas are tens to hundreds of kilometers.

1.2 Features and Limitations

MELSAR is a mesoscale air quality model for predicting pollutant concentrations from releases from up to 20 point and area sources. Two pollutants can be treated during any run. MELSAR is a Lagrangian puff model for application in complex terrain, principally at long source-to-receptor transport distances (tens to hundreds of kilometers) and short averaging times (1 to 24 hr). The ground-level concentrations are computed on up to four 25- by 25-receptor grids and up to 10 individual receptors. The pollutants are assumed to be nondepositing and inert. This is a conservative assumption for computing air concentrations of primary pollutants.

MELSAR is set up to operate on a 500- by 450-km region covering western Colorado, eastern Utah, and southern Wyoming (refer to Figure 1-1 and the figures in Appendix A). This region is referred to as the GRAMA region in this user's guide. The coordinate system for the GRAMA region is a rectangular system, and input data can be specified in either the GRAMA, Universal Transverse Mercator (UTM), or latitude-longitude coordinate systems.

Simulation periods from hours to days (maximum 30 days) can be accommodated by MELSAR. In addition, intermediate meteorological and terrain output files can be saved and cataloged for later applications of MELSAR, thus saving the cost and time of regenerating these files. A file tracking and cataloging system is provided with MELSAR.

MELSAR utilizes a three-dimensional mass-consistent flow model to determine the time-varying and space-varying winds over the region. The model is a diagnostic model and uses upper-air data from up to 10 stations and surface weather data from up to 15 stations as input. The flow model also accounts for flow channeling around major terrain features during stable atmospheric conditions by using the concept of a dividing streamline height. This height is calculated from available upper-air data and from analysis of the terrain data. The winds are specified on up to nine levels above the terrain surface. Using the same upper-air and surface weather data that are used to determine the winds, MELSAR produces hourly gridded fields of temperature, pressure, friction velocity, convective velocity, Monin-Obukov length, mixing height, and stability classification. These gridded quantities are written to disk files and can be used during other applications of MELSAR.

The puffs diffuse in a Gaussian fashion where the vertical distribution is modified by multiple reflections from the ground and an upper mixing lid. The horizontal and vertical diffusion coefficients are computed as functions

of travel time and the standard deviations in the horizontal winds, a_v, and vertical winds, σ_w, respectively. Two options are available in MELSAR for computing σ_v and σ_w: 1) from empirical equations relating σ_v and σ_w to boundary layer parameters (e.g., friction velocity, convective velocity), where the required boundary layer parameters are determined from the input meteorological data, and 2) from empirical equations relating a and σ_w to terrain roughness. The effects of wind shear on horizontal diffusion are treated, and initial diffusion caused by buoyant plume rise is incorporated.

Sources located within valleys are treated in a special way in MELSAR. If, from analysis of the meteorological data, the valley atmosphere is 'decoupled' (primarily nighttime) from the regional flow, then the pollutants released into the valley remain in the valley. These pollutants travel down-valley in mean down-valley winds until sunrise, at which time the valley winds are stopped and MELSAR immediately begins ventilating pollutants from the valley. Pollutants are ventilated from the valley to the regional winds at a rate determined by the rate of inversion destruction within the valley.

The MELSAR code was designed to operate on any subpart of the GRAMA region, although the code has not been fully tested for this application. In addition, certain of the meteorological and diffusion algorithms were adapted for or developed for MELSAR, considering only regional-scale applications. Consequently, these parameterizations may not necessarily be appropriate for local-scale applications. Because of these regional-scale parameterizations and large terrain averaging intervals for regional-scale applications of MELSAR, concentrations computed at receptors near (within 10 to 20 km) a source may not be dependable estimates of impacts from that source. This would only apply to pollutant releases from the near source.

Applying MELSAR to sites other than the GRAMA region would require examination of some parameterizations in MELSAR which were developed from site-specific data. In particular, the ventilation rate of pollutants from valleys is based on empirical relations developed from data collected in Colorado valleys.

1.3 System Description

MELSAR consists of four main programs: TERRAIN, MET, POLUT, and POLPRC. TERRAIN uses a base terrain file and produces files of spatially averaged terrain statistics for use by MET and POLUT. MET produces hourly winds, gridded mixing heights, stabilities, friction velocities, convective velocities, Monin-Obukov lengths, temperatures, pressures, and valley coupling coefficients, using upper-air and surface weather observations. POLUT uses the output files from MET and TERRAIN and produces pollutant concentrations, corrected to standard conditions, on a user-specified receptor network for each time step of a simulation. The concentration fields are used by POLPRC to compute moving-average concentrations of pollutants for up to three averaging times. The output data from POLPRC are tables of highest and second highest pollutant concentrations at each

receptor. Tables are produced for the sum of all sources along with the resulting contribution of each source to the sum. Also, highest and second highest concentration tables are generated for each receptor grid and set of individual receptors, considering each source individually. Figure 1-2 shows how the four main programs interact.

FIGURE 1-2

INTERACTION OF THE FOUR MAIN PROGRAMS IN MELSAR

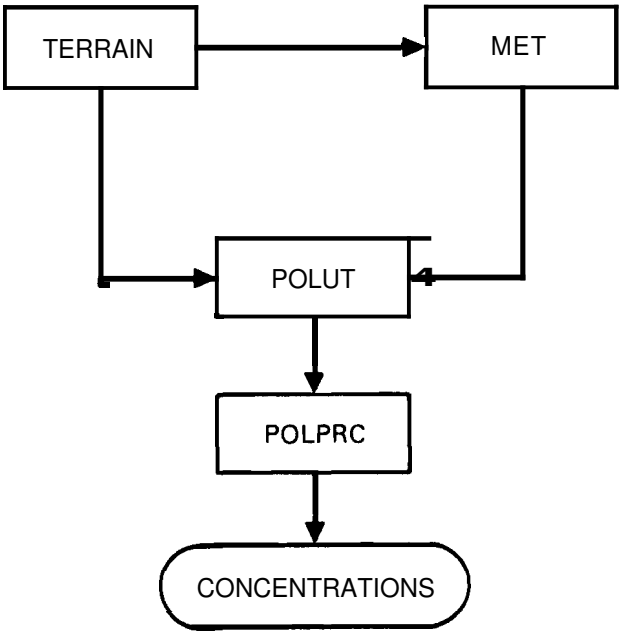

For multiple applications of MELSAR, it may not be necessary to run TERRAIN, MET, and POLUT for each application. The output files for one application may be useable during other applications. Provided with MELSAR is an approach for naming and tracking the input and output files from MELSAR. Tracking the files will ensure that documentation is available for future reference and ensure that all the input and output files will be available and retrievable for future runs of MELSAR.

The TERRAIN program produces gridded fields of terrain statistics from the base terrain file, which contains 500 by 450 terrain heights where each terrain height is the average over a 1-km-square area. This program enables users to compute the necessary terrain statistics for any subdomain in the GRAMA region they want to model. In addition, TERRAIN provides the flexibility necessary to investigate the effects of terrain smoothing on ground-level concentrations during any sensitivity testing of MELSAR. TERRAIN requires approximately 250K words of memory to load on a UNIVAC® 1108 computer.

® UNIVAC is a registered trademark of the SPERRY RAND Corporation.

MET is a very flexible meteorological data processor. It is designed to receive up to one month of upper-air and surface weather input data from up to 10 upper-air and 15 surface stations over different time periods and sampling intervals. It can handle missing data and was designed to handle any data that are available for a specified period of time. That is, observations from National Weather Service stations, special studies, or intensive field programs can be used. MET requires approximately 70K words of memory to load on a UNIVAC® 1108 computer.

POLUT is a Lagrangian puff model where the pollutant distribution is described in a Gaussian fashion about the puff center-of-mass. The distribution in the vertical is modified by the treatment of multiple reflections from the ground and an upper mixing lid. Ground-level concentrations for each modeling time step for two pollutants can be computed for releases from up to five sources, either point or area sources. The area sources are treated as virtual point sources. Concentrations are computed on up to four 25- by 25-receptor grids and up to 10 individual receptors specified anywhere at ground level in the modeling domain. POLUT requires approximately 160K words of memory to load on a UNIVAC® 1108 computer.

POLPRC computes moving-average concentrations of pollutants at each receptor for up to three user-specified averaging times. The averaging times can range from 1 to 24 hr. Up to 20 sources can be processed at one time. The outputs are tables of highest and second highest pollutant concentrations for the duration of the simulation, at each receptor for each pollutant for each averaging time. The highest and second highest moving averages for the sum of all sources and the contribution of each source to the highest and second highest sum are computed. Highest and second highest moving averages can also be computed for each source individually. Tables of the time of occurrence of the highest and second highest values are also listed. POLPRC requires approximately 90K words of memory to load on a UNIVAC® 1108 computer.

1.4 Data Requirements

The input data required by MELSAR are

1. gridded terrain data
2. upper-air weather data
3. surface weather data
4. points to interpolate wind data to (primarily for boundary conditions)
5. gridded land-use categories (for determining surface roughness)
6. source valley characteristics
7. pollutant source inventory
8. receptor layout.

All but the upper-air and surface weather data must be specified within the modeling region. Data from weather stations outside the modeling region can be used by MELSAR.

The gridded terrain data for the GRAMA region are provided with MELSAR and do not have to be developed by the user. Also included with MELSAR are four files of surface and upper-air weather data, one file of wind interpolation points for runs using the entire GRAMA region, and one file of gridded land-use categories for runs using the entire GRAMA region. These data files are described in Appendix D.

New upper-air and surface weather data files can be developed if meteorological periods other than the ones provided are desired for model runs. For applications where the modeling domain is a subset of the GRAMA region, a new wind interpolation point file and a new land-use categories file must be constructed. For each group of sources to be modeled, a new source inventory file and a new source-valley characteristics file must be constructed. New receptor layout files must be constructed for each new receptor configuration. Section 3.0 describes the construction of the input data files.

SECTION 2.0

TECHNICAL DISCUSSION

This section discusses the technical basis of the MELSAR model. Sufficient detail is presented to allow the user to understand the uses and limitations of the model. For more technical detail the user can refer to the computer code, which contains a complete set of comments explaining the code. Table 2-1 provides the names of the subroutines corresponding to the main technical areas presented in this section.

The technical discussion of MELSAR is divided into seven main topic areas, which are discussed in Sections 2.1 through 2.7. These topic areas are Model Structure, Domain and Coordinate System, Terrain, Meteorological Data Processor, Puff Model, and Averaging Process.

2.1 Model Structure

MELSAR consists of four computer programs named TERRAIN, MET, POLUT, and POLPRC. TERRAIN uses a base terrain file for the region of interest and produces disk files of spatially averaged terrain statistics (e.g., heights, roughness) for use by the MET and POLUT programs. MET produces hourly winds, gridded mixing heights, stabilities, friction velocities, convective velocities, Monin-Obukov lengths, temperatures, pressures, and valley coupling coefficients, using upper-air and surface winds and temperature observations. POLUT uses the output files from MET and TERRAIN and produces pollutant concentrations on a user-specified receptor network for each time step of a simulation. The concentration fields are output to a disk file that is then used by POLPRC to compute moving-average concentrations of pollutants for up to three averaging times. The outputs from POLPRC are tables of highest and second highest pollutant concentrations at each receptor. Tables are produced for the sum of all sources along with the resulting contribution of each source to the sum. Also, highest and second highest concentration tables are generated for each receptor grid and set of individual receptors, considering each source individually. The interaction of the four main computer programs is given in Figure 1-2.

TABLE 2-1

MAIN COMPUTER CODE ROUTINES WITHIN EACH TECHNICAL AREA

Report Section No.	Technical Area	Main Programs	Main Subroutines
2.2	Domain and Coordinate System	MET	LAT,UTM,GRID
2.3	Terrain	TERRAIN	ROUGH
2.4	Meteorological Data Processor	MET	UPPER,SRFC,AMPLIT,COEFF,MIXSTB,BLPARS
2.4.1	Wind Fields	MET	AMPLIT,AMPL,FROUDE,TEMP,LAPSE
2.4.2	Mixing Heights	MET	MIXSTB,SOLAR,HPROF,WINDS
2.4.3	Stability Classification	MET	MIXSTB,STAB,WINDS
2.4.4	Valley Coupling Coefficient	MET	COEFF,CUP,BETA,VALGAM,WARM,SUBAO,DESCNT
2.4.5	Friction Velocity	MET	BLPARS,USTAR
2.4.6	Convective Velocity	MET	BLPARS,WSTAR
2.4.7	Monin-Obukov Length	MET	BLPARS,MONIN
2.4.8	Temperature	MET	BLPARS
2.4.9	Pressure	MET	BLPARS
2.5	Puff Model	POLUT	
2.5.1	Gaussian Puff Equation	POLUT	CONS,VERTDF
2.5.2	Plume Rise	POLUT	PRISE
2.5.3	Receptors	POLUT	INIT
2.5.4	Source Representation	POLUT	INIT
2.5.5	Puff Treatment	POLUT	SIGGS,NEWLOC,CLEAN,CLEANV
2.5.6	Puff Transport	POLUT	NEWLOC
2.5.7	Sampling Function	POLUT	CALC,CALCVA,DEFINE,DIVIDE
2.5.8	Valley Treatment	POLUT	VALY,VALMA
2.5.9	Interpolation	POLUT	BLPINT,TETRI,ROUINT
2.5.10	Diffusion Coefficients	POLUT	SIGGS,SIGMAY,SIGMAZ
2.6	Averaging Process	POLPRC	MOVAVE

2.2 Domain and Coordinate System

The modeling domain in the GRAMA program is a region covering western Colorado, eastern Utah, and southern Wyoming. This region was singled out because of its potential for large-scale energy production, especially that related to oil shale. The modeling region spans approximately 38° to 42° north latitude and 106° to 112° west longitude as shown in Figure 1-1.

A good map projection for projecting this size and location of the earth's surface to a plane is the Transverse Mercator Projection (Richardus and Adler 1972). In fact, this projection is used by the U.S. Army in defining their Universal Transverse Mercator (UTM) grid system (U.S. Army 1973). The UTM grid system covering the northern hemisphere is divided into zones for every 6° longitude. Two UTM grid zones, 12 and 13, cover the GRAMA region and are based on projections about the 111° and 105° meridians, respectively.

Because basing the MELSAR coordinate system on the UTM system is not practical (because of the overlapping of grid zones), and because transposing data to and from a model grid overlayed on maps would be cumbersome and potentially inaccurate, the MELSAR coordinate system was based on a Transverse Mercator projection about the region's central meridian (109° west longitude).

The origin of this projection is the intersection of the central meridian and the equator. For convenience, the MELSAR coordinate system is specified as a subset of the above projection, such that the origin is near the intersection of the 38° north latitude and 112° west longitude and a rectangular domain fits within the 38° to 42° latitude by 106° to 112° longitude boundaries. The domain was chosen to be 500 km in the east-west direction by 450 km in the north-south direction. Figure 2-1 shows the relationship of the MELSAR coordinate system and latitude-longitude for the GRAMA region.

The general transformation equations for a Transverse Mercator Projection from latitude-longitude to the MELSAR grid, based on the earth as a sphere, are

$$X = \frac{1}{2} CR \ln \left[\frac{1 + \cos\sin (\lambda_o - A)}{1 - \cos\phi\sin (\lambda_o - \lambda)} \right] + X_o \qquad (2\text{-}1)$$

$$Y = CR \left\{ \frac{\pi}{2} - [\tan^{-1}(\cot\phi\cos (\lambda_o - \lambda))](\frac{\pi}{180}) \right\} - Y_o \qquad (2\text{-}2)$$

where

X = X-coordinate in MELSAR coordinate system (km)
Y = Y-coordinate in MELSAR coordinate system (km)
ϕ = latitude (deg)
λ = longitude (deg)

FIGURE 2-1

RELATIONSHIP OF THE MELSAR COORDINATE SYSTEM AND LATITUDE-LONGITUDE FOR THE GRAMA MODELING REGION

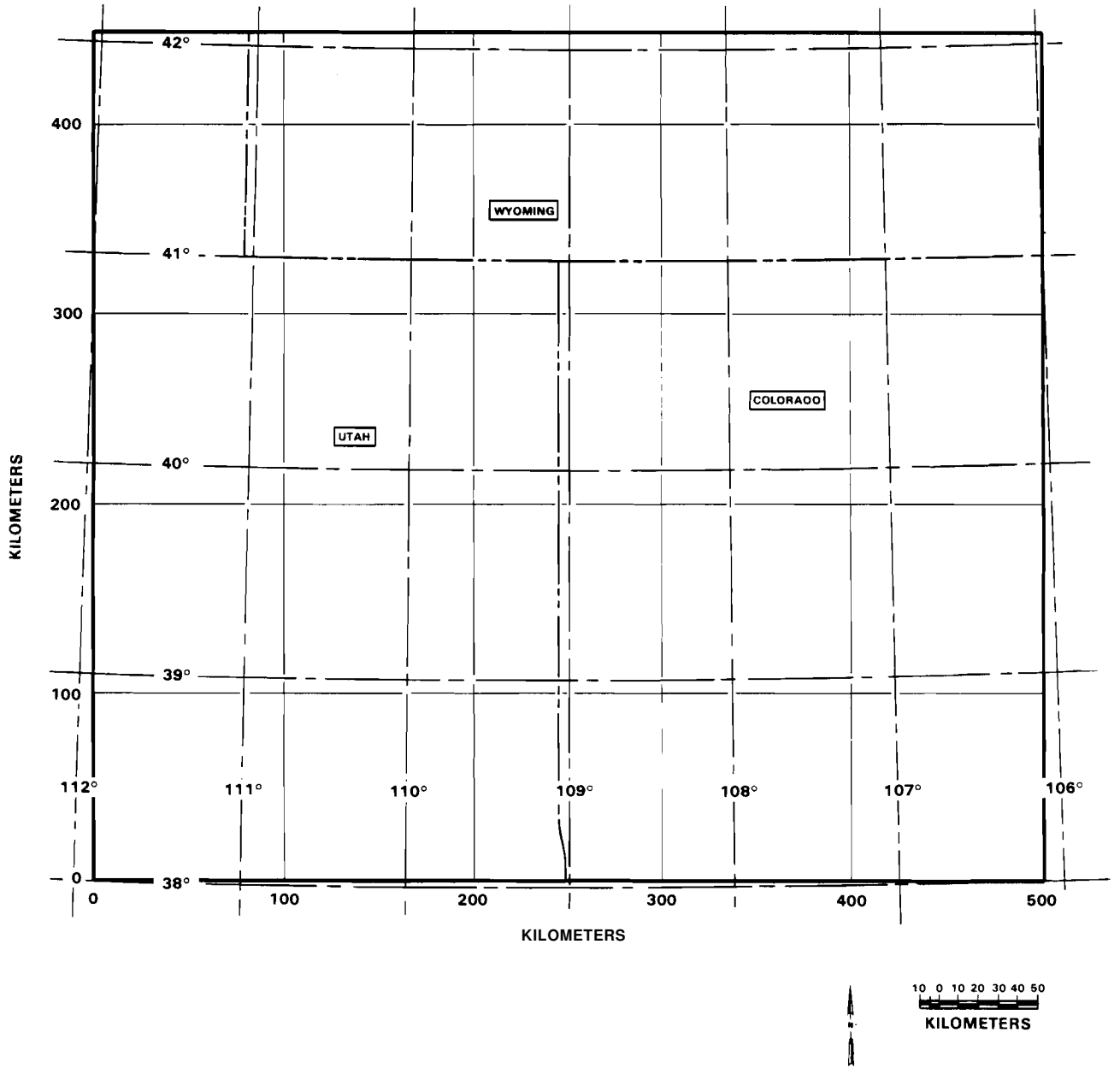

λ_o = central meridian (deg)
X_o = distance of MELSAR grid origin west of λ_o (km)
Y_o = distance of MELSAR grid origin north of equator (km)
R = ab = mean radius of earth (km)
a = 6378.206 km, (Richardus and Adler 1972) equatorial axis of earth
b = 6356.584 km, (Richardus and Adler 1972) polar axis of earth
C = 0.9996, scale factor to distribute the distortion more evenly.

For the GRAMA region, λ is 109°, X_o is 250.500 km, and Y is 4224.697 km. X_o and Y_o are determine8 by solving Equations (2-1) and (9-2) assuming $X = 0$, $Y = 0$, ϕ = latitude of desired origin, λ = longitude of desired origin, and λ_o = central meridian of projection. Table 2-2 gives the latitude-longitude coordinates of the four corner points of the MELSAR grid for the GRAMA region.

TABLE 2-2

LATITUDE-LONGITUDE COORDINATES OF THE FOUR CORNERS OF THE GRAMA REGION

MELSAR Coordinates			
X (km)	Y (km)	Latitude (deg N)	Longitude (deg W)
0.	0.	38.00	111.86
500.	0.	38.00	106.14
0.	450.	42.05	112.03
500.	450.	42.05	105.97

The transformation equations from the MELSAR coordinate system to latitude-longitude for output purposes, are

$$\phi = \sin^{-1}(A) \tag{2-3}$$

$$\lambda = \begin{cases} \lambda_o + \cos^{-1}\left[\dfrac{Y'A}{(1 - A^2)^{1/2}}\right]; & X' < 0 \\ \lambda_o - \cos^{-1}\left[\dfrac{Y'A}{(1 - A^2)^{1/2}}\right]; & X' \geq 0 \end{cases} \tag{2-4}$$

where

$$X' = \frac{\exp\left[2(X - X_o)/(CR)\right] - 1}{\exp\left[2(X - X_o)/(CR)\right] + 1}$$

$$Y' = \tan\left\{\left[\frac{\pi}{2} - (Y + Y_o)/(CR)\right]\left(\frac{180}{\pi}\right)\right\}$$

$$A = \left[\frac{1 - X'^2}{1 + Y'^2}\right]^{1/2}$$

Equations (2-1), (2-2), (2-3), and (2-4) are based on the assumption that the earth is in the shape of a sphere; whereas, the earth can be better represented as an ellipsoid (Richardus and Adler 1972; U.S. Army 1973). Transformation equations based on the earth as an ellipsoid are very complex and are accurate to within a few meters for projections the size of the GRAMA region. Comparison of the results of spherical-based equations with ellipsoidal-based equations shows that spherical-based equations differ from ellipsoid-based equations by about 0.09 km/100 km in the north-south direction and about -0.30 km/100 km in the east-west direction over the GRAMA region. This level of accuracy using the spherical-based equations is much better than the uncertainty in predicting the pollutant trajectories. Therefore, the improved accuracy from ellipsoidal-based equations will not improve the prediction of pollutant impacts.

In addition to receiving input data in latitude-longitude coordinates, MELSAR is configured to receive input data in UTM coordinates from two UTM grid zones. The UTM transformation equations are based on an ellipsoidal shape of the earth; however, spherical-based equations are used in MELSAR to transform from UTM coordinates to latitude-longitude. The transformation equations from UTM to latitude-longitude are of the same form as Equations (2-3) and (2-4) and are listed below:

$$\phi = \sin^{-1}(A) \tag{2-5}$$

$$\lambda = \begin{cases} \lambda_o + \cos^{-1}\left[\dfrac{N'A}{(1 - A^2)^{1/2}}\right] & ; \quad E' < 0 \\ \lambda_o - \cos^{-1}\left[\dfrac{N'A}{(1 - A^2)^{1/2}}\right] & ; \quad E' > 0 \end{cases} \tag{2-6}$$

where

$$E' = \frac{\exp\left[2(E - E_o)/(CR)\right] - 1}{\exp\left[2(E - E_o)/(CR)\right] + 1}$$

$$N' = \tan\left\{\left[\frac{\pi}{2} - (N + N_o)/(CR)\right]\left(\frac{180}{\pi}\right)\right\}$$

$$A = \left[\frac{1 - E'^2}{1 + N'^2}\right]^{1/2}$$

λ_o = central meridian of UTM grid zone (deg)
N = UTM northing (km)
E = UTM easting (km)
N_o = northing coordinate of origin relative to equator (km)
E_o = easting coordinate of origin west of central meridian (km).

The actual UTM origin for any grid zone is located on the equator 500 km west of the central meridian. But because spherical-based equations are used in MELSAR, the UTM origin, (E_o, N_o), will be slightly translated from the actual location. The adjusted origin, for each grid zone of interest, can be computed by solving Equations (2-5) and (2-6) for E_o and N_o knowing the UTM coordinates and the latitude-longitude of the point where the central meridian intersects the southern boundary of the modeling domain. The final E_o is equal to the E_o from Equations (2-5) and (2-6) minus 500 km. This computed origin (E_o, N_o) can then be used in Equations (2-5) and (2-6) to compute the latitude-longitude for any point in a UTM grid zone given the UTM coordinates of the point. Equations (2-1) and (2-2) are then used to complete the transformation from UTM to MELSAR coordinates.

Features of the GRAMA region within the MELSAR grid are given in Appendix A. Figure A-1 shows the major roads and towns, Figure A-2 shows the PSD Class I areas in relation to oil shale development areas, Figure A-3 shows the topography of the region, Figure A-4 shows the main rivers and streams, and Figure A-5 shows the boundaries of the major river drainages.

2.3 Terrain

MELSAR requires certain terrain statistics averaged over grid cells for its operation. The MET program requires 'lower' terrain elevations, terrain obstacle heights and drainage directions on a 10 x 10 grid for Froude number modification to the flow field. MET also requires smoothed terrain elevations on up to a 50 x 50 grid. POLUT requires smoothed terrain elevations, and terrain 'roughness' in the X-direction and terrain 'roughness' in the Y-direction on up to a 50 x 50 grid. The description of the creation of the base terrain file and computation of the above-listed terrain statistics are given below.

Once the MELSAR coordinate system has been defined for a region, as described in the previous section, the base terrain file for that region can be constructed. From this base terrain file, the required terrain statistics for any run of MELSAR can be computed. The elements of this file must be terrain heights averaged over 1-km squares, denoted the '1-km resolution' base terrain file. The 500- by 450-km base terrain file used by MELSAR for the GRAMA modeling region was constructed from U.S. Geological Survey 0.001" resolution digitized terrain data. First the 0.001" data were averaged to 0.01" resolution for each 1°-latitude by 1°-longitude cell between 106° to 112° west longitude and 38° to 42° north latitude. This resulted in a total of twenty-four 0.01"-average terrain files. Next, all of the files were combined into one file and the location of each terrain element in this file was transformed into the MELSAR grid system using Equations (2-1) and (2-2) as described in Section 2.2. Since 0.01" longitude is about 0.86 km at the latitude of the GRAMA region and 0.01" latitude is about 1.11 km, then some of the 1-km grid points in the base terrain file contained no value on transformation. These missing values were subsequently filled by assigning the grid points the value of the average of the four surrounding grid points. From this base terrain file of 500 km by 450 km with 1-km resolution, all of the required terrain statistics for a run of MELSAR for the GRAMA region are computed. Figure 2-2 gives a perspective plot of the 1-km base terrain file for the GRAMA modeling region.

MELSAR is designed to operate over the entire modeling domain or any portion of it. Therefore, the terrain processing routines were designed to compute terrain statistics given any origin, any domain size, any smoothing interval, and any grid cell size up to 50 km by 50 km. Figure 2-3 shows the grid points in the first 30 km of the southwest corner of the GRAMA modeling domain for 10-km-square grid cells covering the entire GRAMA domain. For this configuration, there is a total of 50 grid cells in the X-direction by 45 grid cells in the Y-direction. (The maximum number of cells that MELSAR can treat is 50 by 50.) The terrain statistics for each grid cell are computed from the one hundred 1-km data points in each cell (shown in the first cell in Figure 2-3) for this example assuming that the smoothing interval is the same as the cell size. If the smoothing interval was specified larger than the cell size, then some overlap of the averaging process would be accomplished. The smoothing interval must be greater than or equal to the cell size.

The smoothed terrain height and standard deviation (used to compute obstacle height) of the terrain height for each grid cell in the example in Figure 2-3 are simply the arithmetic mean and standard deviation computed from the 1-km terrain elements within each grid cell.

Figure 2-4 gives a plot of the 1-km base terrain data with 10-km smoothing. This is to illustrate what effect smoothing has on the base terrain file. In this plot every 1-km data point has a 10-km average terrain height associated with it. Obtaining a 50 x 45 grid of 10-km smoothed terrain heights by the process illustrated in Figure 2-3 would give

FIGURE 2-2

DISPLAY OF THE BASE TERRAIN FILE FOR THE GRAMA MODELING REGION
(The file consists of terrain heights averaged over 1-km square cells)

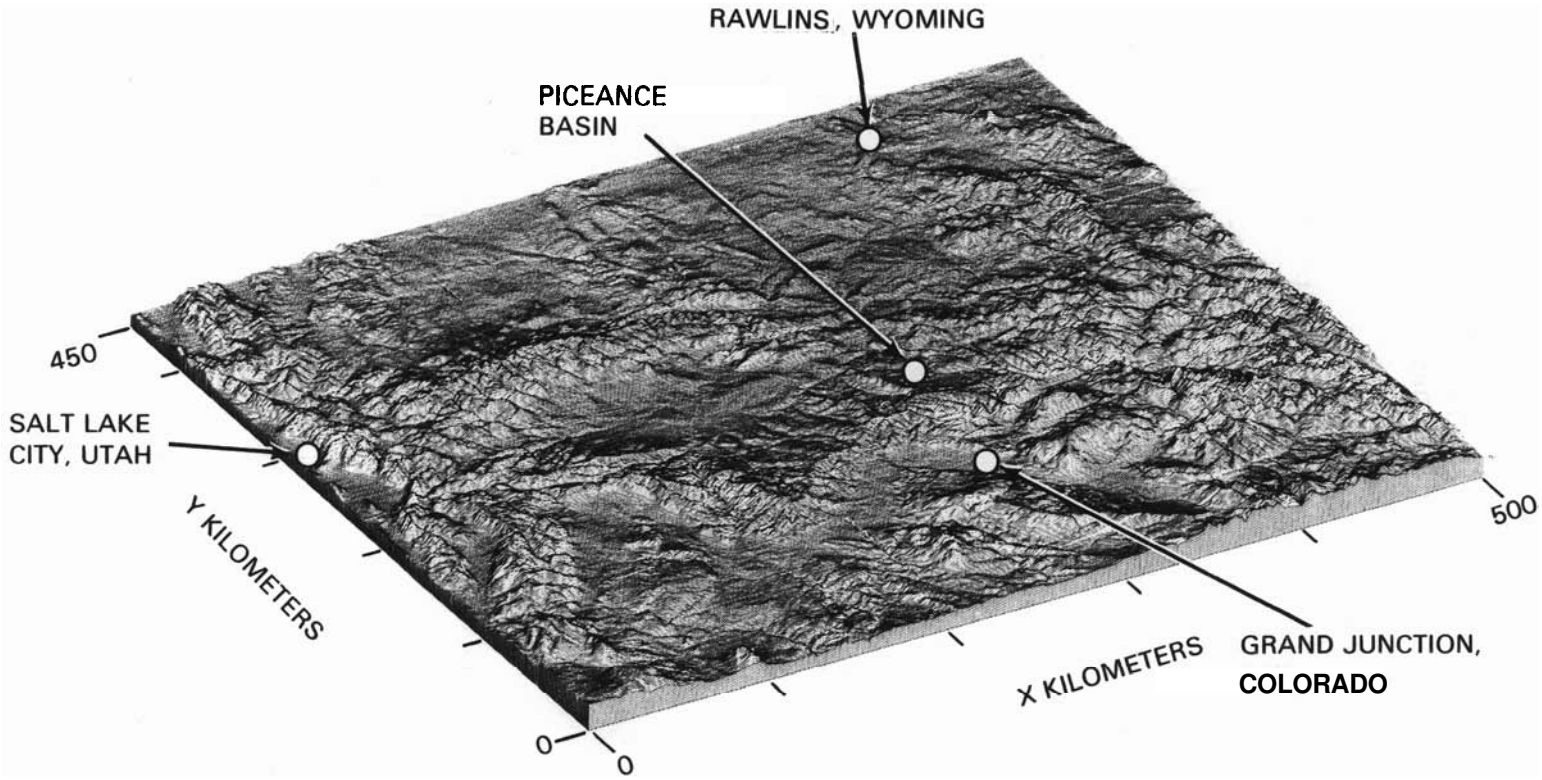

VERTICAL EXAGGERATION 5X

FIGURE 2-3

LOCATION OF GRID POINTS FOR 10-km-SQUARE GRID CELLS IN THE SOUTHWEST CORNER OF THE GRAMA MODELING REGION
(Shown in the first cell are the 1-km-square cells making up the base terrain file)

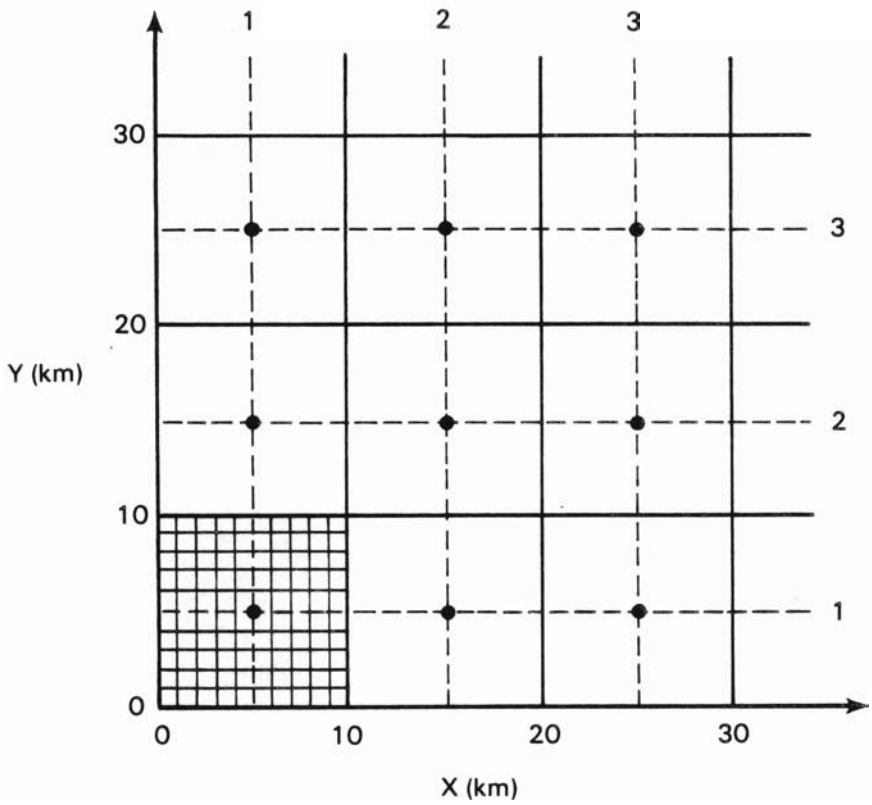

the same results as overlaying a 50 x 45 grid over the smoothed terrain surface in Figure 2-4 and registering the terrain elevation below each grid point.

A measure of terrain roughness, R_T, (not to be confused with surface roughness, Z_0) is used for computing turbulence, and was derived by MacCready, Baboolal and Lissaman (1974) based on a best correlation with the turbulence data that they analyzed. The average terrain roughness for a grid cell is computed by first determining a measure of terrain roughness for each 1-km data element and then finding the average of all the 1-km elements in a grid cell. The terrain roughness is computed in the Xdirection and Ydirection, resulting in two numbers for each grid cell. The terrain roughness for each 1-km-grid element is computed by centering a 14-km-long line segment over the point of interest oriented in the desired direction and using equations:

FIGURE 2-4

DISPLAY OF TERRAIN SURFACE FOR GRAMA MODELING REGION FOR A SMOOTHING INTERVAL OF 10 KILOMETERS

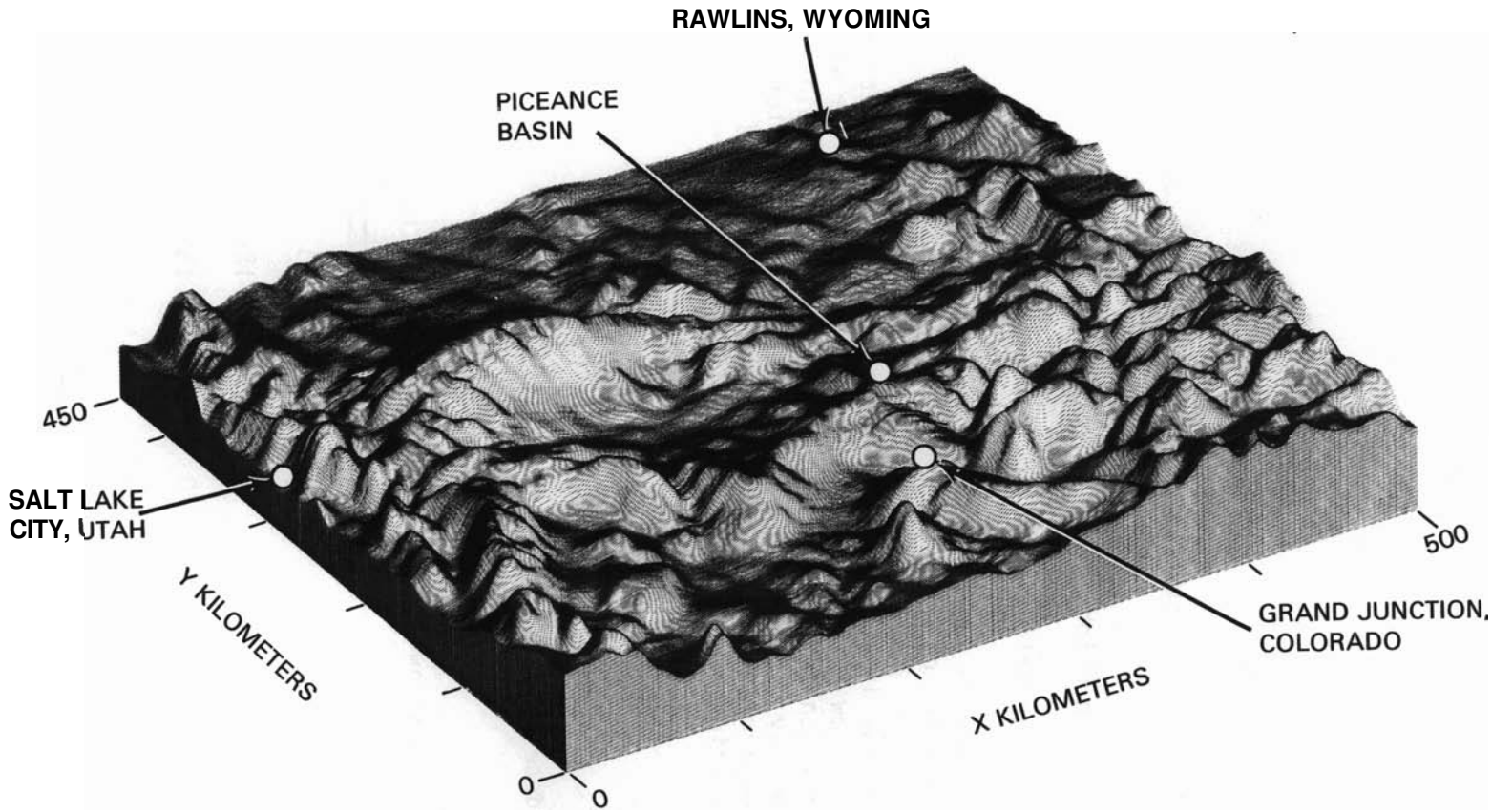

VERTICAL EXAGGERATION 20X

$$R_T = 2.3 \left[\frac{\sum_{i=1}^{14} (Z_{T_i} - \overline{Z_T})^2}{14} \right]^{1/2} \qquad (2\text{-}7)$$

$$\overline{Z_T} = \frac{1}{14} \sum_{i=1}^{14} Z_{T_i}$$

where

R_T = terrain roughness in direction of orientation of line segment (km)

Z_{T_i} = terrain height of one element on 14-km segment (km)

$\overline{Z_T}$ = average height of 14-km segment (km).

Plots of the terrain roughness for 10-km grid cells for the entire GRAMA modeling region are given in Figures 2-5 and 2-6.

The drainage direction, Θ_D, is an important terrain statistic used in modifying the flow field in conjunction with Froude number values. The drainage direction is defined as the direction that a drainage wind would come from for any given terrain cell. It is determined for a grid cell by computing the average slopes in the X-direction, AX, and the Y-direction, ΔY, across a grid cell and using the following equations:

$$\Theta_D = 90 - \Theta; \quad 0 < \Theta < 90 \qquad (2\text{-}8)$$

$$\Theta_D = 450 - \Theta; \quad 90 < \Theta < 360$$

where Θ is determined from Table 2-3.

TABLE 2-3

RELATIONSHIPS USED IN COMPUTING DRAINAGE DIRECTION

Condition	AX = 0	AX < 0	AX > 0
$\Delta Y = 0$	a	$\Theta' + 180$[b]	$\Theta' + 360$
$\Delta Y < 0$	270	$\Theta' + 180$	$\Theta' + 360$
AY > 0	90	$\Theta' + 180$	Θ'

[a] Terrain is flat, no drainage direction.
[b] $\Theta' = \tan^{-1} [\Delta Y/\Delta X]$.

FIGURE 2-5

DISPLAY OF X-DIRECTION TERRAIN ROUGHNESS AVERAGED IN 10-krn-SQUARE GRID CELLS FOR THE GRAMA MODELING REGION

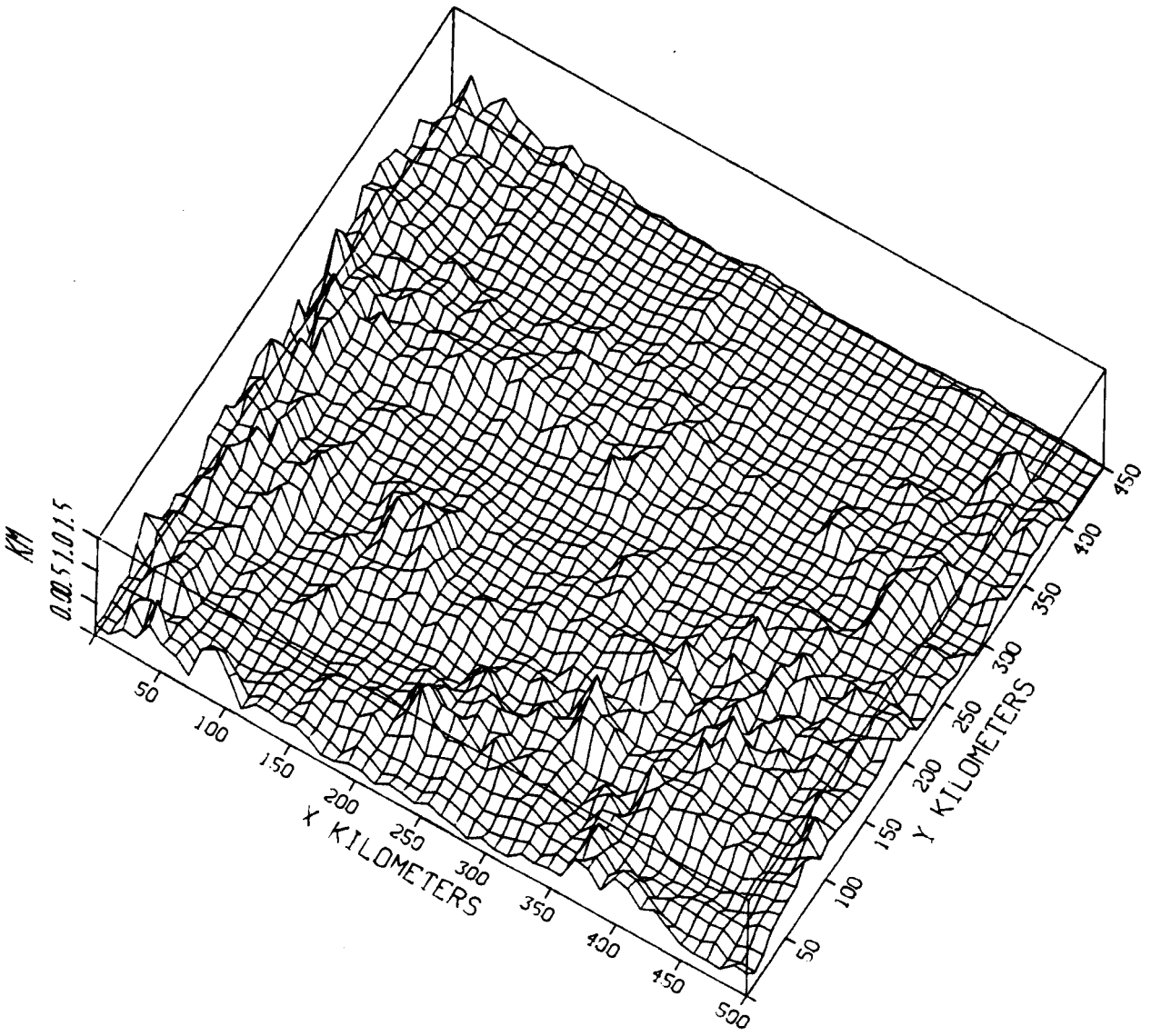

FIGURE 2-6

DISPLAY OF Y-DIRECTION TERRAIN ROUGHNESS AVERAGED IN 10-km-SQUARE GRID CELLS FOR THE GRAMA REGION

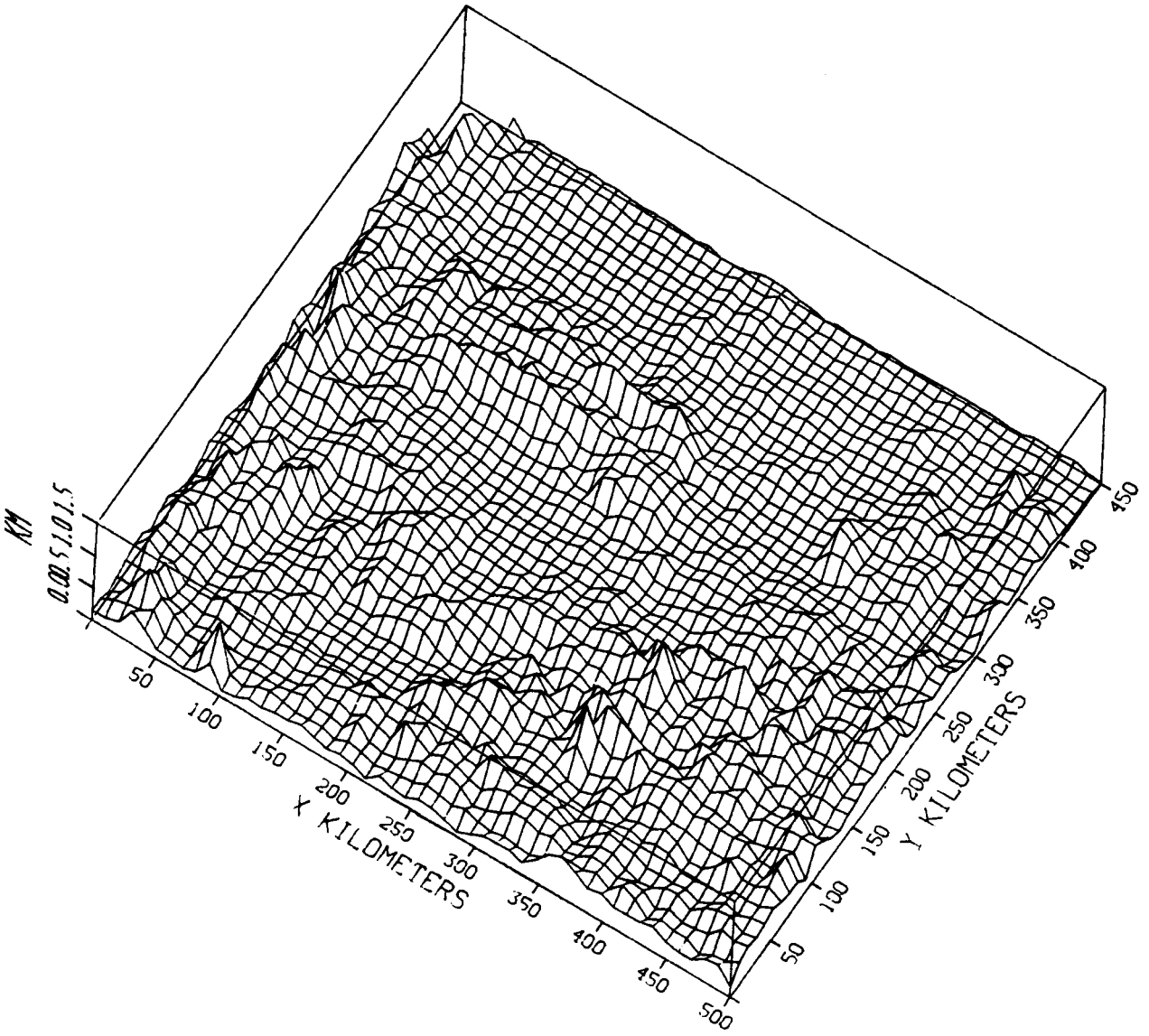

Shown in Figure 2-7 are drainage directions computed for 50- by 50-km average terrain cells across the whole GRAMA domain. The drainage vectors are plotted on a map of the major river drainages. The vectors show the downslope direction and the slope angle which is proportional to the vector length. A vector of length equal to half a grid cell is equal to a downslope angle of 1.2°. The computed drainage directions in most cases follow the river drainages, especially for grid cells with a substantial slope. In cells with fairly flat, drainage slopes, the 50-km averaging may be too coarse to resolve the river drainages. On the whole, however, the 50-km smoothing interval appears to provide sufficient resolution of major drainages to be used in regional-scale flow channeling calculations as described in Section 2.4.1.

Two terrain statistics in addition to the drainage direction are required in the calculation of Froude-number-modified winds. They are the terrain obstacle height and 'lower' terrain elevation. The obstacle height, h_o (m), for each grid cell is defined as:

$$h_o = 2 \times S_D \qquad (2\text{-}9)$$

where S_D is the standard deviation (m) of the terrain height for a grid cell. Limited analysis of terrain data has shown that Equation (2-9) will give an accurate measure of obstacle height for terrain obstacles with the same horizontal dimension as the smoothing interval. The computed obstacle heights, for obstacles with horizontal dimensions less than or greater than the smoothing interval, will be less than the actual obstacle height. Consequently it is important to choose a smoothing interval commensurate with the size of the dominant terrain features in the region to be modeled.

A companion statistic to the terrain obstacle height is the 'lower' terrain elevation, T_L (m MSL), defined as

$$T_L = T_A - S_D \qquad (2\text{-}10)$$

where T_A is the smoothed terrain elevation (m MSL). This 'lower' terrain elevation can be thought of as the terrain surface that the obstacles sit on.

2.4 Meteorological Data Processor

Several variables derived from meteorological data are required for the puff model operation. Certain of these are required for individual valleys but the majority are required over the entire modeling domain. The variables required over the modeling domain are specified hourly on a grid covering the domain, except the wind components, which are described analytically. These hourly values are determined from surface and upper air observations. Data from either routine reporting stations (e.g., NWS, FAA) or special observational programs can be used as input. The derived variables required

FIGURE 2-7

DRAINAGE DIRECTION VECTORS COMPUTED FROM 50- by 50-km AVERAGE TERRAIN STATISTICS OVERLAID ON A MAP OF THE MAJOR RIVER DRAINAGES IN THE GRAMA MODELING DOMAIN

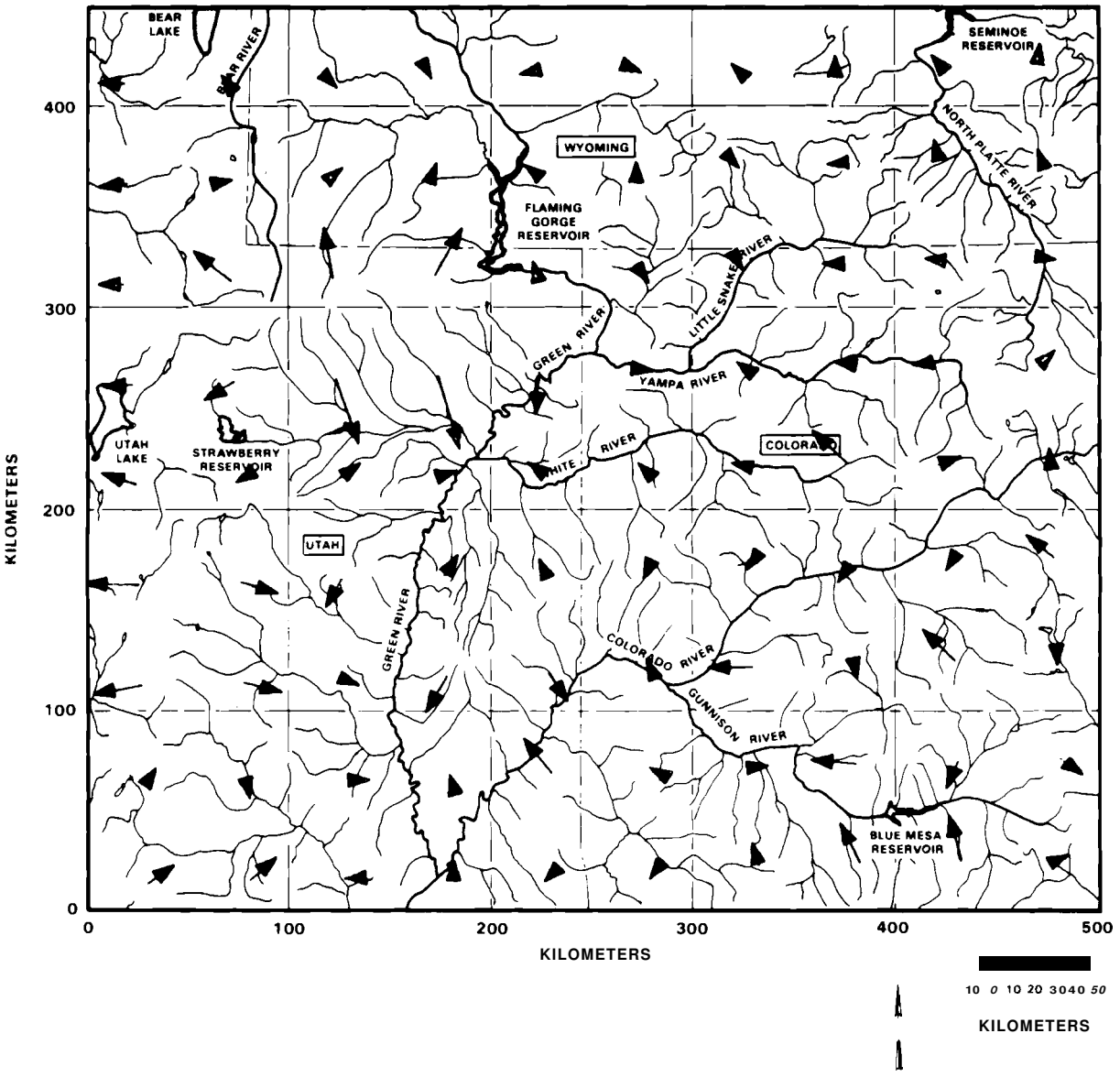

for each valley are specified hourly except the average down-valley wind speed. Single values of the down-valley wind speed for each valley for a simulation period are required. The derived variables from MET are

f_i, g_i = amplitude functions which describe the three components of winds
Z_ℓ = mixing height
S = Pasquill-Gifford stability class
u_* = friction velocity
w_* = convective velocity
L = Monin Obukov length
T = atmospheric temperature
P = atmospheric pressure
u_V = average down-valley wind speed
C_V = valley coupling coefficients for each valley segment.

The methods for determining the quantities listed above are given next.

2.4.1 Wind Field

The wind field is determined by applying a mass-conserving interpolation technique to upper-air and surface-wind observations. The technique was developed by Drake and Huang (1980) and has been described by Drake, Huang and Davis (1981).

The flow algorithm was formulated by transforming the continuity equation from Cartesian coordinates to terrain-following coordinates as shown in Figure 2-8. The computational domain is bounded above by a surface that may be an inversion surface, the tropopause or some other prescribed surface. The lower boundary is the terrain surface. Assuming an anelastic, dry adiabatic atmosphere, the transformed continuity equation reduces to an equation of the same form as the untransformed, incompressible, nonstratified continuity equation. The anelastic assumption eliminates the propagation of sound waves, which is a reasonable assumption for the mesoscale. This assumption simplifies the time-dependent term in the continuity equation. The dry adiabatic assumption simplifies the density-height relationship. The transformed continuity equation is

$$U_{,\alpha} + V_{,\beta} + W_{,\gamma} = 0 \qquad (2\text{-}11)$$

where the (,a) indicates the partial differentiation with respect to a. The terms in Equation (2-11) are defined as

$$U = \rho u h \qquad (2\text{-}12)$$

$$V = \frac{L_x}{L_y} \rho v h \qquad (2\text{-}13)$$

FIGURE 2-8

MASS-CONSISTENT FLOW MODEL COORDINATE SYSTEMS
(The Cartesian system is transformed into a unit cube using the equations shown)

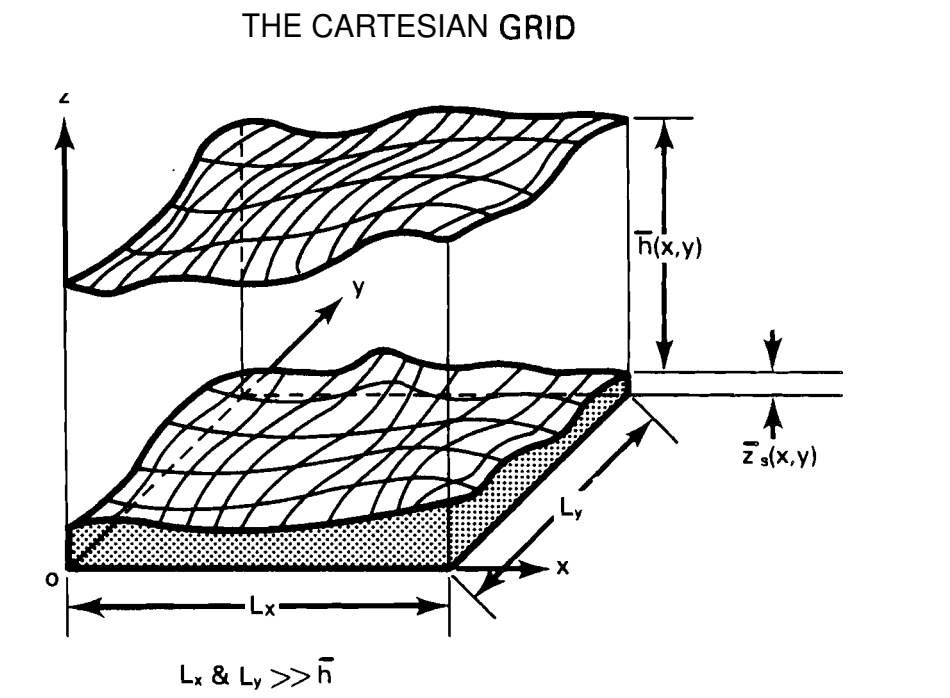

$$W = \rho L_x w - \rho Z_s - \rho \gamma h \tag{2-14}$$

where

u = X-component of velocity
v = Y-component of velocity
w = Z-component of velocity
ρ = density of air at height z
h = height of top sheet above terrain
L_x = domain length in X-direction
L_y = domain length in Y-direction
γ = transformed vertical coordinate

$$Z_s = Z_{s,\alpha}\, u + \frac{L_x}{L_y} Z_{s,\beta}\, v \tag{2-15}$$

$$h = h_{,\alpha}\, u + \frac{L_x}{L_y} h_{,\beta}\, v \tag{2-16}$$

$Z_{s,\alpha}$ = terrain slope with respect to a
$Z_{s,\beta}$ = terrain slope with respect to β
$h_{,\alpha}$ = slope of upper sheet with respect to a
$h_{,\beta}$ = slope of upper sheet with respect to β.

The description of the wind field is accomplished through a general solution of Equation (2-11) assuming there is no regional lifting or subsidence, and no veering or backing of the winds. The general solution is

$$U = \sum_{i=0}^{n} f_i(\gamma)\, B_i(\alpha,\beta) \tag{2-17}$$

$$V = \sum_{i=0}^{n} g_i(\gamma)\, C_i(\alpha,\beta) \tag{2-18}$$

and assuming $B_{i,\alpha}(\alpha,\beta) = -C_{i,\beta}(\alpha,\beta)$, then

$$W = \sum_{i=0}^{n} B_{i,\alpha}(\alpha,\beta) \int_0^{\gamma} [g_i(\gamma) - f_i(\gamma)]\, d\gamma \tag{2-19}$$

where $B_i(\alpha,\beta)$ and $C_i(\alpha,\beta)$ are 'basis' functions given in Table 2-4 and $f_i(y)$ and $g_i(\gamma)$ are 'amplitude' functions. The basis functions currently being used are polynomials, and they are a function only of the transformed orthogonal coordinates alpha and beta.

The mass-consistent wind field is computed at hourly intervals for a simulation. The first step in computing the wind fields is to define the number of computational surfaces. Up to nine surfaces can be specified, where the first surface is at the surface-wind measurement height (e.g., 3 m) and the last surface is the top boundary. Next the upper-air input wind observations are interpolated to each computational surface ('gamma' surface - gamma coordinate in Figure 2-8) at the location of each upper-air station. These input upper-air observations at each gamma level are then spatially interpolated using a $1/r^2$ weighting to each surface weather station, with the ground-level interpolated winds being replaced by the surface-wind observations. The upper-air observations are also spatially interpolated to user-specified points on the boundary of the domain to ensure that the computed wind fields are realistic at the boundaries. Given these input wind 'soundings', and computing the basis functions for each station location knowing alpha and beta, the amplitude functions (or coefficients to each basis function term) for each gamma surface can be computed from Equations (2-17) and (2-18) using a least squares solution technique. The number of polynomial terms used in the solution is 10, corresponding to a third degree polynomial. Now knowing the amplitude functions for each gamma surface, U, V, and W can be computed anywhere in the domain by simply computing the basis functions at the desired point and using Equations (2-17), (2-18), and (2-19). Finally u, v, and w, the velocity components, can be computed from Equations (2-12) through (2-16).

Computer core requirements are reduced significantly by representing the wind field as a set of amplitude functions and not as a gridded wind field. For a 50 by 50 grid, more than a 250-fold decrease in computer core is required to represent one surface of the wind field as 30 amplitude terms (10 polynomial terms times 3 velocity components) rather than 7500 grid values.

When the spatial resolution of the input winds is insufficient to show flow channeling around major terrain features, then a Froude number modification to the flow field can be employed. The Froude number adjustment is based on the concept of a dividing streamline height, H_c, defined as (Snyder 1980)

$$\frac{1}{2} \rho U_c^2 = g \int_{H_c}^{h_o} (h_o - z)(-\frac{\partial \rho}{\partial z}) \, dz \qquad (2\text{-}20)$$

where

ρ = density
U_c = wind speed evaluated at H_c
g = acceleration due to gravity
h_o = height of obstacle
$\partial\rho/\partial z$ = local density gradient.

H_c is the height at which the fluid has just enough kinetic energy to ascend the obstacle. Fluid parcels below H_c will either stagnate or go around the

TABLE 2-4

POLYNOMIAL BASIS FUNCTIONS USED IN MELSAR

i	B_i	C_i	$B_{i,\alpha}$
0	1	-1	0
1	α	$-\beta$	1
2	β	$-\alpha$	0
3	α^2	$-2\alpha\beta$	2α
4	$\alpha\beta$	$-1/2\beta^2$	β
5	β^2	$-\alpha^2$	0
6	α^3	$-3\alpha^2\beta$	$3\alpha^2$
7	$\alpha^2\beta$	$-\alpha\beta^2$	$2\alpha\beta$
8	$\alpha\beta^2$	$-1/3\beta^3$	β^2
9	β^3	$-\alpha^3$	0
10	α^4	$-4\alpha^3\beta$	$4\alpha^3$
11	$\alpha^3\beta$	$-3/2\alpha^2\beta^2$	$3\alpha^2\beta$
12	$\alpha^2\beta^2$	$-2/3\alpha\beta^3$	$2\alpha\beta^2$
13	$\alpha\beta^3$	$-1/4\beta^4$	β^3
14	β^4	$-\alpha^4$	0
15	α^5	$-5\alpha^4\beta$	$5\alpha^4$
16	$\alpha^4\beta$	$-2\alpha^3\beta^2$	$4\alpha^3\beta$
17	$\alpha^3\beta^2$	$-\alpha^2\beta^3$	$3\alpha^2\beta^2$
18	$\alpha^2\beta^3$	$-1/2\alpha\beta^4$	$2\alpha\beta^3$
19	$\alpha\beta^4$	$-1/5\beta^5$	β^4
20	β^5	$-\alpha^5$	0

obstacle and fluid parcels above H_c will go over the obstacle. To simplify, we assume a constant wind and temperature gradient, which reduces Equation (2-20) to

$$H_c = h_o (1 - Fr) \tag{2-21}$$

where Fr is the obstacle Froude number. It is determined by

$$Fr = \frac{U_A}{h_o \sqrt{\frac{g}{\bar{T}} \frac{\partial \Theta}{\partial z}}}, \quad \frac{\partial \Theta}{\partial z} > 0 \tag{2-22}$$

where

U_A = wind speed of flow approaching obstacle
$\bar{T}$ = average temperature through the height of the obstacle
$\partial\Theta/\partial z$ = potential temperature gradient through the height of the obstacle.

For $Fr \to 0$, $H_c \to h_o$, implying that most of the flow goes around the obstacle. When $Fr \to 1$, $H_c \to 0$, implying that most of the flow goes over the obstacle.

Equations (2-21) and (2-22) form the basis for the treatment of flow channeling around major terrain obstacles in MELSAR. The approach is first to specify a 10 by 10 grid over the domain and compute the 'lower' average terrain height, the obstacle height, and the drainage direction for each grid element as described in Section 2.3. Next the winds for each hour are computed at the center of each grid element for all gamma surfaces. These winds are computed using the amplitude functions generated from the input wind observations. The Froude number is then computed, using Equation (2-22), for each grid element. U_A is determined from the computed winds, and $d\theta/dz$ and $\bar{T}$ are determined from input temperature soundings and surface observations. Knowing the Froude number for each grid element, the computed winds are adjusted toward the terrain tangent direction below the dividing streamline height, H_c. Above H_c, no adjustments to the wind direction are made. After the computed winds at each grid element have been adjusted, then these adjusted soundings, in addition to the original input wind soundings, are used in conjunction with Equations (2-17) and (2-18) to compute new amplitude functions, which then define the complete wind field.

The method of calculating $d\theta/dz$ at a grid point for a given hour epends on whether it is daytime or nighttime. The daytime $d\theta/dz$ calculation is a three step process. First, the potential temperature lapse rate is calculated at a weather station location through the obstacle depth at the same MSL elevation as the obstacle. Second, the $d\theta/dz$ is computed at the weather station through the obstacle depth at the MSL elevation of the weather station. The station $d\theta/dz$ corresponding to the given obstacle (for a particular grid point) is the average of the two above calculations of

$d\theta/dz$. Calculating the $d\theta/dz$ for the obstacle as the average of the $d\theta/dz$ at the obstacle height on the sounding plus the $d\theta/dz$ at the station elevation is a means of accounting for surface effects in addition to differences of $d\theta/dz$ with elevation. Third, this obstacle $d\theta/dz$ computed at each weather station is spatially interpolated to the grid point using a $1/r^2$ weighting resulting in a $d\theta/dz$ at a grid point corresponding to the grid point obstacle height.

Typically, only twice daily measures of temperature soundings are available at a station. Consequently, the $d\theta/dz$ at a station must be interpolated in time. This is accomplished using hourly surface potential temperature observations in conjunction with the morning potential temperature sounding. The intersection of the hourly surface potential temperature observation with the morning sounding modifies the lower portion of the sounding to a constant potential temperature. Therefore, a new potential temperature 'sounding' is determined each hour using this technique, These 'soundings' are forced to converge to the afternoon sounding. This approach of 'marching' up the morning sounding using surface potential temperature observations is very similar to that given by Benkley and Schulman (1979) for determining hourly convective mixing heights. Cold or warm air advection is accounted for by looking at the potential temperature difference between the morning and afternoon sounding in the free stream portions of the soundings. The surface potential temperatures are adjusted to account for this warm or cold air advection (Benkley and Schulman 1979).

The nighttime $d\theta/dz$ for an obstacle height at a grid point is determined in the same fashion as the daytime procedure except the $d\theta/dz$ for a given hour is determined by interpolating between the afternoon potential temperature sounding and the next day's morning sounding. The potential temperature sounding is interpolated in time and weighted according to the change in surface potential temperature.

The average temperature, T, through the height of an obstacle is determined for any hour in the same way as the nighttime $d\theta/dz$. But instead of using upper-air and surface potential temperatures, upper-air and surface temperature observations are used. Also the temperature is averaged through the obstacle height rather than determining a lapse rate.

2.4.2 Mixing Heights

Gridded mixing heights are computed for each hour using surface weather observations and upper-air observations. The hourly mixing height at a grid point is the maximum of a convective mixing height or a mechanical mixing height. The convective mixing height is set equal to zero during the night. The mechanical mixing height is computed as 53×10^{-4} Ug, where Ug is the free stream wind speed (m/s). This forniulation for mechanical mixing height is given by Benkley and Bass (1979).

The convective mixing height is computed using a technique described by Benkley and Schulman (1979). The hourly mixing height at a weather station

is estimated by determining the height of the intersection of the surface potential temperature with the morning potential temperature sounding. The technique accounts for warm or cold air advection into the region by adjusting the hourly surface potential temperature values according to an advection rate. The advection rate is determined from the difference in potential temperature between the afternoon and morning sounding at a height above the convective mixing height. The technique also makes adjustments for differences between the temperature at the surface station and the surface temperature at the radiosonde station, or makes adjustments if the minimum surface temperature occurs before the morning sounding. This is accomplished by adjusting the morning sounding to fit the minimum surface temperature observation.

Once the mixing height is computed at each weather station, the mixing height at a grid point is determined by an inverse-distance-square weighting of the station mixing heights to the grid points.

2.4.3 Stability Classification

The Pasquill-Gifford-Turner (PGT) stability classes are determined at a gridpoint for each hour using the approach given by Benkley and Bass (1979). Knowing the wind speed at the surface and the convective mixing height, the PGT stability class is determined from Table 2-5.

TABLE 2-5

DETERMINATION OF PASQUILL-GIFFORD-TURNER STABILITY CLASSES

Wind Speed at 10 m	Day			Night
	Hc>1000 m	500<Hc<1000	Hc<500	
<2 m/s	A	A	B	F
2-3	A	B	C	E
3-5	B	B	C	D
5-6	C	C	D	D
>6	C	D	D	D

2.4.4 Valley Coupling Coefficient

It is well known that local wind circulations regularly form within areas of complex terrain. At nighttime, for example, downslope and down-

valley flows are the rule in valley terrain, caused by the cooling and subsequent drainage of cold air into low-lying areas. Deep temperature inversions can form in valleys during the night as cold air builds up in the valley bottoms. In recent years an improved understanding has been gained of the physical processes through which these nighttime valley inversions are destroyed following sunrise (Whiteman 1980, 1982; Brehm and Freytag 1982; Vergeiner 1982; Bader and McKee 1983). The destruction of the nighttime inversions in valleys has important implications for air pollutant transport out of valleys into regional flows. It is during the inversion breakup period that air pollutants trapped within the valley at night are carried from the valley into the prevailing regional-scale flows above the valley and are dispersed in the regional wind field.

Because valleys are sub-grid scale in MELSAR, a parameterization of valley flow interaction with above-ridgetop flows is used. Each valley with pollutant sources is treated as a segmented line source as described in Section 2.5.7. This is accomplished by dividing the valley into a number of line segments and releasing trapped pollutants from the valley to the regional flow at a rate determined by the temperature inversion breakup rate. This rate of release of pollutants from a valley segment is defined as the 'coupling' coefficient and is computed hourly. A coupling coefficient of zero means no pollutants are venting from the valley segment (valley 'decoupled' from regional flows), and a coefficient of one means all pollutants have vented from the valley (valley 'coupled' with regional flow). A fraction between zero and one is the portion of total pollutant material, trapped in a valley segment, that is vented out during a time step. The fractions during a coupling period add to one. Advection of contaminants from the valley in up-valley (or down-valley) flows is not considered in MELSAR because of the complexity of incorporating this process (convective coupling or advection) into the model. It is uncertain what the dominant process for advection of contaminants from a valley is. This will require further research.

Whether a valley is coupled or decoupled from the regional flows is determined from the morning and afternoon temperature soundings at the nearest upper air station. If the maximum temperature in the lowest 500 m of the morning sounding is >1°C warmer than the sounding surface temperature, then the valley atmosphere is assumed to be decoupled from the regional flows during the morning. Otherwise the valley atmosphere would be coupled with the regional flows. A valley atmosphere is assumed to be coupled in the afternoon if the temperature lapse rate between 500 m above ground level (AGL) and 75 m AGL is ≤-4.9°C/km, otherwise the valley atmosphere would be decoupled in the afternoon. The lower elevation of 75 m is above any surface-based temperature inversions that may be forming in the afternoon (especially during the winter). These criteria for determining whether a valley atmosphere is coupled or decoupled from the regional flow are highly simplified, but correspond with observations made in valley atmospheres in western Colorado by Whiteman (1980). He compared the inversion characteristics of deep valleys in western Colorado with radiosonde observations made at Grand Junction, Colorado. Using the morning and afternoon coupling (1) and decoupling (0) indicators from the nearest upper-air station, the hourly coupling coefficient for a valley segment can be

determined from Table 2-6. The calculation of the coupling coefficient during the period of sunrise to the time of inversion breakup is given next (Period SR_1+1→BU during DAY in Table 2-6).

The basic hypotheses and equations for specifying the time-history of valley-inversion destruction (flow coupling) are those developed by Whiternan and McKee (1982) and used by Whiteman and Allwine (1985) in the local-scale model VALMET.

Whiteman and McKee's model is a 'bulk' thermodynamic model in that it does not differentiate between sensible heat flux over different valley

TABLE 2-6

VALLEY SEGMENT COUPLING COEFFICIENT FROM SUNRISE ON DAY 1 (SR_1) TO SUNRISE ON DAY 2 (SR_2) DETERMINED FROM NEAREST WEATHER STATION COUPLING COEFFICIENT

DAY (SR_1+1→SS)

Station Coefficient		Time Period	
SR_1	SS[a]	SR_1+1→BU[b]	BU+1→SS
0	0 or 1	c	1.0
1	0 or 1	1.0	1.0

NIGHT (SS+1→SR_2)

Station Coefficient		Time Period			
SS	SR_2	SS+1→SS+2	SS+3→MD[d]-2	MD-1→MD+1	MD+2→SR_2
0	0	0.0	0.0	0.0	0.0
0	1	0.0	0.0	0.333	1.0
1	1	1.0	1.0	1.0	1.0
1	0	1.0	0.0	0.0	0.0

[a] SS is time of sunset on Day 1.
[b] BU is time of valley inversion breakup.
[c] Fraction (between 0.0 to 1.0) of valley inversion destroyed for each hour. The sum of the fractions is equal to 1.0.
[d] MD is (SR_2-SS+1)/2 where SR_2=SR_1+24.

surfaces. The heat flux that drives the valley-inversion destruction is partitioned or distributed in a fundamentally different way from that for an inversion over homogeneous terrain. There, the sensible heat flux destroys the inversion by driving an upward growth from the ground of a convective boundary layer, which warms the inversion air mass from below until the temperature deficit is overcome and the inversion is destroyed. In contrast, in a valley the upward heat flux over valley surfaces develops a convective boundary layer, but also, as a result of sensible heat flux convergence over the slopes, causes warmed air parcels to flow up the slopes in an upslope flow that develops within the convective boundary layer (CBL). These upslope flows remove mass from the base of the temperature inversion in the shallow slope flows, and through mass continuity, result in a general subsiding motion over the valley center. The atmospheric energy budget approach used by Whiteman and McKee is capable of partitioning energy between these two different processes to produce inversion destruction solely by CBL growth, solely by inversion descent (assuming a nongrowing CBL is present initially in a simulation), or by a combination of the two processes. The partitioning is controlled by a single parameter, k, defined as the fraction of sensible heat flux going to CBL growth. The remaining fraction, 1 - k, is assumed to be responsible for mass transport up the CBL, which results in inversion descent. A default value for k of 0.15 is used in MELSAR.

The thermodynamic model is composed of two coupled equations. The first equation is a prediction equation for CBL height where, in accordance with the bulk nature of the model, the CBL depth H is assumed not to differ over the valley floor and sidewalls. The first equation is

$$H_{j+1} = H_j + \Delta H_j \tag{2-23}$$

where

$$\Delta H_j = \frac{\theta}{T} \frac{k}{\rho c_p} \frac{w + H_j C}{w + \frac{H_j C}{2}} \frac{A_o A_l}{\gamma H_j} \left(\sin \frac{\pi}{\tau} (t - t_i)\right) \Delta t \tag{2-24}$$

Note that a non-zero initial CBL height is necessary to make this prognostic numerical equation tractable. In the model, this requirement is met by using an initial CBL height at sunrise of 25 m. The second equation, describing the inversion top height h is:

$$h_{j+1} = h_j + \Delta h_j \tag{2-25}$$

where

$$\Delta h_j = -\frac{\theta}{T}\frac{1}{\rho c_p}\frac{[w+h_jC-k(w+H_jC)]A_oA_1\sin\frac{\pi}{\tau}(t-t_i)-\rho c_p\frac{T}{p\theta}\frac{\beta}{2}(h_i-h_j)(w+\frac{h_i+h_j}{2}C)}{h_j\gamma(w+\frac{h_j}{2}C)-\frac{\beta}{2}(t-t_i)(w+h_jC)}\Delta t \qquad (2\text{-}26)$$

$$\frac{\theta}{T} = \left(\frac{1000}{P}\right)^{0.286}$$

P = atmospheric pressure
ρ = air density
w = valley floor width
C_p = specific heat of air at constant pressure
β = warm air advection rate above valley
$C = \cot\alpha_1 + \cot\alpha_2$
α_1 = inclination angle of right sidewall
α_2 = inclination angle of left sidewall
A_o = fraction of extraterrestrial solar flux converted to sensible heat flux, $0 \leq A_o \leq 1$
A_1 = extraterrestrial solar flux on horizontal surface at solar noon
γ = vertical potential temperature gradient
τ = length of daylight period
Δt = modeling time step
$t_i = 0$
$t = (j + 1)\,\Delta t + t_i$
j = 0, 1, 2, 3, ..., n (time steps).

An idealized valley cross-section showing some of the terms used in Equations (2-24) and (2-26) is given in Figure 2-9. The terms in the numerator and denorninator of Equation (2-26) involving the warming coefficient for the air above the inversion, $\beta(^{\circ}Ks^{-1})$, allow the model to incorporate the retarding effect on temperature inversion breakup caused by warm air advection above the valley temperature inversion. Extra energy is required to destroy the valley temperature inversion if this warming occurs during the temperature inversion breakup period because the inversion cannot be broken until the entire valley atmosphere is warmed to the temperature of the air above the valley.

FIGURE 2-9

IDEALIZED VALLEY CROSS SECTION

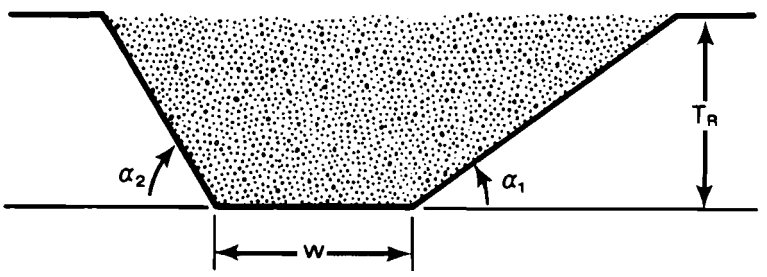

The numerical simulation using these coupled equations proceeds with discrete time steps and is complete when the inversion is destroyed at the first time step, n, at which the CBL height becomes greater than the inversion top height, such that

$$H_n \geq h_n \tag{2-27}$$

The fraction of total pollutant material, Δf, emitted from each valley segment per time step after sunrise is determined using Equations (2-23) through (2-26) in conjunction with the following equation

$$\Delta f_{j+1} = \frac{V_j - V_{j+1}}{V_o} \tag{2-28}$$

where

$V_o = (h_o - H_o)w + C(h_o - H_o)/2$, is the volume of air within valley inversion per unit length of segment at sunrise
h_o = inversion height at sunrise (assumed to be at ridge tops)
H_o = CBL height at sunrise (25 m)
$V_{j+1} = (h_{j+1} - H_{j+1})\, w + C(h_{j+1} - H_{j+1})/2$, is the volume of air within the stable core after $j+1$ time steps after sunrise
$j = 0, 1, 2, 3, \ldots, n$.

At sunrise f is equal to zero, and when the condition of Equation (2-27) is satisfied f is equal to one, also

$$\sum_{j=o}^{n} (\Delta f_{j+1}) = 1.0 \tag{2-29}$$

The hourly coupling coefficient for a valley segment during the morning inversion breakup period is Δf_j.

The warm air advection rate at the top of the valley, and the pressure and average air density through the valley atmosphere used in Equations (2-24) and (2-26) are computed using the morning and afternoon potential temperature soundings of the nearest upper-air station. The fraction of extraterrestrial solar flux converted to sensible heat flux, A_o, is also computed from the two soundings. The warm air advection rate, β, is determined from the difference in temperature, at the elevation of the valley top, between the morning and afternoon sounding divided by the time between the two soundings. The average pressure and density are determined from the morning sounding by averaging the sounding through the valley depth. The quantities are averaged through a layer on the sounding corresponding to the actual MSL elevations of the valley.

The potential temperature lapse rate, γ, in the valley is computed from the lapse rate of the morning sounding, γ_s, through the layer from ground-level up to 200 m AGL. Then the lapse rate of the valley is computed as

$$\gamma = \frac{\gamma_s}{0.04}\gamma_{max} \quad \gamma \leq \gamma_{max} \tag{2-30}$$

where 0.04 (°K/m) is the maximum, average potential temperature lapse rate expected at the upper-air station and γ_{max} (°K/m) is the maximum potential temperature lapse rate expected in deep valleys in western Colorado (typically 0.03 °K/m). The maximum values of 0.04 and 0.03 are from analyses performed by Whiteman (1980) on data he collected in western Colorado valleys and radiosonde data from Grand Junction, Colorado.

The fraction of extraterrestrial solar flux converted to sensible heat flux, A_o, is computed as the ratio of the energy required to warm the air between the morning and afternoon soundings, E_s, divided by the total incoming solar energy, E_R, during the same period. The energy to warm the air is computed from the First Law of Thermodynamics:

$$E_s = 100\,\frac{Cp}{R_a}\int_o^{Z_m}\frac{p}{\theta}\,\Delta\theta\,dZ \tag{2-31}$$

where

Cp = specific heat at constant pressure (1005 J/kg -°K)
R_a = gas constant (287 J/kg -°K)
p = average pressure between soundings (mb)
θ = average potential temperature between soundings (°K)
$\Delta\theta$ = difference in potential temperature between soundings (°K)
Z_m = height above convective mixing height (m AGL).

The factor of 100 in Equation (2-31) results from unit conversions.

Warm or cold air advection is accounted for by translating the afternoon sounding such that the upper portions of the soundings (above convective boundary layer) match.

The total incoming solar energy, E_R, is:

$$E_R = \int_{t_M}^{t_A} R\,dt \tag{2-32}$$

$$R = S_o f_e B \sin v \tag{2-33}$$

where

R = extraterrestrial solar flux at time t (W/m^2)
t_A = time of afternoon sounding (MST)
t_M = time of morning sounding (MST)
S_o = 1367 (W/m^2), solar constant
f_e = factor to account for elliptical orbit of the earth
B = radiation reduction factor caused by clouds
v = solar elevation angle.

The radiation reduction factors used in MELSAR are given in Table 2-7. These are from Scire et al. (1984) as adapted from Maul (1980). The sine of the solar elevation angle is determined from the following set of equations as given by Scire et al. (1984):

TABLE 2-7

SOLAR RADIATION REDUCTION FACTOR B

Cloud Cover (tenths)	B
0	1.00
1	0.91
2	0.84
3	0.79
4	0.75
5	0.72
6	0.68
7	0.62
8	0.53
9	0.41
10	0.23

$$\sin v = \sin \phi \sin K_D + \cos \phi \cos K_D \cos H_A \quad (2\text{-}34)$$

$$H_A = (\pi/12)\ (\tau - E_m) - \lambda \quad (2\text{-}35)$$

$$E_m = 12. + 0.12357 \sin(D) - 0.004289 \cos(D) + 0.153809 \sin(2D) + 0.060783 \cos(2D) \quad (2\text{-}36)$$

$$D = (d-1)(360./365.242)(\pi/180) \quad (2\text{-}37)$$

$$K_D = \sin^{-1}(0.39784989 \sin(n\,\sigma_A/180)) \quad (2\text{-}38)$$

$$\sigma_A = 279.9348 + D(180/\pi) + 1.914827 \sin(D) - 0.079525 \cos(D) + 0.019938 \sin(2D) - 0.00162 \cos(2D) \quad (2\text{-}39)$$

where

ϕ = the latitude (radians)
λ = is the longitude (radians)
d = the Julian day
τ = the time of day in GMT (hours).

The factor, f_e, to account for the fact that the earth-sun distance varies during the year as the earth travels in an elliptical orbit about the sun is computed as

$$f_e = (1 - e \cos \omega d)^{-2} \quad (2\text{-}40)$$

where

$\omega = 2\pi/365$
e = 0.0167, eccentricity of earth's orbit.

The time of sunrise (used to define the morning sounding) in local standard time is

$$t_{SR} = t_{NOON} - \cos^{-1}(-\tan\phi \tan K_D)\left(\frac{180}{15\pi}\right) \quad (2\text{-}41)$$

$$t_{NOON} = \lambda/15 + E_m - T_B \quad (2\text{-}42)$$

where T_B is the correction from Greenwich Mean Time (GMT) to the base time zone. The values of T_B are 5 (Eastern), 6 (Central), 7 (Mountain), and 8 (Pacific).

The time of sunset (used to define the afternoon sounding) in local standard time is

$$t_{SS} = t_{NOON} + \cos^{-1}(-\tan\phi \tan K_D)\left(\frac{180}{15\pi}\right) \quad (2\text{-}43)$$

The solar flux at solar noon, A_1, used in Equations (2-24) and (2-26) is computed as

$$A_1 = S_o f_e \sin \nu_N \quad (2\text{-}44)$$

where ν_N is the solar elevation angle at solar noon, which is computed using Equations (2-34) through (2-39) at the solar noon time of $(t_{SR}+t_{SS})/2$.

Currently, an approximation to the hourly incoming solar radiation, which does not account for solar reduction caused by clouds, is used in Equations (2-24) and (2-26). This is a sine approximation to the total incoming extraterrestrial solar radiation. The term is $A_1 \sin(\tau/(t_{SS}-t_{SR})(\tau-t_{SR}))$. A future modification to MELSAR would be to replace this term by Equation (2-33) to account for reduction resulting from clouds.

2.4.5 Friction Velocity

The surface friction velocity, u_* (m/s), is computed on a grid for each hour using surface weather observations. The approach used is that given by Scire et al. (1984) with the exception that the sensible heat flux, H, computed in Equation (2-49) uses A_o and R as given in Section 2.4.4. The surface friction velocity can be estimated during unstable conditions by the method described by Wang and Chen (1980):

$$u_* = \tilde{u}_* \{1 + a \ln [1 + b\, Q_o/\tilde{Q}_o]\} \quad (2\text{-}45)$$

$$\tilde{u}_* = \frac{k u_m}{\ln (z_m/z_o)} \quad (2\text{-}46)$$

$$z_m = z_{ms} - 4\, z_o \quad (2\text{-}47)$$

$$Q_o = H/(\rho\, c_p) \quad (2\text{-}48)$$

$$H = A_o R + H_o \tag{2-49}$$

$$H_o = 2.4\ C_o - 25.5 \tag{2-50}$$

$$\tilde{Q}_o = \frac{\theta\ \tilde{u}_*^3}{k\ g\ z_m} \tag{2-51}$$

$$a = \begin{cases} 0.128 + 0.005\ \ln\ (z_o/z_m) & z_o/z_m \leq 0.01 \\ 0.107 & z_o/z_m > 0.01 \end{cases} \tag{2-52}$$

$$b = 1.95 + 32.6\ (z_o/z_m)^{0.45} \tag{2-53}$$

where

k = the von Karman constant (~0.4)
c_p = the specific heat of air at constant pressure (996 $m^2/(s^2\ deg)$)
u_m = the wind speed (m/s) measured at height z_{ms} (m)
z_o = the surface roughness (m)
ρ = the density of air (kg/m^4)
g = acceleration due to gravity (9.81 m/s^2)
θ = surface potential temperature (°K)
R = incoming solar radiation from Equation (2-33) (W/m^2)
A_o = fraction of R converted to sensible heat flux (from Section 2.4.4)
C_o = opaque cloud cover (tenths).

During stable conditions, u_* is determined by the following method (Venkatram 1980a):

$$u_* = \frac{C_{DN}\ u_m}{2}\ [1 + C^{0.5}] \tag{2-54}$$

$$C_{DN} = \frac{k}{\ln\ (z_m/z_o)} \tag{2-55}$$

$$C = 1 - \frac{4\ u_o^2}{C_{DN} u_m^2} \qquad C \geq 0 \tag{2-56}$$

$$u_o^2 = \frac{\gamma z_m}{k A} \qquad (2\text{-}57)$$

where γ and A are constants with values of 4.7 and 1100, respectively, and C_{DN} is the neutral drag coefficient.

The surface roughness at a grid point is determined from gridded land-use categories (Scire et al. 1984) using Table 2-8.

TABLE 2-8

SURFACE ROUGHNESS AS A FUNCTION OF LAND USE TYPE

Category	Land Use Type	z_o (m)
1	Cropland and pasture	0.20
2	Cropland, woodland and grazing land	0.30
3	Irrigated crops	0.05
4	Grazed forest and woodland	0.90
5	Ungrazed forest and woodland	1.00
6	Subhumid grassland and semiarid grazing land	0.10
7	Open woodland grazed	0.20
8	Desert shrubland	0.30
9	Swamp	0.20
10	Marshland	0.50
11	Metropolitan city	1.00
12	Lake or ocean	10^{-4}

From: Shieh, Wesely and Hicks (1979).

2.4.6 Convective Velocity

The convective velocity scale, w_* (m/s), is computed on a grid for each hour using surface weather observations. The approach used is that given by Scire et al. (1984). During convective conditions, w_* is calculated from its definition:

$$w_* = \left(\frac{g}{T_o} Q_o Z_i \right)^{1/3} \qquad (2\text{-}58)$$

where T_o is the surface air temperature (OK), Q_o is from Equation (2-48) and Z_i is the mixing height from Section 2.4.2. For Q_o less than zero, w_* is equal to zero.

2.4.7 Monin-Obukov Length

The Monin-Obukov length, L (m), is computed on a grid for each hour using surface weather observations. For unstable conditions it is computed from its definition:

$$L \equiv - \frac{u_*^3 T_o}{g k Q_o} \qquad (2\text{-}59)$$

where the terms are defined in earlier sections. During stable conditions, L is given by Venkatram (1980b) as

$$L = 1100 u_*^2 \qquad (2\text{-}60)$$

2.4.8 Temperature

The surface temperature, T_o (°K), is computed on a grid for each hour using surface observations and seasonal temperature lapse rates from analysis of climatological data in western Colorado (PEDCO 1981). PEDCO analyzed up to 40 years of surface temperature observations for nine stations in western Colorado. They determined the average temperature change with elevation for each month of the year. These monthly temperature lapse rates were plotted versus Julian day and the points connected with straight lines. The slopes and intercepts of these lines are given in Table 2-9. The hourly temperature observation at each surface station is interpolated to each grid point using an inverse-distance-squared weighting factor. The

interpolated temperature from each weather station is corrected for altitude differences between the weather station and the grid point. The corrected temperature is

$$T_G = T_S + (E_G - E_S) * LR/548.6 \qquad (2\text{-}61)$$

where

T_G = temperature at grid point (°K)
T_S = temperature at weather station (°K)
E_G = elevation at grid point (m MSL)
E_S = elevation of weather station (m MSL)
LR = correction lapse rate (°F/1000 ft).

The lapse rate, LR, to correct surface temperature for variation in altitude is computed by

$$LR = md + b \qquad (2\text{-}62)$$

where d is Julian day, and m and b are given in Table 2-9.

2.4.9 Pressure

The surface pressure, P_o (mb), is computed on a grid for each hour using a density relationship derived by Drake, Huang and Davis (1981) assuming dry adiabatic conditions, and the gridded temperature values from Section 2.4.8:

$$P_o = R_u T_o \bar{\rho}(o) \left[1 - \frac{E_G}{H_a}\right]^{5/2} \qquad (2\text{-}63)$$

where

R_u = universal gas constant (2.869 $(m^3\text{-mb})/(kg\text{-}°K)$)
T_o = surface temperature at grid point (°K)
E_G = elevation of grid point (m MSL)
$\bar{\rho}(o)$ = $353.1/\theta$, air density at sea level (kg/m^3)
H_a = $C_p\theta/g$ = 102.4 θ, height of the adiabatic atmosphere (m).

The value, θ, in the definition for H_a and $\bar{\rho}(o)$ above, is the average sea-level potential temperature for an hour from all surface weather stations. It is determined by solving Equation (2-63) for θ for each surface station.

TABLE 2-9

SLOPE AND INTERCEPT OF TEMPERATURE LAPSE RATE CORRECTION BY JULIAN DAY

Julian Day (d)	Slope (m)	Intercept (b)
$1 \leq d \leq 16$	-0.0152	-1.6950
$16 < d \leq 75$	-0.0607	-0.9592
$75 < d \leq 105$	0.0093	-6.2100
$105 < d \leq 136$	-0.0552	0.5619
$136 < d \leq 166$	0.0180	-9.3880
$166 < d \leq 197$	-0.0135	-4.1510
$197 < d \leq 228$	0.0116	-9.1077
$228 < d \leq 258$	0.0037	-7.2960
$258 < d \leq 289$	0.0832	-27.8223
$289 < d \leq 319$	0.0500	-18.2200
$319 < d \leq 350$	0.0261	-10.6052
$350 < d \leq 366$	-0.0152	3.8600

2.5 Puff Model

The puff model is configured to treat the transport and diffusion of a nondepositing inert pollutant from point and line sources in complex terrain situations. The model is intended for use at source-to-receptor transport distances on the order of fifty to hundreds of kilometers. The model can be operated at shorter source-receptor distances (ten to tens of kilometers) provided the proper input data are available and the model is scaled accordingly. The results from the model are hourly ground-level pollutant concentrations to be used for computing short-term averages for comparison with standards.

This section contains the technical description of the puff model divided into ten major topic areas:

1. Gaussian puff equation

2. plume-rise equations used for buoyant plumes from point sources

3. receptor layout

4. source representation

5. method for handling puffs emitted above the top of the mixed layer and puff 'housekeeping' techniques

6. method for transporting puffs

7. techniques used to compute ground-level concentrations from each puff

8. treatment of nighttime drainage flows in valleys and ventilation of pollutants from valleys during the morning transition period

9. equations for interpolating gridded quantities (e.g., mixing heights) to a specific location

10. the formulation of the dispersion coefficients used in the Gaussian puff equation.

2.5.1 Gaussian Puff Equation

A continuous plume can be represented by a series of overlapping puffs. In fact, the Gaussian plume equation is derived by integrating the Gaussian formula for an instantaneous point source (i.e., puff) from $t = 0 \rightarrow \infty$ (Slade 1968). The plume is regarded as resulting from the addition of an infinite number of overlapping averaged puffs, carried along the X-axis by the mean wind. The Gaussian formula for an instantaneous point source is a fundamental solution of the Fickian differential equation for diffusion (Slade 1968).

The pollutant concentration distribution within a puff is described in a Lagrangian (moving) coordinate system. The origin of this coordinate system in a fixed Cartesian coordinate system is the point where the puff center-of-mass projected vertically down intersects the terrain surface. A puff traveling from time t to time $t + \Delta t$ imbedded in the fixed coordinate system X-Y-Z is shown in Figure 2-10. For the purpose of illustration, the terrain in Figure 2-10 is flat at a height of $Z = 0$. The X' axis is oriented along the plume axis in the downwind direction, and the Z' axis is perpendicular to the terrain along the plume path and vertical in the cross-path direction. In the case of flat terrain, Z' is parallel to Z. This orientation of X'-Y'-Z' will be discussed later. The pollutant concentration at some receptor R at ground level is computed using the Gaussian puff equation in the X'-Y'-Z' coordinate system. The basic equation for describing the ground-level pollutant concentration for a single puff is

$$x_i(t) = \frac{M(t)}{2\pi\sigma_Y^2(t)} f_h(t)\, f_v(t)$$

$$f_h(t) = \exp\left[-\frac{r^2}{2\sigma_y^2(t)}\right] \qquad (2\text{-}64)$$

$$f_v(t) = \frac{2}{\sqrt{2\pi}\,\sigma_z(t)} F_1$$

where

$x_i(t)$ = average ground-level pollutant concentration over the modeling time step for the i^{th} puff ($\mu g/m^3$)
$M(t)$ = mass of pollutant within puff (μg)
$\sigma_y(t)$ = horizontal diffusion coefficient for the modeling time step (m)
t = total travel time of puff (s)
r = perpendicular distance from puff center axis (Z') to receptor (m)
$\sigma_z(t)$ = vertical diffusion coefficient for the modeling time step (m)
F_1 = multiple reflection terms.

The average concentration over the model time step at any ground-level receptor is determined by simply summing the contribution of all puffs to that receptor. The concentration at any receptor is

$$x_R = \sum_{i=1}^{k} x_i \qquad (2\text{-}65)$$

where

x_R = average ground-level concentration for the modeling time step at a fixed receptor ($\mu g/m^3$)
k = number of puffs impacting the receptor.

The ground-level concentration can be corrected to standard conditions by

$$x = x_R \frac{P_o}{P} \frac{T}{T_o} \qquad (2\text{-}66)$$

FIGURE 2-10

UNIFORMLY MIXED PUFF IN VERTICAL, TRANSPORTED FROM POSITION AT TIME t TO POSITION AT TIME t + Δt TRAVELING DISTANCE Δs
(The ground-level concentration at receptor R is computed using the Gaussian puff equation in the X'-Y'-Z' coordinate system)

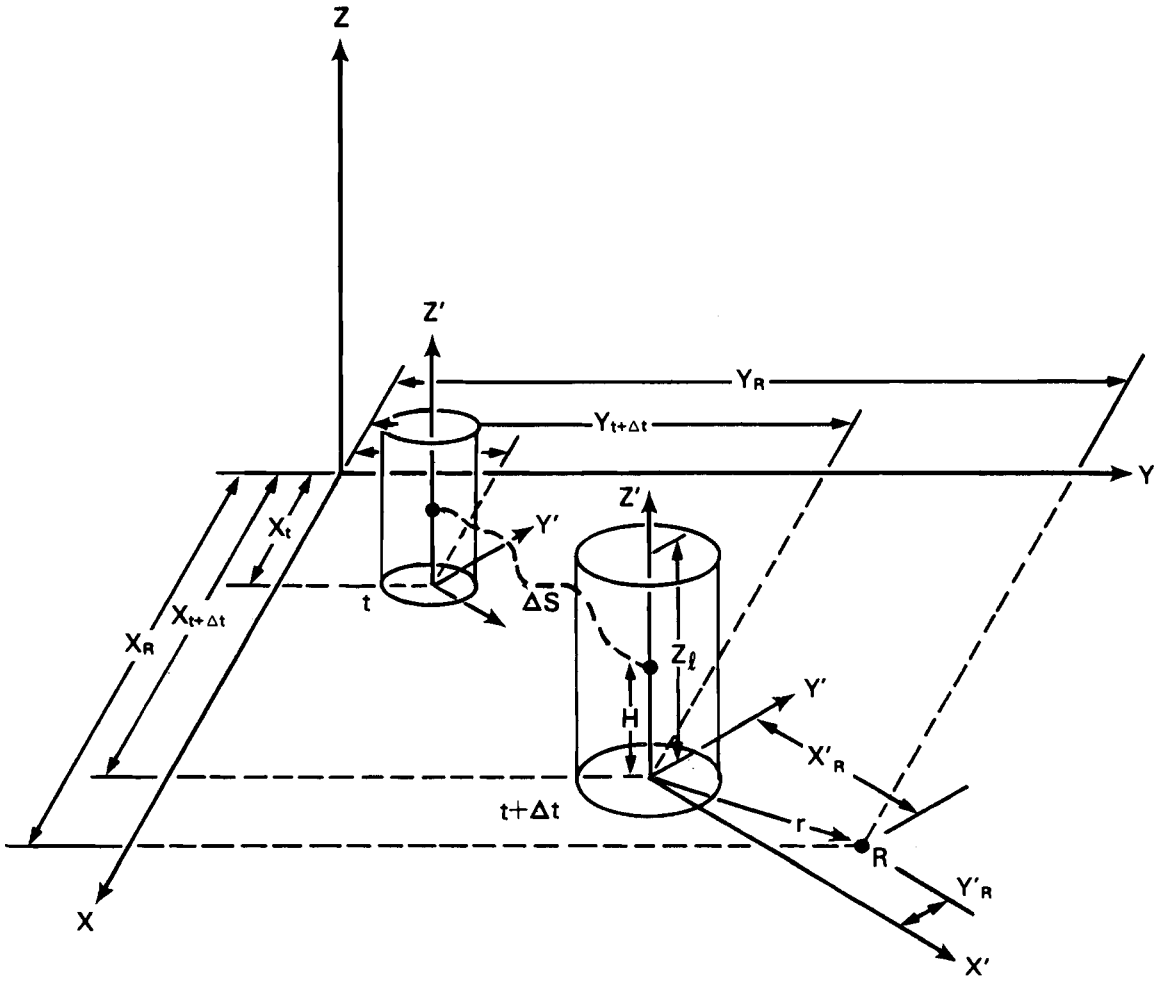

where

P_o = 1013 mb
T_o = 293.16°K
P = ambient pressure (mb)
T = ambient temperature (°K).

The multiple reflection terms in Equation (2-64) can be represented by an infinite series:

$$F_1 = \sum_{n=-\infty}^{\infty} \exp\left[- \frac{(H + 2nZ_\ell)^2}{2\sigma_z^2(t)} \right] \qquad (2\text{-}67)$$

or a Fourier series:

$$F_1 = \frac{\sigma_z(t)}{Z_\ell} \left(\frac{\pi}{2}\right)^{1/2} \left[1 + \sum_{j=1}^{\infty} 2 \cos(j\pi h) \exp(-j^2\pi^2 A/2)\right] \qquad (2\text{-}68)$$

as given by Schulman and Scire (1980), where

H = height aboveground of puff center-of-mass (m AGL)
Z_ℓ = mixed layer height above ground (m AGL)
$h = H/Z_\ell$
$A = (\sigma_z/Z_\ell)^2$.

Equation (2-67) converges rapidly for values of $A < 0.6$ (usually less than three or four terms), and Equation (2-68) converges quickly for values of $A \geq 0.6$. As discussed by Schulman and Scire, for these restricted values of A only a few terms are needed to evaluate the series. The equations for F_1 become

$$F_1 = \exp\left[-\frac{h^2}{2A}\right] \left\{1 + \exp\left[-\frac{2(1-h)}{A}\right] + \exp\left[-\frac{2(1+h)}{A}\right] + \exp[-4(2+h)] + \exp\left[-\frac{4(2+h)}{A}\right]\right\} \qquad A < 0.6$$

$$F_1 = \frac{\sigma_z}{Z_\ell} \left(\frac{\pi}{2}\right)^{1/2} \left\{1 + 2\cos(nh) \exp\left[-\frac{a^2 A}{2}\right] + 2\cos(2\pi h) \exp[-2\pi^2 A]\right\} \qquad A \geq 0.6 \qquad (2\text{-}69)$$

which contain a sufficient number of terms to obtain a high degree of precision. To optimize the computation of F_1 further, the exponential terms in Equation (2-69) can be evaluated by

$$\exp(-a) = \begin{cases} 1 - a & a < a_{min} \\ \exp(-a) & a_{min} \leq a \leq a_{max} \\ 0. & a > a_{max} \end{cases} \qquad (2\text{-}70)$$

where a_{min} is 0.1, and a_{max} is 7.0. This equation will give an estimate of the exponential to within about two decimal places.

As the ratio (σ_z/Z_ℓ) becomes larger, the vertical concentration distribution becomes more uniform. For values of $(\sigma_z/Z_\ell) \geq 1.6$, the vertical distribution can be assumed to be uniform, and the function f_v in Equation (2-64) becomes equal to $1/Z_\ell$. For pollutant concentrations distributed uniformly in the vertical direction, Equation (2-64) can be rewritten as

$$x_i(t) = \frac{M(t)}{2\pi\ \sigma_Y^2(t)\ Z_\ell}\ \exp\left[-\frac{r^2}{2\ \sigma_y^2(t)}\right] \qquad (2\text{-}71)$$

In MELSAR, the user has the option of specifying either an initial uniform vertical distribution or initial vertical Gaussian distribution. This decision will be based on how close the receptors are to the sources. In general, puffs within the daytime mixed layer will satisfy the condition of $\sigma_z/Z_\ell \geq 1.6$ within a couple of hours after release. In addition, for plume travel distances $\gtrsim 100$ km, the criteria of $\sigma_z/Z_\ell \geq 1.6$ will most likely be satisfied.

The orientation of the X'-Y'-Z' puff coordinate system, as described earlier, is a convenient way of representing a terrain-following continuous plume. Terrain following in this definition does not mean the height of the plume above ground is necessarily constant, but that the vertical distribution of pollutant material is described on an axis (Z' axis) that is perpendicular to the terrain along the plume path and vertical in the cross-path direction. This is equivalent to 'pulling' on the ends of the plume path until the along-path 'kinks' of the terrain features are removed. The cross-path terrain variations are still maintained. Figure 2-11 shows the along-path representation of the terrain and plume centerline using a

FIGURE 2-11

MELSAR's REPRESENTATION OF THE PLUME AND TERRAIN
WHEN COMPUTING GROUND-LEVEL CONCENTRATIONS
(A 'half-height' correction was assumed on the plume height)

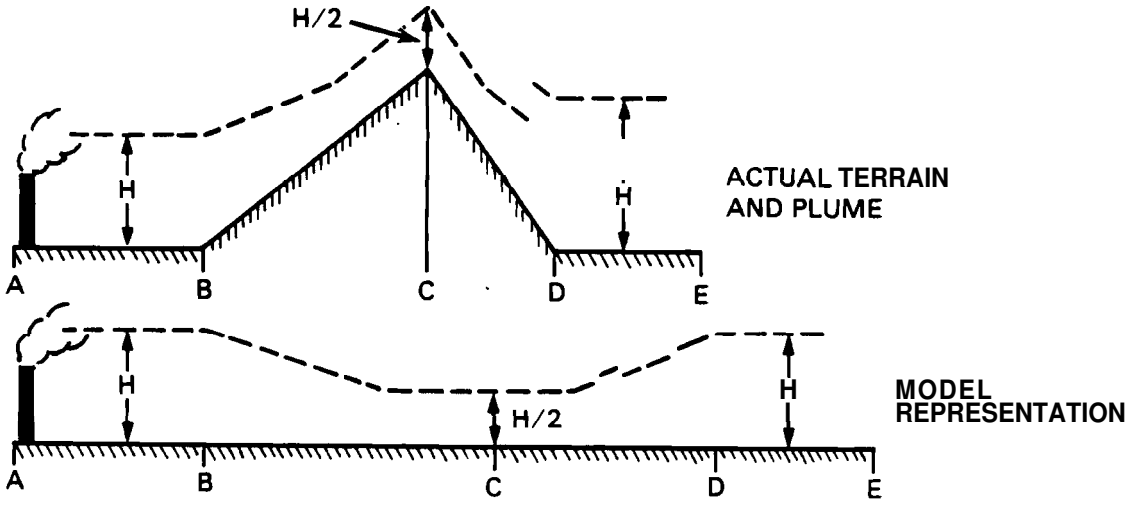

'half-height' correction to the plume height (refer to section on Puff Transport for an explanation of half-height correction).

To compute ground-level concentrations from a puff, the only quantities that must be computed in the X'-Y'-Z' coordinate system are the perpendicular distance, r, from the puff center axis (Z') to the receptor and the distance, H_L, parallel to the Z' axis from the receptor to a plane perpendicular to Z' containing the puff center of mass.

Using equations for lines and planes in space and vector analysis, the following relationship for r can be derived:

$$r = \left[|\vec{R}|^2 - \frac{(\vec{R} \cdot \vec{C})^2}{|\vec{C}|^2} \right]^{1/2}$$

$$|\vec{R}|^2 = (X_R - X_{PO})^2 + (Y_R - Y_{PO})^2 + (Z_R - Z_{PO})^2$$

$$|\vec{C}|^2 = \left[\frac{(X_P - X_{PO})(Z_P - Z_{PO})}{(X_P - X_{PO})^2 + (Y_P - Y_{PO})^2} \right]^2 + \left[\frac{(Y_P - Y_{PO})(Z_P - Z_{PO})}{(X_P - X_{PO})^2 + (Y_P - Y_{PO})^2} \right]^2 + 1$$

$$\vec{R} \cdot \vec{C} = -(X_R - X_{PO}) \frac{(X_P - X_{PO})(Z_P - Z_{PO})}{(X_P - X_{PO})^2 + (Y_P - Y_{PO})^2}$$

$$- (Y_R - Y_{PO}) \frac{(Y_P - Y_{PO}) + (Z_P - Z_{PO})}{(X_P - X_{PO})^2 + (Y_P - Y_{PO})^2} + (Z_R - Z_{PO}) \qquad (2\text{-}72)$$

where

$\vec{R}$ = position vector for receptor

$\vec{C}$ = position vector for puff axis (Z')

X_R, Y_R, Z_R = coordinates of receptor in fixed coordinate system (km)

X_{PO}, Y_{PO}, Z_{PO} = coordinates of the X'-Y'-Z' origin for puff for which ground-level concentrations are being computed (km)

X_P, Y_P, Z_P = coordinates of the X'-Y'-Z' origin of next puff downwind from puff of interest (km).

If the Z' axis is vertical (flat terrain along the path of the puff, $Z_P - Z_{PO} = 0$) then $\vec{C}$ is

$$\vec{C} = 0\vec{i} + 0\vec{j} + \vec{k} \qquad (2\text{-}73)$$

and Equation (2-72) reduces to

$$r = [(X_R - X_{PO})^2 + (Y_R - Y_{PO})^2]^{1/2} \quad . \tag{2-74}$$

The second quantity needed relative to the X'-Y'-Z' coordinate system is H_L. This is a 'local' puff height aboveground used to treat puff interaction with sloping terrain in the cross-path direction. Ramsdell, Athey and Glantz (1983) use this approach in the MESOI puff model. Figure 2-12 gives an example of H_L. A plume is traveling horizontally along a two-dimensional side-hill (into the page) at a height, H, aboveground at the plume centerline. Shown are two receptors and a cross section of a puff in the X'-Y'-Z' coordinate system (X' is into the page). H_L is the difference between H and d where d is the perpendicular distance from the receptor to the plane defining the base of the puff (X'-Y' plane at Z' = 0).

The equation for computing H_L is

$$H_L = H - d \tag{2-75}$$

where

H = height of puff center-of-mass above ground at puff centerline

$d = [(X_{RO}-X_R)^2 + (Y_{RO}-Y_R)^2 + (Z_{RO}-Z_R)^2]^{1/2}$ for $(Z_{RO}-Z_R) \leq 0$

$d = -d$ for $(Z_{RO}-Z_R) > 0$

X_R, Y_R, Z_R = coordinates of receptor in fixed coordinate system

X_{RO}, Y_{RO}, Z_{RO} = coordinates of the receptor projected to the base plane of the puff.

X_{RO}, Y_{RO}, Z_{RO} are computed from the following equations:

$$\begin{aligned} X_{RO} &= Ek + X_R \\ Y_{RO} &= Fk + Y_R \\ Z_{RO} &= Gk + Z_R \end{aligned} \tag{2-76}$$

where

$$E = - \frac{(X_P - X_{PO})(Z_P - Z_{PO})}{(X_P - X_{PO})^2 + (Y_P - Y_{PO})^2}$$

$$F = - \frac{(Y_P - Y_{PO})(Z_P - Z_{PO})}{(X_P - X_{PO})^2 + (Y_P - Y_{PO})^2}$$

$$k = \frac{E(X_P-X_R) + F(Y_P-Y_R) + G(Z_P-Z_R)}{(E^2+F^2+G^2)}$$

If the Z' axis is vertical, then d in Equation (2-75) reduces to

$$d = Z_P-Z_R. \qquad (2\text{-}77)$$

FIGURE 2-12

EXAMPLES OF THE LOCAL PUFF HEIGHT, H_L, FOR A PLUME TRAVELING ALONG A TWO-DIMENSIONAL RIDGE (INTO THE PAGE) AT A HEIGHT H ABOVEGROUND AT THE PLUME CENTERLINE

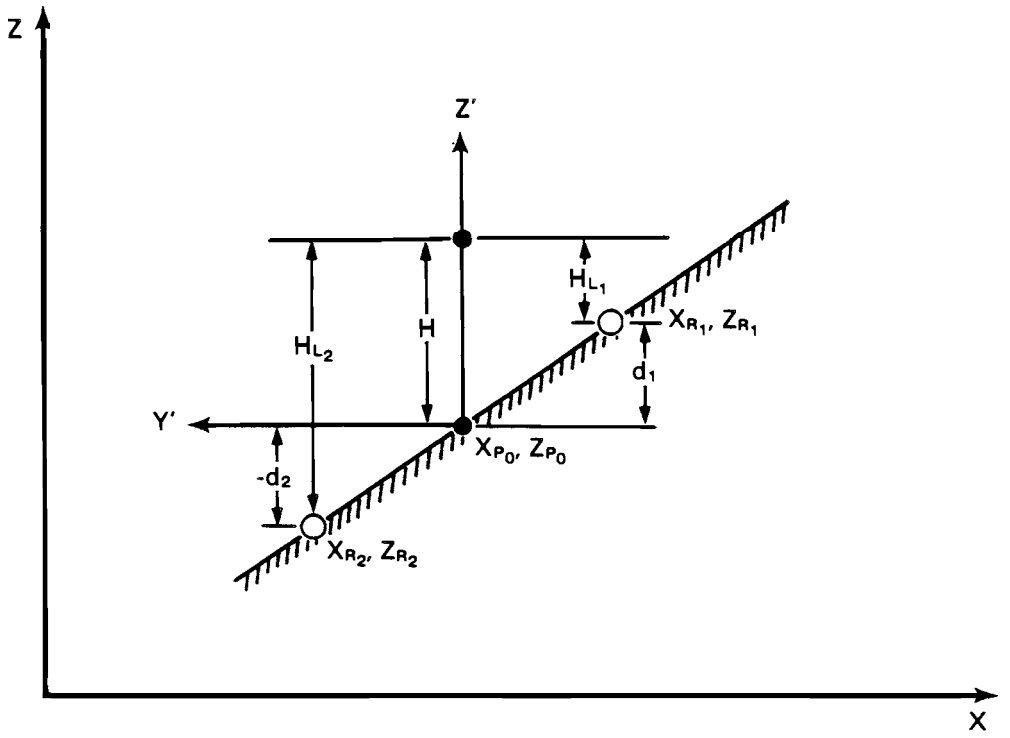

As discussed by Eagan, D'Errico and Vaudo (1979) adjusting the height of the plume to account for a plume approaching sloping terrain may cause the peak concentration in the plume to increase as the plume gets closer to the terrain. This is physically impossible because of the nature of the diffusion process. Eagan, D'Errico and Vaudo propose an answer for the problem, but this will require further investigation to see if it can be incorporated into MELSAR.

2.5.2 Plume Rise

The plume rise equations used in MELSAR are those described by Briggs (1975) for final plume rise and incorporated by Renkley and Bass (1979) in the MESOPUFF model. The following technical discussion on plume rise is taken principally from Benkley and Bass.

The effective emission height, H, of a puff center of mass aboveground is computed as $H = h_s + \Delta h$, where h_s is the stack height (m AGL) and Δh is the plume rise (m). For unstable and neutral conditions when the puff center does not rise above the top of the boundary layer, Δh is computed by

$$\Delta h = 1.6\ F^{1/3}\ (3.5\ x^*)^{2/3}/u_m \qquad (2\text{-}78)$$

$$x^* = \begin{cases} 34.49\ F^{2/5} & F > 55\ m^4/S^3 \\ 14\ F^{5/8} & F \leq 55\ m^4/S^3 \end{cases}$$

where the initial stack plume buoyancy flux, F (m^4/s^3), is

$$F = 9.8\ V_E\ R_E^{\ 2}\ \frac{T_E - T_A}{T_E}$$

u_m = maximum {u, 1.37}

u = wind speed at stack height (m/s)

V_E = velocity of gases at stack exit (m/s)

R_E = radius of stack exit (m)

T_E = temperature of gases at stack exit (°K)

T_A = ambient air temperature (OK).

For unstable and neutral conditions when the puff center penetrates into an elevated stable layer above the boundary layer, Δh is computed by:

$$\Delta h = \text{minimum} \left\{ \begin{array}{l} 1.6\ F^{1/3}\ (3.5\ x^*)^{2/3}/u_m \\ [1.8\ Z_b^{\ 3} + 18.75\ F/(u_m S)]^{1/3} \end{array} \right\} \qquad (2\text{-}79)$$

where

Z_b = the distance from the stack top to the top of the boundary layer (m)

$S = (9.8/T_A)\ (\partial\theta/\partial Z)$, stability parameter

$\partial\theta/\partial Z$ = potential temperature gradient, assumed to be 0.0137 °K/m.

For stable conditions, Δh is given by

$$\Delta h = \begin{cases} 2.6\ F^{1/3}/(u\ S)^{1/3} & u \geq 1.37 \text{ m/s} \\ 4.0\ F^{1/4}/S^{3/8} & u < 1.37 \text{ m/s} \end{cases} \qquad (2\text{-}80)$$

2.5.3 Receptors

Up to ten individual receptors and up to four receptor grids can be specified anywhere in the modeling domain. Each receptor grid can contain a maximum of 25 by 25 receptors. If all receptor options are used, the result is 2510 receptors.

A receptor grid is defined by specifying the horizontal coordinates of the lower left corner, X_G and Y_G, the number of receptors in the X-direction, N_x, the number of receptors in the Y-direction, N_y, and the spacing between receptors, Δr. Figures 3-2 and 3-3 show an example of the locations of two receptor grids and three individual receptors in the modeling domain. Table 2-10 gives the specifications on these receptors. The receptor heights are determined by interpolation of the gridded terrain heights.

TABLE 2-10

SPECIFICATIONS OF RECEPTORS IN FIGURES 3-2 and 3-3

	Receptor Grids				
Name	X_G(km)	Y_G(km)	N_x	N_y	Δr(km)
Flat Tops	375.0	200.0	6	11	4.0
Dinosaur	246.0	266.0	11	3	2.0

	Individual Receptors	
Name	X_r(km)	Y_r(km)
So. Flat Tops	385.0	195.0
Meeker, Colorado	343.0	223.0
Dinosaur	227.0	262.0

Two characteristics of the rectangular receptor grids are used in the sampling function routines to determine if 'tracking' puffs should be split and ground-level concentrations computed. The quantities required are the coordinates of the grid center and half the diagonal distance. The equations for these quantities are

$$X_{GC} = X_G + \Delta r(N_x-1)/2$$

$$Y_{GC} = Y_G + \Delta r(N_y-1)/2 \quad (2\text{-}81)$$

$$D_G = [\Delta r(N_x-1)/2]^2 + [\Delta r(N_y-1)/2]^{2\ 1/2}$$

where

X_{GC} = X-coordinate of receptor grid center (km)
Y_{GC} = Y-coordinate of receptor grid center (km)
D_G = half the diagonal distance of the receptor grid (km).

2.5.4 Source Representation

Up to 5 point sources can be represented during any run of the pollution model POLUT, although the post-processor, POLPRC, can compute averages for up to a total of 20 sources (four runs of POLUT). The user also has the option of representing area sources as virtual point sources by specifying an initial sigma-y for each source. This is a simplified approach but adequate for long source-to-receptor distances (>100 km).

The information required for each source is:

1) name
2) location (UTM, latitude-longitude, or GRAMA coordinates)
3) stack height
4) stack gas exit velocity
5) stack gas exit temperature
6) stack exit radius
7) number of pollutants (not more than two)
8) names of pollutants
9) pollutant emission rates.

If the source is an area source, then only items 1, 2, 7, 8, 9, and the initial sigma-y are required.

2.5.5 Puff Treatment

Puffs emitted above the top of the mixed layer diffuse in the horizontal direction at D, E, or F stability conditions depending on the stability at that time and location. If the gridded stability is A, B, or C, the puff diffuses at D stability conditions.

Any puff above the top of the mixed layer does not contribute to ground-level concentrations. Only when the mixed layer has grown to a height above the puff center of mass does the puff contribute to ground-level concentrations, and then the puff is assumed to be immediately

uniformly distributed through the mixed layer. For transport purposes the puff center of mass is assumed to be at one-half the depth of the mixed layer after the fumigation. As the mixed layer continues to deepen as a result of convection, the puff remains uniformly mixed in the vertical direction through the growing mixed layer. Once the mixed layer begins to collapse as the convection decreases, the puff remains uniformly distributed through the maximum depth of the mixed layer encountered by the puff.

Certain puff 'housekeeping' functions are required to keep the number of puffs being treated on the grid to a reasonable number. Three situations allow the number of puffs to be reduced: 1) if the puff is advected off the grid, it is eliminated; 2) if the concentration at the center of a puff drops below a minimum value, x_{min}, the puff is eliminated; and 3) if the centers of any two puffs in the same plume are separated by less than a minimum separation distance, d_{min}, the two puffs are combined.

Note that individual puffs are not tracked from a source located in decoupled valley flows. Instead, the total pollutant mass is accumulated in the valley throughout the duration of the decoupled period, as described in Section 2.5.8. Once this trapped pollutant material begins to be released into the above ridgetop flows, puffs are then tracked by the model.

2.5.6 Puff Transport

A puff is transported from time t to time $t+\Delta t$ in the mean wind field. The mass-consistent wind fields are specified hourly (see Section 2.4.1). Three components of wind velocity, u, v, and w, are specified at up to nine levels above the ground.

The user has the option of computing the puff movement with or without the vertical velocity. If the vertical velocity field is representative of the actual atmosphere, then computing puff movement using the vertical velocities could give better descriptions of the puff movement relative to the terrain than empirical correction techniques. However, it is uncertain how well the flow model represents the actual vertical velocities. This aspect of the flow model will require further testing.

The procedure for transporting a puff from time t to $t+\Delta t$ is based on a two-step iteration procedure described by Hales, Powell and Fox (1977). If vertical velocities are not used, the procedure shown in Figure 2-13 is used. This figure shows transport over a ridge of constant elevation aligned in the Y direction (into the page). The transport vectors are viewed from above (X-Y) and from one side (X-Z) in Figure 2-13. The puff center of mass at time t (position $[X(t),Y(t),Z(t)]$) is moved over Δt to position $[X_1,Y_1,Z(t)]$ using the horizontal winds at position $[X(t),Y(t),Z(t)]$ at time t. The equations for position 1 are

FIGURE 2-13

TWO-STEP APPROXIMATION OF PUFF TRANSPORT FROM TIME **t** TO TIME **t+Δt** WITHOUT USING VERTICAL VELOCITIES (The puff is moving over a ridge aligned in the Y-direction into the page.)

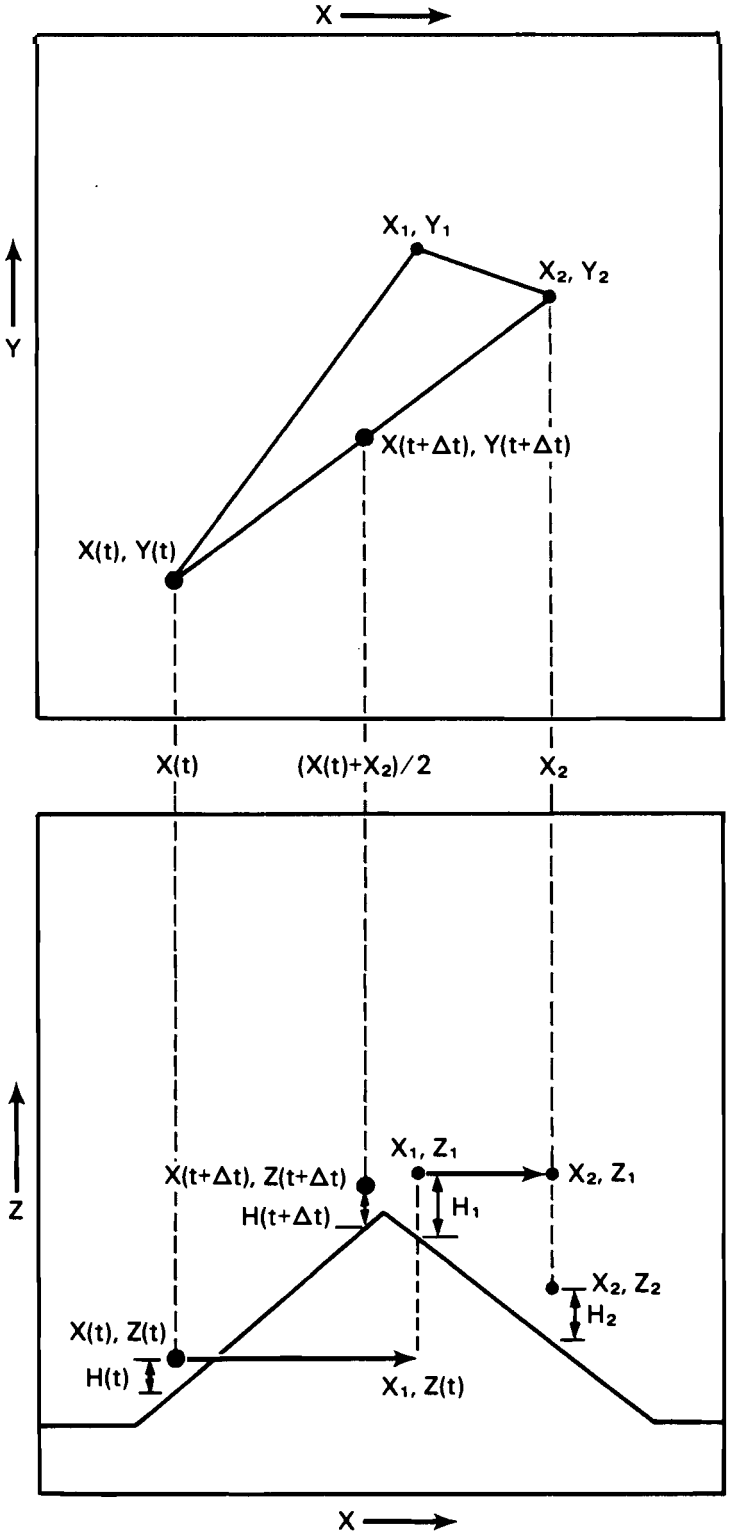

$$X_1 = X(t) + u[t;X(t),Y(t),Z(t)]\Delta t$$

$$Y_1 = Y(t) + v[t;X(t),Y(t),Z(t)]\Delta t \qquad (2\text{-}82)$$

$$Z_1 = T_1 + H_1$$

where T_1 is the elevation of terrain at position 1, and H_1 is the height of the puff center of mass aboveground.

To account for changes in the winds over Δt, a second advection increment is added to position $[X_1,Y_1,Z_1]$. The horizontal winds at position 1 at time $t+\Delta t$ are used to move the puff to position $[X_2, Y_2, Z_1]$. The equations for position 2 are

$$X_2 = X_1 + u[t+\Delta t;X_1,Y_1,Z_1]\Delta t$$

$$Y_2 = Y_1 + v[t+\Delta t;X_1,Y_1,Z_1]\Delta t \qquad (2\text{-}83)$$

$$Z_2 = T_2 + H_2$$

The equation for Z_2 is given here for completeness, although it is not actually needed to determine the puff position at $t+\Delta t$. On the other hand, Z_1 is required in the computation because we must know the air density, which is a function of elevation, to determine the horizontal wind components at position 1. The equations for computing the winds are given in Section 2.5.9.

Finally, the new X and Y puff position at $t+\Delta t$ is found by adding the vector average of the horizontal components of the two advection increments to the X and Y puff position at time t. This is taken to be halfway along the horizontal line from $[X(t),Y(t)]$ to $[X_2,Y_2]$. The Z coordinate of the puff at time $t+\Delta t$ is equal to the terrain height at $[X(t+\Delta t),Y(t+\Delta t)]$ plus the height of the puff center of mass aboveground, $H(t+\Delta t)$. The determination of H affected by terrain elevation changes is discussed later. The equations for the puff at time $t+\Delta t$ are

$$X(t+\Delta t) = 0.5[X(t) + X_2]$$

$$Y(t+\Delta t) = 0.5[Y(t) + Y_2] \qquad (2\text{-}84)$$

$$Z(t+\Delta t) = T(t+\Delta t) + H(t+\Delta t)$$

When vertical velocities are used in the modeling, the same basic two-step iteration procedure described above and shown in Figure 13 is used to transport puffs, except the vertical travel of the puff is determined using the vertical velocity. The X-, Y-, and Z-coordinates of the puff at positions 1 and 2 and $t+\Delta t$ are determined using Equations (2-82), (2-83), and (2-84), respectively. The height aboveground, H, at positions 1, 2, and $t+\Delta t$ are determined using the following equations:

$$H_1 = H(t) + \{w[t;X(t),Y(t),Z(t)] - w_T[t;X(t),Y(t),Z(t)]\}\ \Delta t$$

$$H_2 = H_1 + \{w[t+\Delta t;X_1,Y_1,Z_1] - w_T[t+\Delta t;X_1,Y_1,Z_1]\}\ \Delta t \qquad (2\text{-}85)$$

$$H(t+\Delta t) = 0.5[H(t) + H_2]$$

where w is the vertical velocity (m/s), and w_T is the vertical velocity sufficient to follow terrain (m/s). When the puff becomes uniformly mixed in the vertical direction, the height of the puff center of mass aboveground is simply half the nixing depth. Equation (2-85) becomes

$$H_1 = 0.5(Z_{\ell_1} - T_1)$$

$$H_2 = 0.5(Z_{\ell_2} - T_2) \qquad (2\text{-}86)$$

$$H(t+\Delta t) = 0.5[Z_\ell(t+\Delta t) - T(t+\Delta t)]$$

where Z_ℓ is the height of mixed layer (m MSL), and T is the terrain height (m MSL).

2.5.6.1 Determination of Puff Height Aboveground - H

The approach for determining the puff path height aboveground without using vertical velocities is that given by Schulman and Scire (1980),

$$H(t+\Delta t) = H_o - (1-C_T)(\text{minimum } \{H_o, T(t+\Delta t) - T_o\}) \qquad (2\text{-}87)$$

where

$H_o = h_s + \Delta h$, h_s is the stack height (m AGL) and Δh is plume rise (m)
$T(t+\Delta t)$ = terrain height at puff position at time $t+\Delta t$ (m MSL)
T_o = terrain height at stack base (m MSL)
C_T = height adjustment coefficient.

Example values of the height adjustment coefficient as given by Schulman and Scire (1980) are given in Table 2-11 by Pasquill-Gifford stability class. The user can input any values of C_T for use by MELSAR. If no adjustment is desired then C_T equal to 1.0 should be specified.

For neutral and unstable conditions, the puff is lifted one-half of the difference between the elevation of the terrain at the puff location and the elevation of the stack base, with the additional restriction that the height of the plume always be at least half of the height aboveground that it would be with flat topography. With stable conditions, the puff is lifted about one-third of the difference between the elevation of the terrain at the puff location and the elevation of the stack base, and is restricted to be at least one-third of the height aboveground that it would be with flat topography. An example of the height adjustment scheme is given in Figure 2-14.

TABLE 2-11

EXAMPLE VALUES FOR
THE HEIGHT ADJUSTMENT COEFFICIENT (Schulman and Scire 1980)

Pasquill-Gifford Stability	Adjustment Coefficient C_T
A, B, C, and D	0.5
E and F	0.3

FIGURE 2-14

PUFF PATH HEIGHT ABOVEGROUND FROM EQUATION (2-87) FOR UNSTABLE AND NEUTRAL CONDITIONS (C_T = 0.5) AND STABLE CONDITIONS (C_T = 0.3) (The line of C_T = 1 is plotted for reference. It is the path of the puff following the terrain at H_0 aboveground level.)

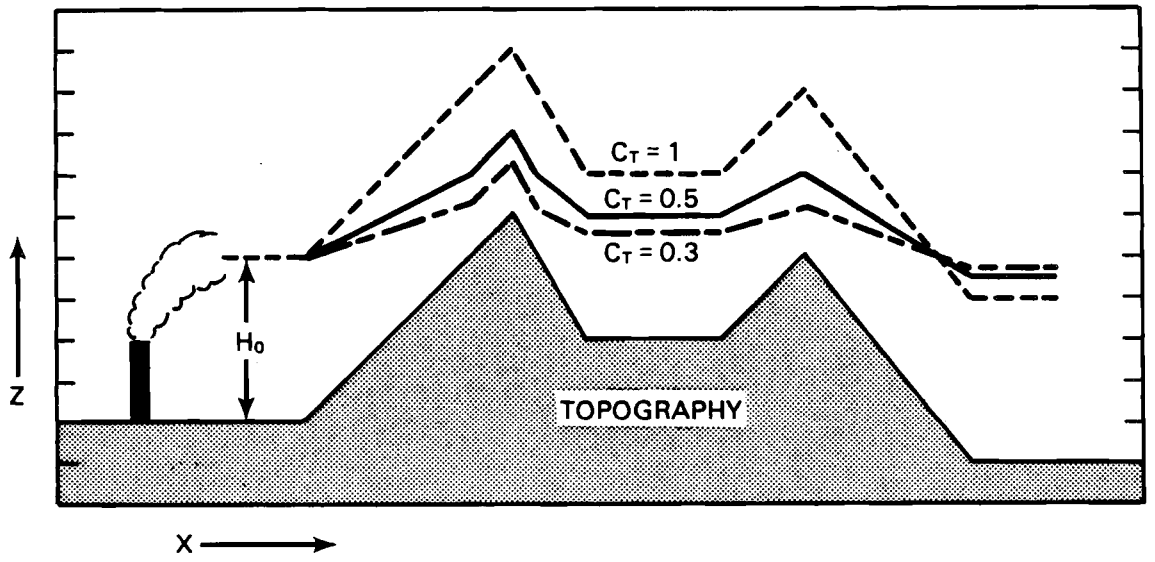

2.5.7 Sampling Function

In MELSAR, 'tracking' puffs are used to define the plume. These puffs are from 10 min to 1 hr apart depending on the user's choice of puff release rate (6 puffs/hr to 1 puff/hr). In most applications of MELSAR with meteorological inputs at 1-hr intervals and long source-to-receptor distances (>100 km), the release rate of 1 puff/hr will be used. As pointed out by Zannetti (1981), a continuous plume is accurately represented by a series of overlapping puffs if the separation distance between adjacent puffs, Δd, is less than or equal to the streamwise standard deviation of the Gaussian concentration, a_y, of each puff

$$\Delta d \leq \sigma_y \qquad (2\text{-}88)$$

A puff splitting routine is used in MELSAR to satisfy Equation (2-88) between tracking puffs.

The splitting routine follows the approach of Zannetti's (1981) for treating nonstationary and nonhomogeneous conditions and is used only when a tracking puff is close enough to a receptor to contribute to the ground-level pollutant concentration.

Figure 2-15 gives an example of a plume from a point source represented by a series of tracking puffs. Shown is a plume after 2 hr of travel time (ABC) and then after 3 hr (AA'B'C'). The winds were from the west at 2 m/s for the first 2 hr and from the southwest at 2 m/s for the last hour. Several characteristics are determined for each tracking puff:

1. the X, Y, Z coordinates
2. the horizontal and vertical diffusion coefficients
3. the height of the mixed layer
4. code identifying whether the puff is above or below the top of the mixed layer
5. a code identifying whether or not the puff is uniformly distributed in the vertical direction.

FIGURE 2-15

PLUME LOCATION AFTER 2 HOURS OF TRANSPORT (time t)
AND AFTER 3 HOURS (t + Δt)
(The winds were from the west at 2 m/s for the first 2 hr
and from the southwest at 2 m/s for the last hour.
The boundaries for the tracking puffs are shown at 1 σ_y.)

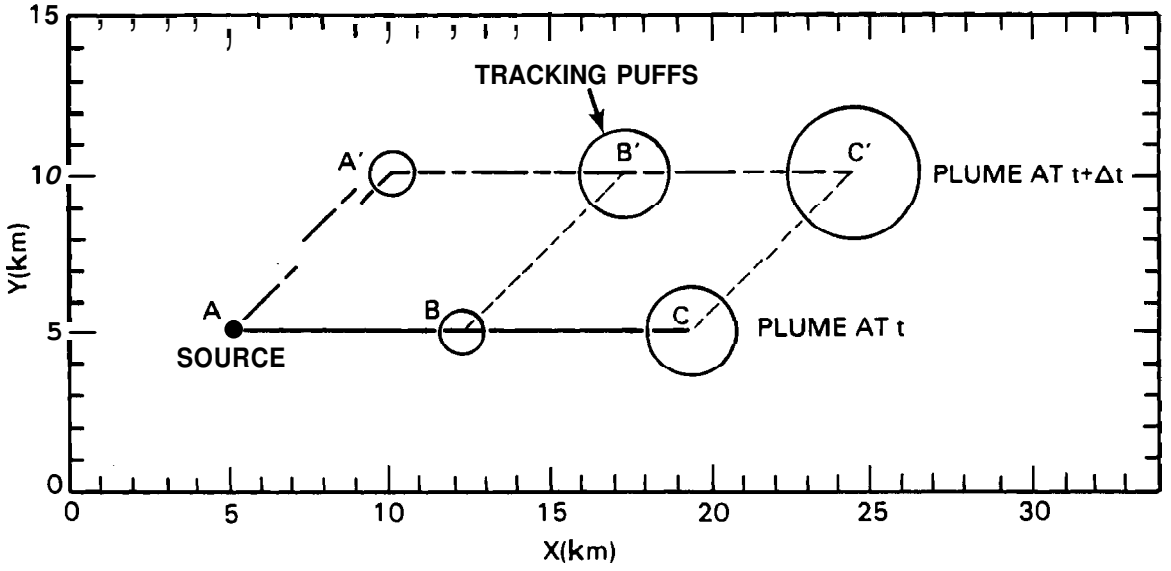

If the splitting routine is used, then the puff characteristics 2, 3, 4, and 5 are interpolated to the intermediate puffs.

The procedure for puff splitting is illustrated in Figure 2-16.[1] The quadrilateral is BB'C'C from Figure 2-15. First, the number of puffs required along the 's' segments, segments (1) and (3), to satisfy Equation (2-88) are determined. Then the minimum number of puffs required on each 's' segment is set to the maximum from either segment. That is

FIGURE 2-16

EXAMPLE OF PUFF-SPLITTING ROUTINE

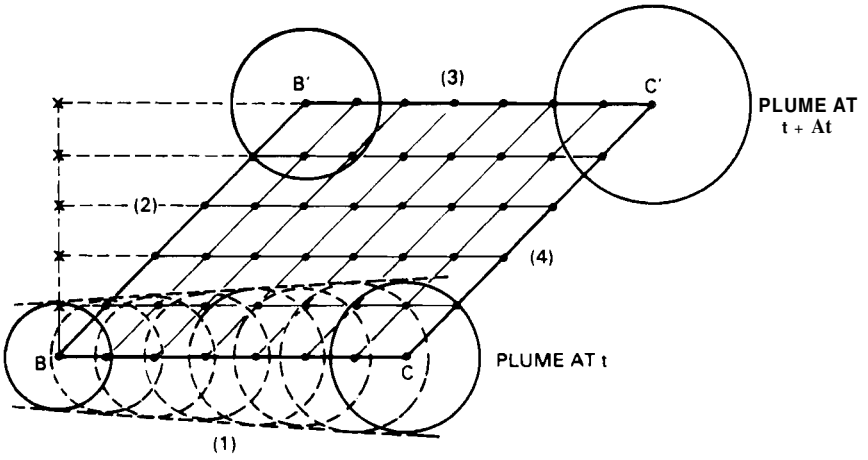

$$N_s = \text{NINT}\left\{\text{MAX}\left[\frac{s_1}{(\sigma_y)_B}, \frac{s_3}{(\sigma_y)_{B'}}\right] + 0.5\right\} \qquad (2\text{-}89)$$

where

N_s = number puffs on 's' segments [(1) and (3) in Figure 2-16]
NINT = find nearest integer of quantity in brackets
MAX = find maximum value of quantity in brackets
$(\sigma_y)_B$ = horizontal standard deviation of pollutant distribution at point B in quadrilateral (m)
$(\sigma_y)_{B'}$ = horizontal standard deviation of pollutant distribution at point B' in quadrilateral (m)
s_1 = terrain-following length of segment (1) (m)
s_3 = terrain-following length of segment (3) (m).

[1] A more efficient puff splitting technique is currently in the code. The results are not affected. Contact the authors if more information is desired.

The distances s_1 and s_3 are the terrain-following distances from point B to C and B' to C', respectively. They are estimated from the following equations:

$$s_1 = \left[(X_C - X_B)^2 + (Y_C - Y_B)^2 + (Z_C - Z_B)^2 \right]^{1/2} \quad (2\text{-}90)$$

$$s_2 = \left[(X_{C'} - X_{B'})^2 + (Y_{C'} - Y_{B'})^2 + (Z_{C'} - Z_{B'})^2 \right]^{1/2} \quad (2\text{-}91)$$

Next the number of puffs required on the 't' segments, (2) and (4), are determined by finding the number of puffs on line segments perpendicular to segment (1). The perpendicular line for segment (2) is shown in Figure 2-16. A similar line is required for segment (4). The minimum number of puffs required on each **t** segment is set to the maximum from either perpendicular segment. That is

$$N_t = \text{NINT} \left\{ \text{MAX} \left[\frac{s_2'}{(\sigma_y)_B} , \frac{s_4'}{(\sigma_y)_C} \right] + 0.5 \right\} \quad (2\text{-}92)$$

where

N_t = number of puffs on **t** segments [(2) and (4) in Figure 2-16]

s_2' = length of component of segment (2) perpendicular to segment (1), (m)

s_4' = length of component of segment (4) perpendicular to segment (1), (m).

The distances s_2' and s_4' are computed from the following equations

$$s_2' = s_2 \sin \left\{ \cos^{-1} \left[\frac{\vec{BB'} \cdot \vec{BC}}{|\vec{BB'}| \, |\vec{BC}|} \right] \right\} \quad (2\text{-}93)$$

$$s_4' = s_4 \sin \left\{ \cos^{-1} \left[\frac{\vec{CC'} \cdot \vec{CB}}{|\vec{CC'}| \, |\vec{CB}|} \right] \right\}$$

where

s_2 = terrain-following length of segment (2)

$\vec{BB'} \cdot \vec{BC}$ = dot product of vectors $\vec{BB'}$ and $\vec{BC}$

$= (X_{B'} - X_B)(X_C - X_B) + (Y_{B'} - Y_B)(Y_C - Y_B) + (Z_{B'} - Z_B)(Z_C - Z_B)$

s_4 = terrain-following length of segment (4)

$$\vec{CC'} \cdot \vec{CB} = (X_C'-X_C)(X_B-X_C) + (Y_C'-Y_C)(Y_B-Y_C) + (Z_C'-Z_C)(Z_B-Z_C)$$

$$|BB'| = [(X_B'-X_B)^2 + (Y_B'-Y_B)^2 + (Z_B'-Z_B)^2]^{1/2}$$

$$|CC'| = [(X_C'-X_C)^2 + (Y_C'-Y_C)^2 + (Z_C'-Z_C)^2]^{1/2}$$

$$|\vec{BC}|=|\vec{CB}| = [(X_C-X_B)^2 + (Y_C-Y_B)^2 + (Z_C-Z_B)^2]^{1/2}.$$

The distances s_2 and s_4 are computed in the same manner as s_1 and s_3 described earlier.

Once the total number of puffs for a quadrilateral are known, then the splitting process can proceed. First, segments (1) and (3) are each divided into N_s puffs with the puff sigmas, mixing heights, and vertical distribution codes linearly interpolated between the end tracking puffs on each segment. The height of each interpolated puff aboveground is determined using the procedure described in Section 2.5.6. Now, using the interpolated 's' segment puffs as end points, the puffs on the 't' segments are interpolated from the 's' segment puffs. Figure 2-16 shows an example of interpolated puffs on segment (1) in addition to showing the locations of all the required puffs.

The tracking puffs must be split when the puffs are close enough to any receptor to contribute to the ground-level concentration. This minimum separation distance in MELSAR is defined as 5 a_y. This test is not sufficient in itself because receptors can be located near the internal portions of the quadrilateral and still be greater than 5 σ_Y from the four tracking puffs. An additional constraint is imposed on the test to ensure that no internal receptors are overlooked. Puff splitting will occur if the distance from the puff to receptor is less than the quadrilateral segment length adjacent to the puff. This is expressed in mathematical form as

$$d_{P-R} \leq \text{maximum } (5\ a_y,\ s) \qquad (2\text{-}94)$$

where d_{P-R} is the horizontal distance between a puff and a receptor, and s is the horizontal length of a segment between two tracking puffs on a quadrilateral.

This is illustrated in Figure 2-17, which shows a receptor located within quadrilateral BB'C'C. The receptor is outside the range of 5 a_y from each tracking puff, but well within the boundaries of the quadrilateral segment lengths; if no receptors are within the outer boundaries shown in Figure 2-17, the puff splitting will not be necessary.

Note that Equation (2-94) uses only horizontal distances. To save computer time, we assumed that Equation (2-94) is sufficiently conservative

without using vertical distances and that no receptors will be overlooked even in steeply sloping terrain. However, this assumption needs further testing.

To save computer time, Equation (2-94) is not tested for every receptor in the receptor grids, but rather once for each receptor grid. This is done by determining a characteristic puff-to-receptor distance, d_{P-R}, for each receptor grid

$$d'_{P-R} = [(X_P - X_{GC})^2 + (Y_P - Y_{GC})]^{1/2} - D_G \qquad (2\text{-}95)$$

where

X_P = X-coordinate of puff (km)
Y_P = Y-coordinate of puff (km)
X_{GC} = X-coordinate of receptor grid center (km)
Y_{GC} = Y-coordinate of receptor grid center (km)
D_G = half the diagonal distance of the receptor grid.

The puff-to-receptor distance from Equation (2-95) is then used in Equation (2-94). The computing of X_{GC}, Y_{GC}, and D_G is given in Section 2.5.3.

The plume from each source is sampled during every model time step. This is done by starting at the 'oldest' tracking puff from the source and working back toward the source, identifying each quadrilateral and determining whether a quadrilateral should be split based on the test of Equations (2-94) and (2-95). If splitting is required, then the contribution of each split puff to the ground-level concentration at each receptor within 5 a_y of the puff is computed using the equations described in Section 2.5.1. When the source is reached, the plume segment between the source and the newest tracking puff must be tested for close receptors and split if necessary. In other words, both the quadrilateral AA'B'B and plume segment AA' shown in Figure 2-15 must be treated separately in the analysis.

When a quadrilateral is split, the pollutant mass, M, carried along with the primary tracking puff of the quadrilateral must be divided among all the puffs in the quadrilateral. The pollutant mass per puff is

$$M_P = \frac{M_T}{(n_s-1)(n_t-1)} \qquad (2\text{-}96)$$

where

M_P = pollutant mass per puff (pg)
M_T = $Q\Delta t$, pollutant mass associated with a tracking puff (μg)
Q = pollutant emission rate at time of tracking puff release from source (μg/s)
Δt = modeling time step (s)
n_s = number of puffs on s segment [refer to Equation (2-89)]
n_t = number of puffs on t segment [refer to Equation (2-90)].

FIGURE 2-17

ILLUSTRATION OF CRITERIA FOR DECIDING WHETHER TO DIVIDE A QUADRILATERAL INTO OVERLAPPING PUFFS

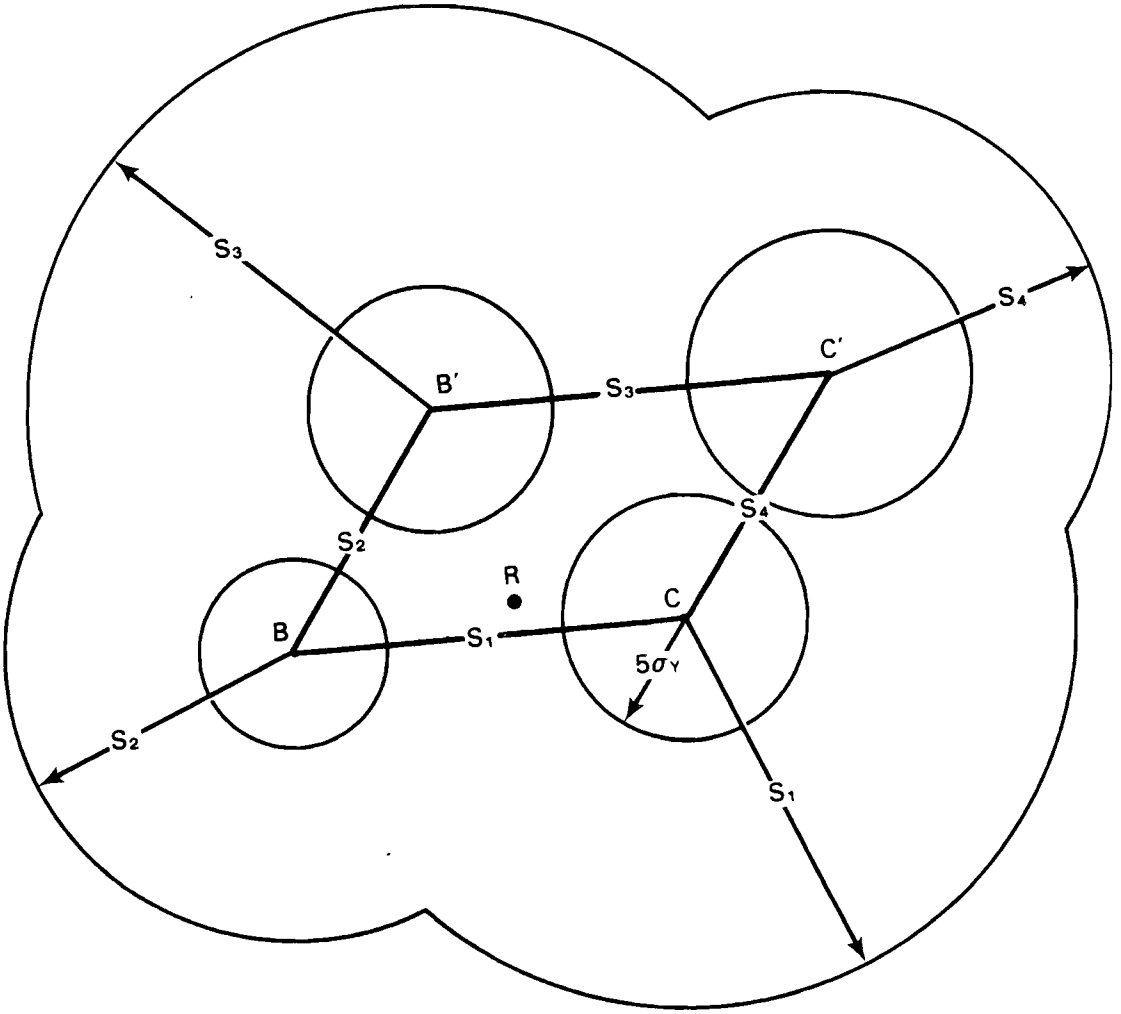

The primary tracking puff of quadrilateral BB'C'C in Figure 2-16 is located at C. The pollutant material associated with this tracking puff is split among all the puffs in the quadrilateral except those along segment RB' and segment BC. The puffs along segments BB' and BC are not used so that their impacts are not counted twice when the model looks at the quadrilateral closer to the source and the quadrilateral during the previous time step, respectively.

2.5.8 Valley Treatment

Air pollutants released in valleys can be transported down-valley in noctural drainage flows and then at sunrise be advected up the valley sidewalls and carried away in the above ridgetop winds. The process is demonstrated in Figure 2-18 for a hypothetical situation where pollutants are trapped in Clear Creek Valley, which is about 50 km NNE of Grand Junction, Colorado. Frame A shows pollutant material trapped in Clear Creek Valley at the time of sunrise. The continuous source is located at the head of Clear Creek and the pollutants have transported about 25 km down-valley through the night. The pollutants are assumed to be uniformly mixed throughout the valley.

At sunrise, the continuous source is assumed to begin emitting pollutants into the above ridgetop winds, which are from the WSW at 10 km/hr. In addition, the valley inversion begins to be destroyed and the pollutant material trapped in the valley begins to be carried away in the above ridgetop winds. Frame B of Figure 2-18 shows the pollutant cloud 1 hr after sunrise when the leading edge of the pollutant cloud is 10 km downwind from the valley.

For purposes of illustration, the valley inversion is assumed to be completely destroyed at 3 hr after sunrise, and hence, the pollutants trapped in the valley are gone after 3 hr. Frame C of Figure 2-18 shows the pollutant cloud at 4 hr after sunrise. Here the continuous plume from the stack and the leading edge of the pollutant cloud from the valley are 40 km downwind. The trailing edge of the cloud from the valley is 10 km downwind. Frame D of Figure 2-18 shows the Clear Creek area in a portion of the GRAMA modeling domain.

This idealized description of valley coupling-decoupling with above ridgetop flows is treated in MELSAR for each valley containing a source. The first step is to characterize the geometry of each source valley. This is done by dividing the valley into linear segments under 10 km in length. The segments are defined using one of three criteria: 1) 10-km-maximum length, 2) valley axis changes direction, or 3) valley cross section changes. A computational limit of 100 km is set for maximum valley length (10 segments). Thus, for any pollutant transported in down-valley flows to distances greater than 100 km, the total pollutant material will be assumed to be uniformly distributed in the 100 km down-valley volume.

Knowing the mean down-valley wind speed, the total length of valley filled with pollutants at sunrise is

$$\ell_T = u_v \, (\Delta t_D) \qquad (2\text{-}99)$$

FIGURE 2-18

TRANSPORT OF POLLUTANTS OUT OF CLEAR CREEK DURING THE VALLEY INVERSION BREAKUP PERIOD. (Frame A shows the pollutants trapped in the valley at sunrise. Frame B shows the plume from the point source at the head of the valley and the pollutant cloud from the valley after 1 hr of transport time in the 10-km/hr regional winds.)

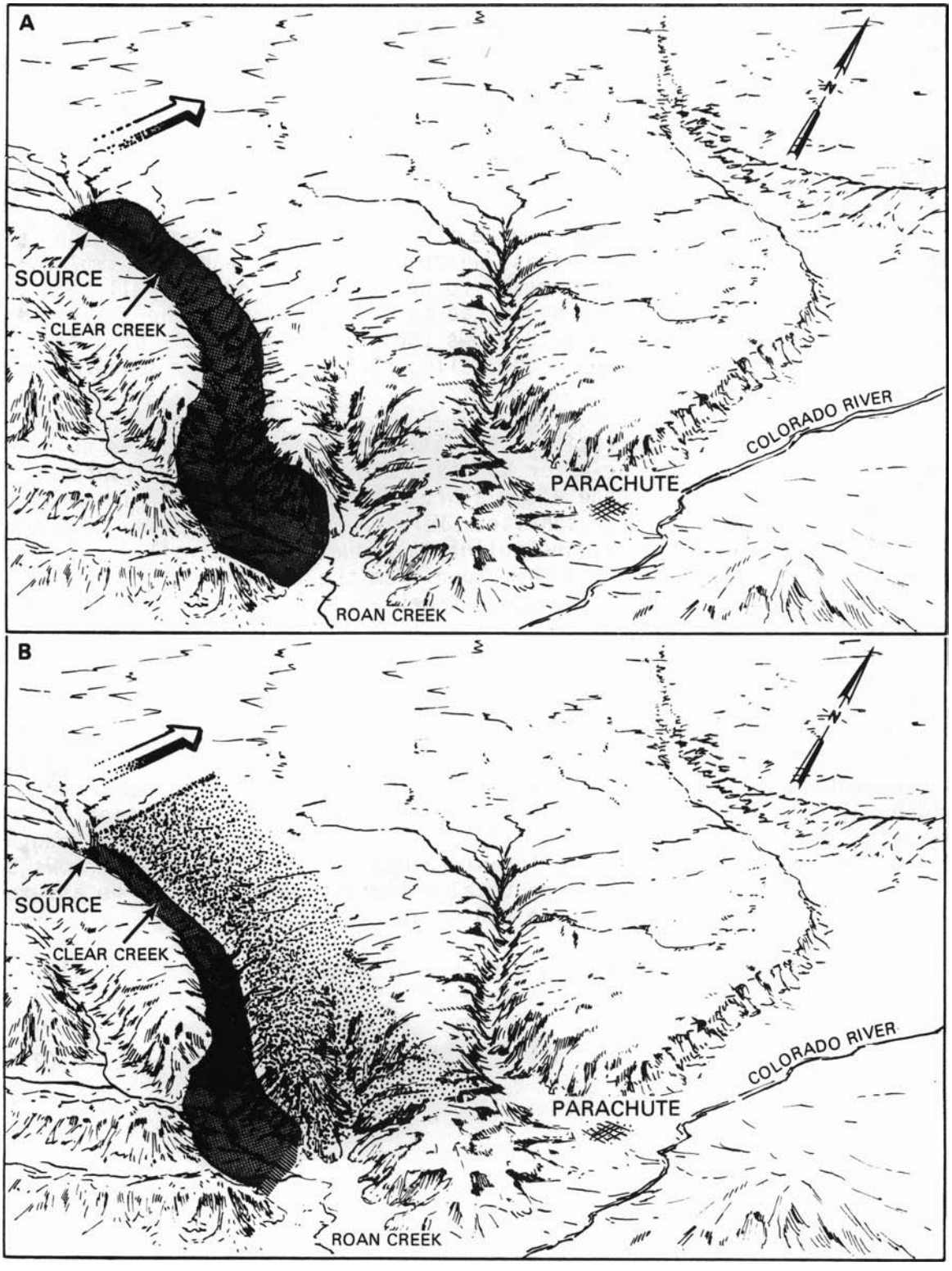

FIGURE 2-18 (continued)

(Frame C shows the pollutant transport 4 hr after sunrise for the valley inversion completely breaking up at 3 hr after sunrise. Frame D shows the area represented in Frames A, B, and C in the GRAMA modeling domain.)

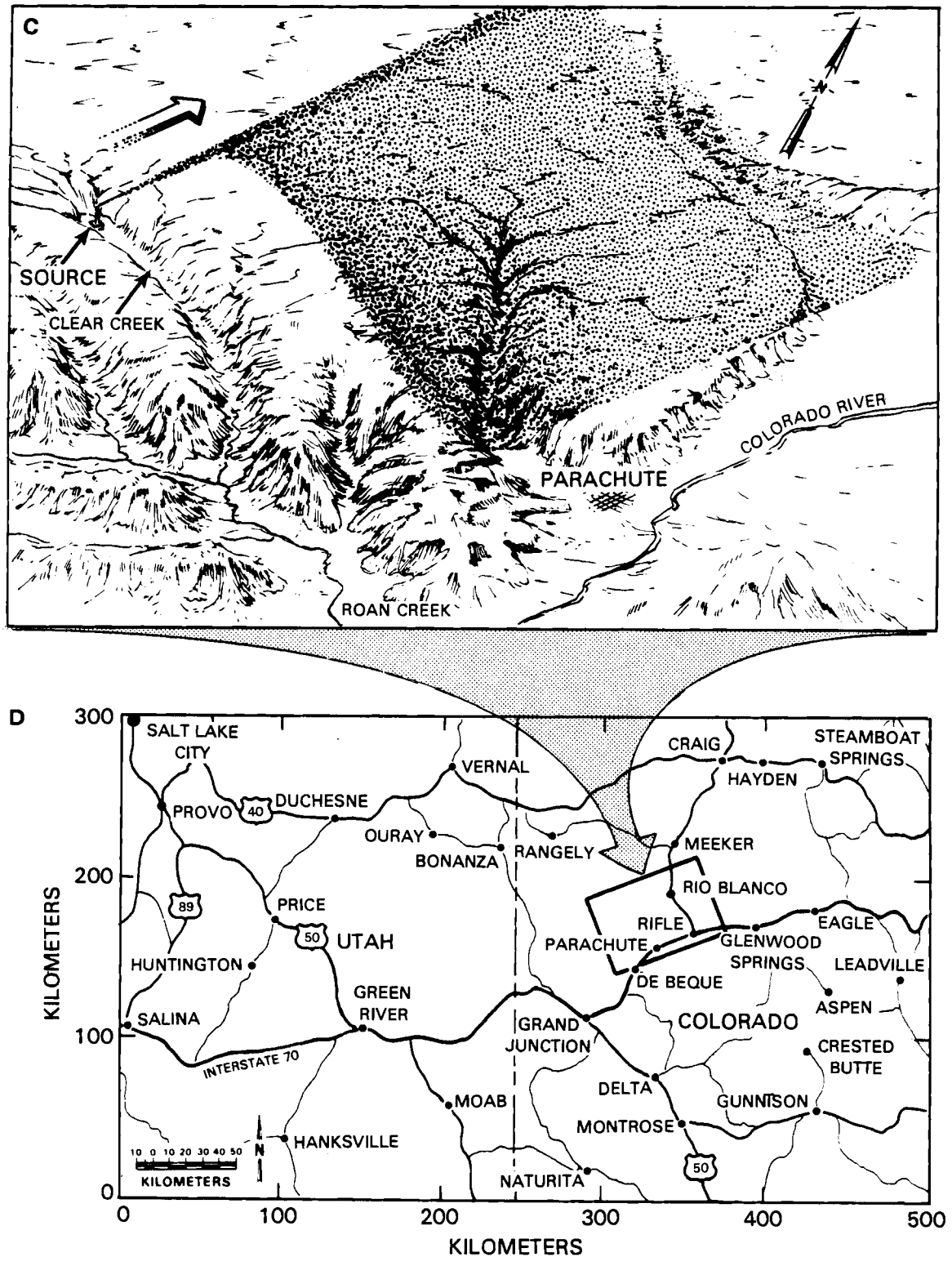

where

ℓ_T = distance down-valley from source to which valley is filled with pollutants (m)
u_v = mean down-valley wind speed (m/s)
Δt_D = total time valley flow is decoupled from above ridgetop flow (s).

From ℓ_T the number of valley segments, n_s, used in modeling the particular episode can be determined by choosing the valley segment end point nearest to ℓ_t. This is demonstrated in Figure 2-19 where two down-valley distances, ℓ_{T_1} and ℓ_{T_2}, are shown. ℓ_{T_1} is nearest to the end point of segment 2 and ℓ_{T_2} is nearest to the end point of segment 3. Thus, segments 1 and 2 are used in the simulation of ℓ_{T_1}, and segments 1, 2, and 3 are used for a_{T_2}.

FIGURE 2-19

DETERMINATION OF NUMBER OF VALLEY SEGMENTS USED TO REPRESENT TWO DIFFERENT DOWN-VALLEY TRANSPORT DISTANCES, ℓ_{T_1} and ℓ_{T2}

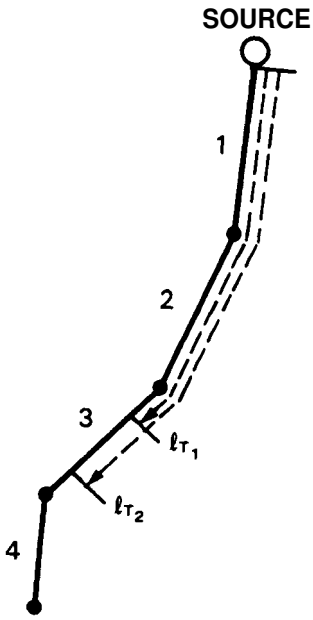

At sunrise the coupling process begins, and the valley is treated as a segmented line source in the mesoscale model. The line source extends from the point source in the valley to a distance ℓ_T' down-valley where

$$\ell_T' = \sum_{i=1}^{n_s} \ell_i \qquad (2\text{-}100)$$

Tracking puffs are released at each valley segment end point and the start of the first segment. The movement of these tracking puffs over the modeling time step defines quadrilaterals, which are then treated as described in Section 2.5.7. Before the puff simulation can start, the initial a_y and a_z of the tracking puffs must be defined. The initial σ_Y and σ_z of the valley tracking puffs are defined as

$$\sigma_y = 1/2\ W_{vt}$$
$$\sigma_z = \sigma_z(W_{vt}/U) \qquad (2\text{-}101)$$

where W_v is the valley width at ridge tops (m), and U is the above ridge-tops win6 speed (m/s). The σ_z is determined by evaluating σ_z (using the equations in the section on Diffusion Coefficient) for a travel time of W_{vt}/U.

The total amount of pollutant material present in each valley segment at sunrise is

$$M_{s_i} = \frac{Q\ \Delta t_D}{\ell_i/\ell_T} \qquad (2\text{-}102)$$

where

M_{s_i} = mass of pollutant in the i^{th} valley segment (μg)
Q = emission rate from source ($\mu g/s$)
Δt_D = total time valley flow is decoupled from above ridgetop flow (s)
ℓ_i = length of i^{th} valley segment (m).

This pollutant material is released over the duration of time required to break up the valley temperature inversion. This release rate is described in Section 2.4.4, in addition to the criteria for determining when a valley atmosphere is coupled or decoupled from the above-ridgetop winds.

2.5.9 Interpolation

Several quantities are required by the puff model that vary in time and space over the modeling region and are supplied to the model in discrete time and space steps. Consequently, interpolation techniques are necessary to get values for the desired quantities at locations and times other than those supplied. These quantities are the three components of winds, terrain heights, mixed-layer heights, stability classifications, temperatures, pressures, friction velocities, convective velocities, and Monin-Obukov lengths.

Linear interpolation techniques are applied in MELSAR, although three different approaches are used depending on the quantity being interpolated. Because the winds are described in three dimensions and are described analytically in space, they are treated differently than the other quantities, which are described in a gridded fashion in the horizontal direction only. The gridded terrain heights are treated differently from the mixed-layer heights and other meteorological quantities. Given below are descriptions of the three approaches.

2.5.9.1 Interpolation of Winds

In MELSAR the three components of winds are described analytically on up to 15 'surfaces' above the ground for each hour. The winds at a point, P, at time, t, and space (X_p, Y_p, Z_p), are determined by linearly interpolating between the surface, Z_2, above the point and the surface, Z_1, below the point for the hour, t_1, before t and the hour, t_2, after t and then interpolating in time. The spatial interpolation factors are

$$S_2 = \frac{Z_p - Z_1}{Z_2 - Z_1} \qquad (2\text{-}103)$$

$$S_1 = 1 - S_2$$

The temporal interpolation factors are

$$T_2 = \frac{t - t_1}{t_2 - t_1} \qquad (2\text{-}104)$$

$$T_1 = 1 - T_2$$

Using the results of Equations (2-103) and (2-104), the winds at the point (X_p, Y_p, Z_p) at time t are

$$\begin{aligned} u &= T_2[S_2u_2(t_2) + S_1u_1(t_2)] + T_1[S_2u_2(t_1) + S_1u_1(t_1)] \\ v &= T_2[S_2v_2(t_2) + S_1v_1(t_2)] + T_1[S_2v_2(t_1) + S_1v_1(t_1)] \\ w &= T_2[S_2w_2(t_2) + S1w1(t2)] + T1[S2w2(t1) + S1w1(t1)] \end{aligned} \qquad (2\text{-}105)$$

where

u,v,w = components of winds at desired point

$u_2(t_2), v_2(t_2), w_2(t_2)$ = winds at surface above point, at hour after point

$u_1(t_2), v_1(t_2), w_1(t_2)$ = winds at surface below point, at hour after point

$u_2(t_1), v_2(t_1), w_2(t_1)$ = winds at surface above point, at hour before point

$u_1(t_1), v_1(t_1), w_1(t_1)$ = winds at surface below point, at hour before point.

The determination of the winds, on the surfaces used for interpolation, is given in Section 2.4.1.

2.5.9.2 Interpolation of Mixing Height and Meteorological Parameters

Mixing height, stability, and other meteorological parameters are determined at a point (X,Y) at time, t, from gridded values, by linear interpolation in time and bilinear interpolation in space.

Assume we have some gridded quantity, Q, at discrete times $t_1, t_2, \ldots, t_n$. The value of Q at point P and time t, which is between times t_1 and t_2 is computed using the following procedure. The configuration and definition of terms is given in Figure 2-20. The spatial interpolation factors are

$$S_{2X} = \frac{X_p - X_i}{X_{i+1} - X_i}$$

$$S_{1X} = 1 - S_{2X} \qquad (2\text{-}106)$$

$$S_{2Y} = \frac{Y_p - Y_i}{Y_{i+1} - Y_i}$$

$$S_{1Y} = 1 - S_{2Y}$$

and the temporal interpolation factors are

$$T_2 = \frac{t - t_1}{t_2 - t_1}$$

$$T_1 = 1 - T_2 \qquad (2\text{-}107)$$

FIGURE 2-20

NOMENCLATURE USED FOR THE INTERPOLATION
OF GRIDDED VALUES OF Q TO POINT P

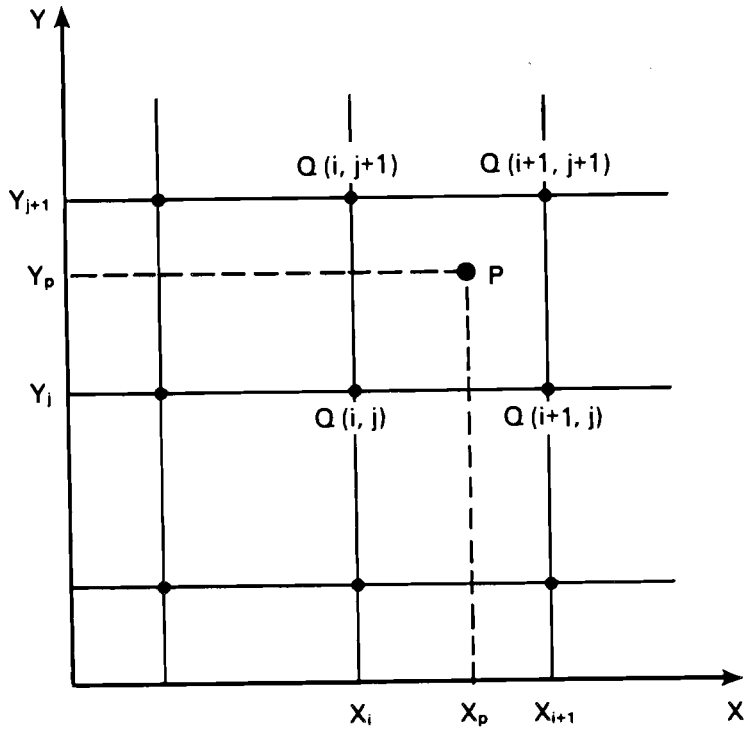

Therefore, the quantity Q at point P and time t is

$$Q = T_2[S_{1X}S_{1Y}Q(i,j;t_2) + S_{2X}S_{1Y}Q(i+1,j;t_2) + S_{1X}S_{2Y}Q(i,j+1;t_2) + S_{2X}S_{2Y}Q(i+1,j+1;t_2)] + T_1[S_{1X}S_{1Y}Q(i,j;t_1) + S_{2X}S_{1Y}Q(i+1,j;t_1) + S_{1X}S_{2Y}Q(i,j+1;t_1) + S_{2X}S_{1Y}Q(i+1,j;t_1)] \quad (2\text{-}108)$$

2.5.9.3 Interpolation of Terrain Heights

The terrain surface is represented by averaged elevations given at discrete points on a rectangular grid covering the region (refer to

Section 2.3). Using bilinear interpolation, as described above, to find elevations defines a shape to the terrain internal to the grid points that is probably not realistic. A more realistic representation of the area internal to grid points can be determined by using more than the four terrain points around the point, P, at which the terrain height is desired. Using sixteen grid points around the desired point, as shown in Figure 2-21, results in the elevation at point P coniputed as

$$\begin{aligned} P_H = {} & \beta_1[\alpha_1 TH(i-1,j-1) + \alpha_2 TH(i,j-1) + \alpha_3 TH(i+1,j-1) + \alpha_4 TH(i+2,j-1)] \\ & + \beta_2[\alpha_1 TH(i-1,j) + \alpha_2 TH(i,j) + \alpha_3 TH(i+1,j) + \alpha_4 TH(i+2,j)] \\ & + \beta_3[\alpha_1 TH(i-1,j+1) + \alpha_2 TH(i,j+1) + \alpha_3 TH(i+1,j+1) + \alpha_4 TH(i+2,j+1)] \\ & + \beta_4[\alpha_1 TH(i-1,j+2) + \alpha_2 TH(i,j+2) + \alpha_3 TH(i+1,j+2) + \alpha_4 TH(i+2,j+2)] \end{aligned} \quad (2\text{-}109)$$

where

P_H = elevation at point P (m MSL)

TH = elevation at grid points (m MSL)

$\alpha_1 = -1/6\ a\ (1-a)(2-a)$

$a_2 = 112\ (1+a)(1-a)(2-a)$

$\alpha_3 = 1/2\ a\ (1+\alpha)(2-\alpha)$

$\alpha_4 = -116\ a\ (1+\alpha)(1-\alpha)$

$\beta_1 = -1/6\ \beta\ (1-\beta)(2-\beta)$

$\beta_2 = 1/2\ (1+\beta)(1-\beta)(2-\beta)$

$\beta_3 = 1/2\ \beta\ (1+\beta)(2-\beta)$

$\beta_4 = -116\ \beta(1+\beta)(1-\beta)$

$a = (X_P - X_i)/\Delta X$

$\beta = (Y_P - Y_j)/\Delta Y$

X_P = X-coordinate of point P (km)

X_i = X-coordinate of i^{th} grid point (km)

AX = terrain grid spacing in X-direction (km)

Y_P = Y-coordinate of point P (km)

Y_j = Y-coordinate of j^{th} grid point (km)

ΔY = terrain grid spacing in Y-direction (km).

FIGURE 2-21

DEFINITION OF TERMS USED TO COMPUTE TERRAIN HEIGHT, AND X- AND Y- DIRECTION SLOPES, AT POINT P

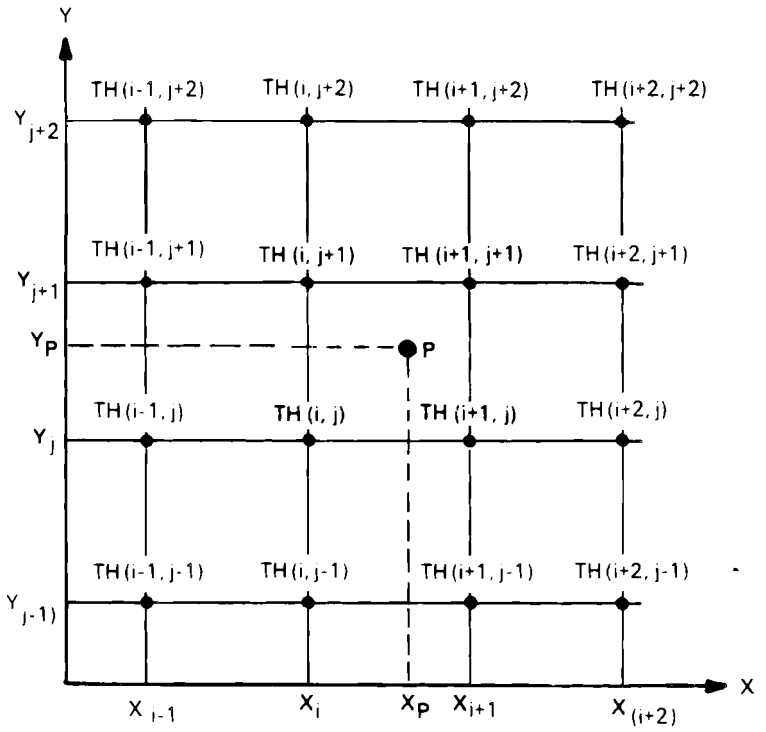

The terrain slopes at point P are computed as

$$P_X = \frac{TH(i+1,j) - TH(i-1,j)}{2\Delta X} \qquad (2\text{-}110)$$

$$P_Y = \frac{TH(i,j+1) - TH(i,j-1)}{2\Delta Y}$$

where

P_X = terrain slope in X-direction
P_Y = terrain slope in Y-direction.

2.5.10 Diffusion Coefficients

The horizontal and vertical diffusion coefficients are based on an approach presented by Pasquill (1976) and further discussed by Irwin (1979) and Ramsdell, Hanna and Cramer (1982). The square of the total horizontal diffusion is the sum of the squares of three components: 1) an initial diffusion resulting from nonatmospheric processes (e.g., buoyant plume rise), 2) diffusion resulting from atmospheric turbulence, and 3) diffusion resulting from horizontal wind-direction shear. The square of the total vertical diffusion is the sum of the squares of two components: 1) an initial diffusion resulting from nonatmospheric processes, and 2) diffusion resulting from atmospheric turbulence. In mathematical form, the horizontal diffusion coefficient is

$$\sigma_y = (A_y^2 + B_y^2 + C_y^2)^{1/2} \qquad (2\text{-}111)$$

where

a_y = the horizontal diffusion coefficient (m)
A_y = initial diffusion resulting from buoyant plume rise (m)
B_y = horizontal diffusion resulting from atmospheric turbulence (m)
C_y = horizontal diffusion resulting from horizontal wind shear (m).

The vertical diffusion coefficient is

$$\sigma_z = (A_z^2 + B_z^2)^{1/2} \qquad (2\text{-}112)$$

where

σ_z = vertical diffusion coefficient (m)
A_z = initial diffusion due to buoyant plume rise (m)
B_z = vertical diffusion due to atmospheric turbulence (m).

In the rest of this section the determinations of A_Y and A_z, C_y, B_y, and B_z are given.

2.5.10.1 Diffusion Resulting from Buoyant Plume Rise - A_Y and A_z

As discussed by Pasquill (1976) and recommended by the AMS Workshop (Hanna et al. 1977), for strongly buoyant plumes the vertical motion of the plume relative to the surrounding air contributes to both vertical and horizontal plume spread. Numerous observations of plumes near the stack by Briggs (1972) show that the plume radius is approximately equal to half the plume rise. Based on this and assuming the horizontal and vertical

diffusion to be affected equally by plume rise, Bjorkland and Bowers (1982) compute initial diffusion as $0.5\ \Delta h/2.15$. Therefore, A_Y in Equation (2-111) and A_z in Equation (2-112) are evaluated by

$$A_y = A_z = \frac{0.5\ \Delta h}{2.15} \qquad (2\text{-}113)$$

2.5.10.2 Diffusion Resulting from Wind Direction Shear - C_y

As pointed out by Pasquill (1976), horizontal wind shear adds a component to total horizontal diffusion. As a rough rule, Pasquill suggests adding a component of variance to σ_Y^2 (C_Y^2 in Equation (2-111)), which is equal to $0.03\ \Delta\theta^2 s^2$ where $\Delta\theta$ is the turning of wind direction over the total depth of the plume, in radians. This correction is for a steady-state plume. In MELSAR the diffusion resulting from wind shear must be numerically accumulated along the path of the puff. This is done using the equation

$$C_y(s+\Delta s) = C_y(s) + \Delta s \left.\frac{dCy(s)}{ds}\right|_{s+\Delta s/2} \qquad (2\text{-}114)$$

where

$$\frac{dC_y(s)}{ds} = 0.173\ \Delta\theta$$

$\Delta\theta$ = wind direction shear through depth of puff evaluated at $s+\Delta s/2$ (radians)
Δs = distance puff center of mass traveled in one time step (m)
s = puff travel distance (m).

$\Delta\theta$ is determined by computing the difference in wind direction between the winds at three σ_z above the puff center of mass and three σ_z below the puff center of mass. If three σ_z above the puff center of mass is above the top of the mixed layer, then the height of the mixed layer is used as the upper limit. If three σ_z below the puff center of mass is below the terrain, then the terrain is used as the lower limit. For a uniformly distributed puff in the vertical direction, the upper boundary is the mixing height and the lower boundary is the ground surface.

2.5.10.3 Horizontal Diffusion Resulting from Atmospheric Turbulence - B_y

The modeling of the horizontal diffusion process in puff trajectory models requires that both plume diffusion and puff diffusion be treated.

Hanna, Briggs and Hosker (1982) and Gifford (1982) both point out the need for caution when using plume diffusion coefficients extrapolated to long travel distances in puff trajectory models.

The transition from plume diffusion to puff diffusion is dependent on the frequency of the input meteorology. As discussed by Hanna, Briggs and Hosker (1982), plume horizontal diffusion coefficients are measured experimentally when the sampling time, t_s, is much greater than the travel time, t, from the release point to the receptor arc. When t_s is much less than t, then instantaneous plume diffusion or puff (relative) diffusion is measured. The same principle applies to puff trajectory modeling. The sampling time is specified by the period of input meteorology, t_m (e.g., 1 hour). For any pollutant travel times in the model less than t_m, plume diffusion should be used. For any travel times much greater than t_m, puff diffusion should be used. A mix of plume and puff diffusion treatment is required when t_m is approximately equal to travel time.

The use of plume diffusion coefficients in puff trajectory models out to long travel distances (>50 to 100 km) could theoretically lead to the underprediction of short-term pollutant concentrations at these distances. This would result from the overprediction of horizontal diffusion caused by the double-counting of plume meander, by using plume diffusion coefficients, and by the integration of individual puffs in a time- and space-varying wind field. 'True' plume diffusion should already account for this integration of puffs in a varying wind field.

Gifford (1982) points out that if typical short-range plume diffusion coefficients are extrapolated to travel times corresponding to distances on the order of 100 to 200 km, the results will fall short of both observed and theoretical values by amounts ranging up to nearly an order of magnitude. Gifford attributes this to short-period turbulence sampling in determining horizontal plume diffusion. In other words, the sampling time was too short in comparison to the Lagrangian time scale and, therefore, not all the turbulent fluctuations were accounted for. Consequently, the particle spread more nearly resembles relative diffusion than time-averaged diffusion.

It can be deduced from Gifford's observations that, in light of the current state of knowledge on this subject, the use of extrapolated empirical 'plume' diffusion coefficients in puff trajectory models may not be a bad estimate of near-field plume diffusion as well as later 'puff' diffusion. However, the air pollution modeler should be aware that approaches for bounding the problem do exist (Gifford 1982), and the extrapolation of short-range plume diffusion coefficients is certainly not the final answer.

The approach used in MELSAR for treating horizontal diffusion combines a method proposed by Pasquill (1976) for plume diffusion and Gifford's approach for treating both plume and puff diffusion.

Near-Field Plume Diffusion--The horizontal diffusion coefficient for plumes used in MELSAR is of the form recommended by Hanna et al. (1977) after Pasquill and described by Irwin (1979)

$$B_y = \sigma_v \, t \, f_y \tag{2-115}$$

where

σ_v = the standard deviation of the horizontal cross-wind component of the wind (m/s)
f_y = a nondimensional function of travel time
t = puff travel time (s).

For nonstationary, nonhomogeneous conditions, B_y is evaluated using a 'virtual time', t_v, in Equation (2-115) for a puff traveling from time t to time $t+\Delta t$, where Δt is the model time step. The virtual time is the total time a puff would have had to travel to be the size of the puff at time t for atmospheric conditions at time $t+\Delta t$. The equation for B_y then becomes

$$B_Y \, (t+\Delta t) = \sigma_v \, [t_v+\Delta t] \, f_Y \, (t_v+\Delta t) \tag{2-116}$$

The value of t_v is determined from Equation (2-116) using Newton's method.

Rewriting Equation (2-116) in the form

$$g(t_v) = [f_y(t_v)]_{t+\Delta t} \, t_v - \frac{[B_y(t)]_t}{[\sigma_v]_{t+\Delta t}} = 0 \tag{2-117}$$

and then finding the first derivative

$$g'(t_v) = [f_y(t_v)]_{t+\Delta t} \, t_v + [f_y(t_v)]_{t+\Delta t} \tag{2-118}$$

we can set up an iterative scheme to converge on t_v where

$$[t_v]_{n+1} = [t_v]_n - \frac{g([t_v]_n)}{g'([t_v]_n)} \tag{2-119}$$

In Equation (2-119) $[t_v]_n$ at n=l is set equal to the actual puff travel time t. Then $[t_v]_{n+1}$ is evaluated. If the ratio g/g' is ≤ 1 the iteration stops, otherwise the iterative procedure continues until g/g' ≤ 1 or n = 6.

This general form of B_y as given in Equation (2-115) or (2-116) allows the effects of terrain roughness on diffusion to be incorporated directly through specification of σ_v as a function of terrain roughness.

Universal function f_y--Irwin (1983) reviewed several schemes for estimating diffusion coefficients. He described the horizontal diffusion after the-form given in Equation (2-115) and compared the results of several field experiments with five models of the universal function f_y. His results showed that a scheme by Cramer (1976) performed best for elevated releases and Pasquill's (1976) best for surface releases. However, Irwin also concluded that a scheme by Draxler (1976) performed almost as well as Pasquill's for the near-surface releases and almost as well as Cramer's for the elevated releases.

B_y in MELSAR [Equation (2-116)] is written as a function of travel time, and Draxler's forms of f_y are also written as functions of travel time. Irwin (1983) recommends that a simplified set of Draxler's equations be used to overcome some bias in Draxler's equations. Therefore, the 'Model 4' equation proposed by Irwin is used in MELSAR:

$$1/f_y = 1 + 0.9\ (t/1000)^{0.5} \qquad (2\text{-}120)$$

Standard deviation of horizontal component of winds σ_v--Currently the user has the option of specifying σ_v in one of two ways: 1) an interim scheme proposed by Irwin (1979), or 2) empirical relationships developed by MacCready, Baboola'l, and Lissaman (1974) which account for terrain roughness. In the future it will be desirable to set up MELSAR to use measured values of σ_v.

The first method for computing σ_v in MELSAR is a scheme proposed by Irwin (1979) in the absence of onsite measurements of σ_v. He proposes that for unstable conditions a relationship developed by Panofsky et al. (1977) should be used

$$\sigma_v/u_* = (12 - 0.5\ Z_\ell/L)^{1/3} \qquad (2\text{-}121)$$

where

u_* = surface friction velocity (m/s)
Z_ℓ = mixing height (m)
L = Monin-Obukov length (m).

For neutral and stable conditions, Irwin recommends the relationship of Binkowski (1978)

$$\sigma_v/u_* = 1.78 \qquad (2\text{-}122)$$

The determination of u_*, Z_ℓ, and L is given in Section 2.4.

The second option for σ_v that the user can specify is based on an approach given by MacCready et al. (1974) that accounts for the influence of terrain roughness on σ_v. Using the LO-LOCAT (Lo-Low Altitude Clear Air Turbulence Project) turbulence data, MacCready et al. developed empirical equations of σ_v and σ_w as a function of a measure of terrain roughness, wind speed, and height aboveground.

The turbulence data used by MacCready et al. (1974) were from a major observational program (LO-LOCAT) conducted for the Air Force Flight Dynamics Laboratory by Boeing Aircraft Company. LO-LOCAT used jet aircraft with excellent instrumentation to assess complete spectra in three dimensions; along 32-mile path lengths; at 250- and 750-ft altitudes; covering high mountains, low mountains, desert, plains, and water; for all seasons; for three times of day including dawn; for four areas near Edwards Air Force Base (AFB) (California), Griffins AFB (New York), Peterson Field (Colorado). and McConnell AFB (Kansas). The LO-LOCAT goal was to provide statistical data for work on aircraft gust load and control, but the reports do not present the meteorological data stratified in a manner suitable for diffusion studies in complex terrain. However, MacCready et al. examined the LO-LOCAT data from the Edwards AFB flights from the standpoint of diffusion in the mountain-desert regions of the southwest United States.

The empirical equations of σ_v developed by MacCready et al. are

for very stable conditions

$$\sigma_v = 0.186\ R_T^{0.35} U^{0.18} Z^{-0.13} \qquad (2\text{-}123)$$

for stable conditions

$$\sigma_v = 0.231\ R_T^{0.28} U^{0.06} Z^{-0.04} \qquad (2\text{-}124)$$

where

R_T = a measure of terrain roughness (m)
U = average wind speed (m/s)
Z = height aboveground (m).

MacCready et al. (1974) did not present results for neutral and unstable conditions. If these relationships are available, they will be included in MELSAR at a later date. Irwin (1983) pointed out that Hinds and Nickola (1967) concluded from their analysis of the Dry Gulch, Prairie Grass, Green Glow, and Mountain Iron data that the influence of local climate and terrain on diffusion is increased during stable atmospheric conditions and decreased during unstable conditions; that is, the

atmospheric mixing is sufficient during moderately unstable atmospheric conditions to outweigh local terrain effects. Therefore, the interim scheme for determining σ_v for option 2 in MELSAR is as follows: Equation (2-123) will be used for very stable conditions, Equation (2-124) will be used for stable and neutral conditions, and option 1 will be used for unstable conditions. That is, Irwin's (1979) scheme described earlier will be used for determining σ_y during unstable conditions. A plot of Equations (2-123) and (2-124) are given in Figure 2-22 for a height of 50 m and a wind speed of 5 m/s for the neutral case and 2.5 m/s for the very stable case.

R_T is a measure of terrain roughness derived by MacCready et al. (1974) that best correlated with the turbulence data they analyzed. The method for computing R_T is given in Section 2.3.

FIGURE 2-22

PLOT OF a_y VERSUS TERRAIN ROUGHNESS (R_T) FROM MACCREADY et al.'s (1974) EMPIRICAL RELATIONSHIPS ASSUMING A HEIGHT ABOVEGROUND OF 50 m AND A WIND SPEED OF 5 m/s FOR NEUTRAL CONDITIONS AND 2.5 m/s FOR VERY STABLE CONDITIONS

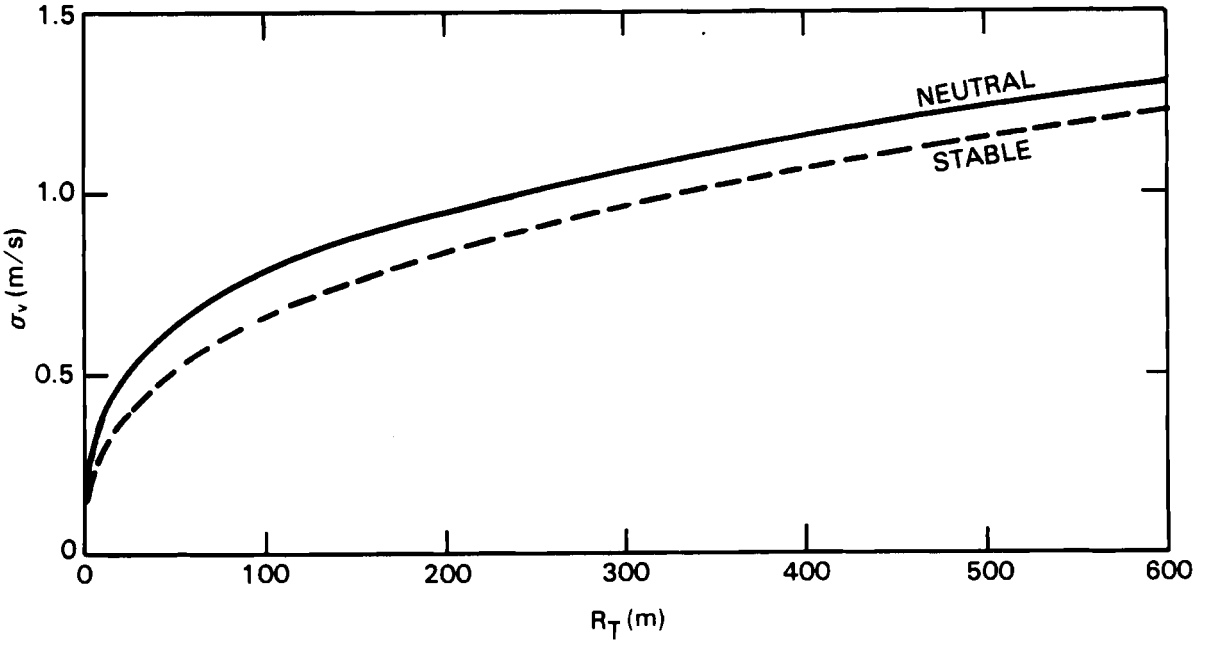

Far-Field Puff Diffusion and the Transition from Plume to Puff--Gifford (1982) solved a form of Lagevin's equation applicable to atmospheric diffusion. The resulting equation describes both puff and plume horizontal diffusion and combinations of the two, for small and large diffusion times. Currently, Gifford's equation is used in MELSAR to describe puff diffusion. However, after more testing of his plume diffusion approach in the future, Gifford's full scheme may be used in MELSAR.

The horizontal diffusion is described using the following equation

$$B_y^2 = 2Kt - \frac{2K^2}{\sigma_v^2}\left[1 - e^{-\frac{\sigma_v^2 t}{K}}\right] - \frac{CK^2}{\sigma_v^2}\left[1 - e^{-\frac{\sigma_v^2 t}{K}}\right]^2 \qquad (2\text{-}125)$$

where

B_y = horizontal diffusion coefficient resulting from atmospheric turbulence (m)
K = large-scale eddy diffusivity (m^2/s)
σ_v = the standard deviation of the horizontal component of the wind (m/s)
t = pollutant travel time (s)
$C = 1 - V_o^2/\sigma_v^2$, where V_o is the instantaneous turbulence level at the source.

The parameter C in Equation (2-125) varies between zero and unity depending on the value of V_o^2/σ_v^2, which, in effect, is the ratio of the instantaneous turbulence level at the source to that of the entire flow. Therefore, when $C = 0$, plume diffusion is described by Equation (2-125) and when $C = 1$, puff diffusion is described. A typical value of the large-scale eddy diffusivity, K, is 1.5×10^4 m^2/s, which is the default value specified in MELSAR.

Figure 2-23 gives a plot of B_y versus travel time for the two extremes of Equation (2-125): plume diffusion ($C = 0$) and puff diffusion ($C = 1$). The K value is 1.5×10^4 m^2/s and σ_v is 0.6 m/s. The σ_v is representative of neutral atmospheric stability determined from a relationship by Binkowski (1978) where $\sigma_v/u_* = 1.78$. The surface friction velocity, u_*, for this example case was determined from the logarithmic wind profile, $U = u_*/0.4 \ln (Z/Z_o)$; assuming the surface roughness, $Z_o = 0.03$ m; the height, $Z = 10$ m; and the wind speed, $U = 5$ m/s.

Also plotted in Figure 2-23 are curves of horizontal plume diffusion coefficients based on universal functions proposed by various researchers, determined from diffusion data. Shown are curves using Cramer (1976), Doran, Horst and Nickola (1978), Draxler (1976), and Pasquill-Gifford (Turner 1970) relationships. These are all assumed to be representative of neutral atniospheric stability. Doran, Horst and Nickola's and Cramer's curves are plotted from the relationship $B = \sigma_v\, t\, f_y(x/U)$ assuming σ_y = 0.6 m/s and U = 5 m/s, Draxler's curve is {lotted from $B_y = \sigma_y\, t\, f_y(t)$, and Pasquill-Gifford's curve from the well-known curves in Turner's Workbook (1970) assuming U = 5 m/s to convert from downwind distance to travel time. The f_y functions for Doran, Horst, and Nickola (1978), Cramer (1976), and Draxler (1976) are given in Table 2-12.

The plume curves are shown extrapolated beyond the limits of the data used to derive them. All the empirical plume curves are below the theoretical plume curve of Gifford's. It is not clear why Gifford's curve is

TABLE 2-12

f_y FUNCTIONS USED TO COMPUTE HORIZONTAL PLUME DIFFUSION

Doran, Horst and Nickola (1978)	X (km)	0.1	0.2	0.4	0.8	1.6	3.2	$10^{(a)}$
	f_y^{b}	1.04	0.98	0.92	0.85	0.77	0.67	0.54
Cramer (1976)	$f_y = (50/X)[(X-5)/45]^{0.9}$							
Draxler (1976)	$f_y = [1 + 0.9(t/1000)0.5]-1$							

(a) Extrapolated.
(b) Sampling time = 3600 s.

above all the empirical curves, especially for travel times less than 100 to 200 s. Since the experimental sampling times were on the order of 10 min to 1 hr, one would think that most of the turbulent fluctuations contributing to the diffusion at these short travel times would have been accounted for through the relatively long sampling times. This point will require further investigation.

At travel times near or longer than the experimental sampling times one would expect the empirical plume curves to depart from Gifford's theoretical plume curve. That is, the measured diffusion is more and more representative of puff diffusion for longer travel times. This is shown in Figure 2-23, especially for Draxler's curve. Based on the hypothesis that Draxler's 'plume' curve is actually more and more representative of puff diffusion for longer and longer travel times, and considering that there are no data on transition from plume to puff, then the extrapolated Draxler curves will be used to represent plume to puff transition in the Melsar model. Consequently, Draxler's curves will be followed by MELSAR from point-of-release to their intersection with Gifford's theoretical puff curve. Beyond that time, the MELSAR model will specify the puff growth rate by Equation (2-125) with C = 1 (puff). Figure 2-24 shows plots of Draxler's curve followed by Gifford's 'puff' curve for four values of a

As in Equation (2-115), Equation (2-125) is evaluated using the concept of a virtual time, t_y, when the puff travels from time t to time $t + \Delta t$. The solution of Equation (2-125) uses the same procedure as that described for Equation (2-115). To determine when puff growth is transferred from Draxler's curve to Gifford's curve, MELSAR evaluates Equations (2-115) and (2-125) for all time steps. As soon as B_y from Equation (2-125) is greater than that from Equation (2-115), the results from Equation (2-125) are used to grow the puff and Equation (2-115) is no longer evaluated.

FIGURE 2-23

HORIZONTAL DIFFUSION VERSUS TRAVEL TIME FOR NEUTRAL CONDITIONS
(σ_V = 0.6 m/s)

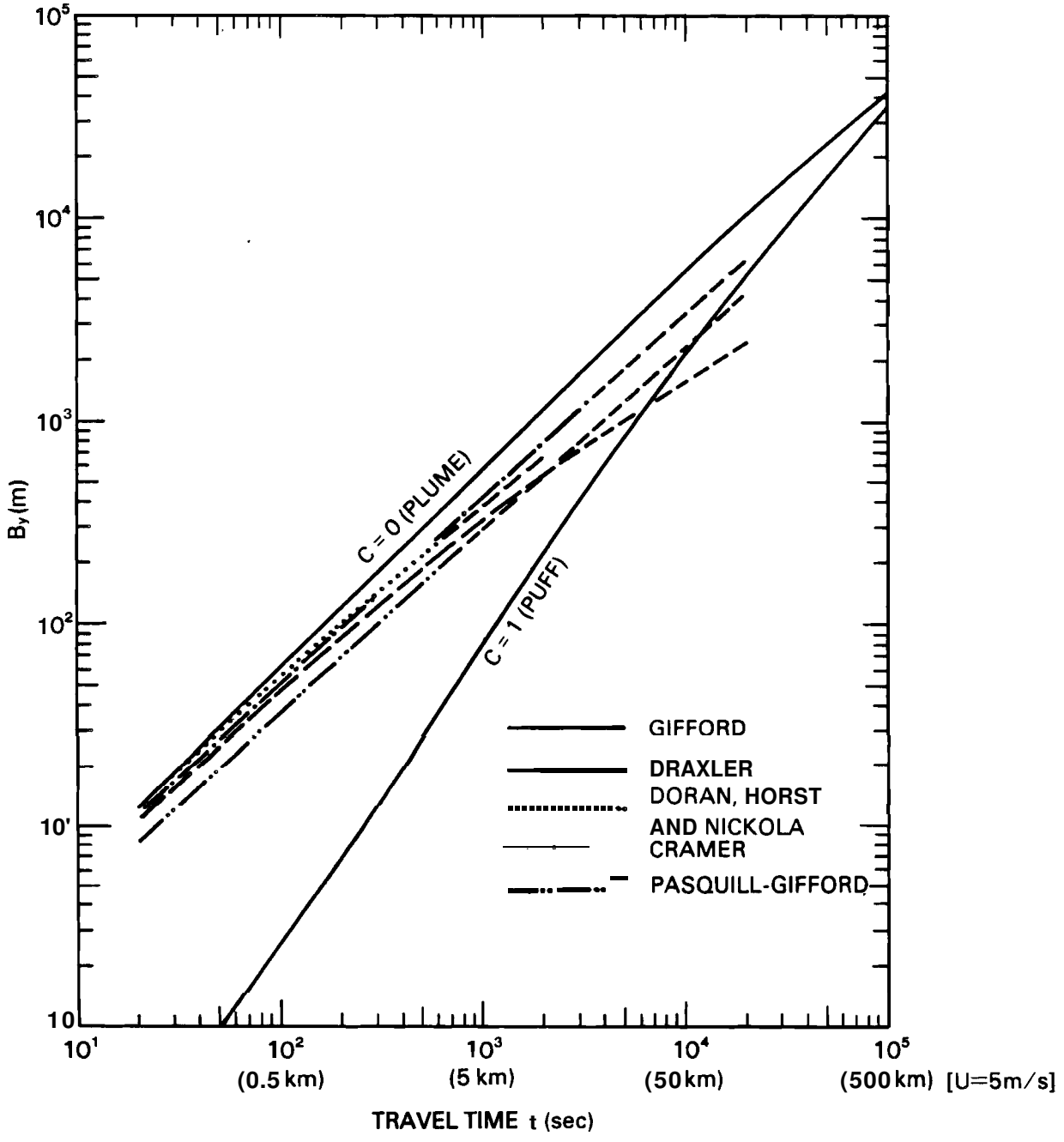

FIGURE 2-24

HORIZONTAL DIFFUSION VERSUS TRAVEL TIME USING DRAXLER'S (1976) EQUATION FOR THE NEAR FIELD AND GIFFORD'S (1982) EQUATION FOR THE FAR FIELD

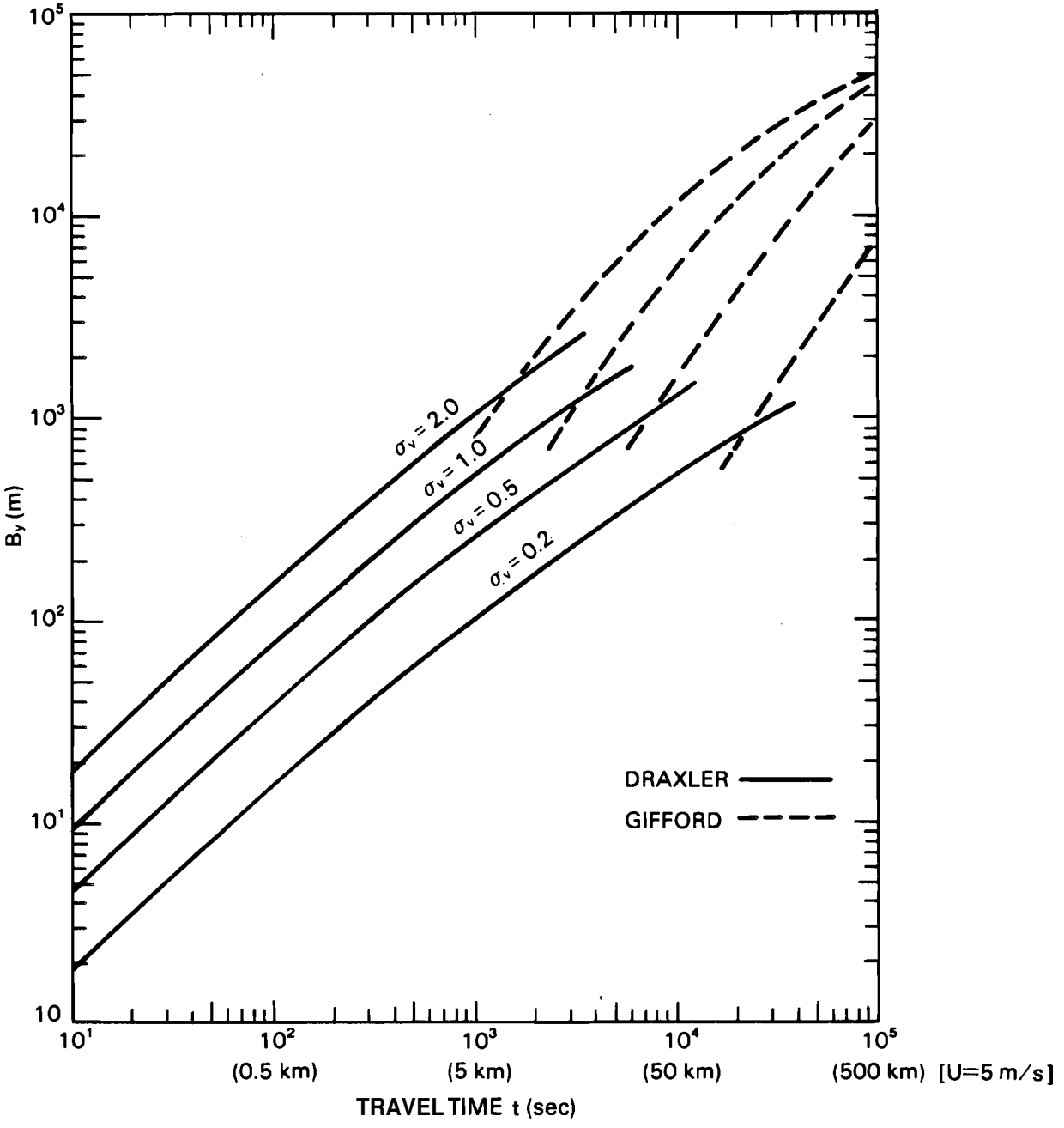

2.5.10.4 Vertical Diffusion Resulting from Atmospheric Turbulence - B_z

Few data exist for characterization of vertical diffusion, especially at long travel times. In addition, characterization for long travel times of vertical diffusion is not as important as that for horizontal diffusion because the pollutant becomes uniformly mixed through the mixing depth relatively quickly. Therefore, properly characterizing the mixing depth and the puff height relative to the mixing depth is more important than characterizing the vertical diffusion coefficient for long travel times. Based on these considerations, plume versus puff diffusion will not be treated in detail as was done for horizontal diffusion. The vertical diffusion in MELSAR will be determined from empirical plume coefficients extrapolated out to travel times of 2×10^4 s (100 km at 5 m/s winds) and by a method recommended by Heffter (1965) for travel times greater than 2×10^4 s.

The vertical diffusion resulting from atmospheric turbulence used in MELSAR for travel times less than 2×10^4 s is of the form described by Irwin (1979)

$$B_z = \sigma_w \, t \, f_z \qquad (2\text{-}126)$$

where

σ_w = the standard deviation of the vertical component of the wind (m/s)
t = travel time (s)
f_z = a nondimensional function, primarily a function of travel time.

Equation (2-125) is evaluated using the concept of a virtual time, t_v, for the puff traveling from time t to time $t+\Delta t$. Equation (2-126) becomes

$$B_z(t+\Delta t) = \sigma_w \, (t_v+\Delta t) \, f_z(t_v+\Delta t) \qquad (2\text{-}127)$$

The solution of Equation (2-127) uses the same procedure as that described for Equation (2-116).

This general form of B_z as given by Equation (2-126) or (2-127) allows the effects of terrain roughness on diffusion to be incorporated directly through specification of σ_w.

For travel times greater than 2×10^4 s, B_z is evaluated using the relationship given by Heffter (1965):

$$B_z(t+\Delta t) = B_z(t) + \frac{0.5 \, (2 \, K_z)^{1/2} \, \Delta t}{\sqrt{t}} \qquad (2\text{-}128)$$

where

t = puff travel time (s)
Δt = model time step (s)
K_z = the vertical eddy diffusivity (m^2/s).

The default values of K_z are given in Table 2-13 and are equal to those used in MESOPUFF II (Scire et al. 1984).

TABLE 2-13

VERTICAL DIFFUSIVITIES BY PASQUILL-GIFFORD STABILITY CLASS

P-G	A	B	C	D	E	F
K_z (m^2/s)	50	30	15	7	3	1

Universal Function f_z--Irwin (1983) reviewed several schemes for estimating diffusion coefficients. He described the vertical diffusion after the form given in Equation (2-126) and compared the results of several field experiments with five models of the universal function f_z. His results showed that a scheme by Draxler (1976) performed best in characterizing the vertical diffusion. However, Irwin (1983) proposed a simplified set of Draxler's equations which perform as well as the full set and eliminate some bias at longer travel times. Irwin's 'Model 4' equations for f_z are used in MELSAR:

for unstable conditions

$$1/f_z = 1 + 0.9\ (t/500)^{0.5} \qquad (2\text{-}129)$$

for stable conditions

$$1/f_z = 1 + 0.9\ (t/50)^{0.5} \quad .$$

Standard Deviation of the Vertical Wind Component of a_w--Currently the user has the option of specifying σ_w in one of two ways: 1) an interim scheme proposed by Irwin (1979) or 2) empirical relationships developed by MacCready, Baboolal and Lissaman (1974) which account for terrain roughness. In the future it will be desirable to set up MELSAR to use measured values of σ_w.

The first method for computing a_w in MELSAR is a scheme proposed by Irwin (1979) to be used in the absence of onsite measurements of a_w. He proposes that the following relationships be used for unstable conditions:

$$\sigma_w/w_* = 1.342\ (Z/Z_\ell)^{0.33} \qquad Z/Z_\ell \leq 0.03$$

$$\sigma_w/w_* = 0.763\ (Z/Z_\ell)^{0.175} \qquad 0.03 < Z/Z_\ell \leq 0.40 \qquad (2\text{-}130)$$

$$\sigma_w/w_* = 0.722\ (1-Z/Z_\ell)^{0.207} \qquad 0.40 < Z/Z_\ell \leq 0.96$$

$$\sigma_w/w_* = 0.37 \qquad Z/Z_\ell > 0.96$$

where

w_* = convective velocity (m/s)
Z = height aboveground (m)
Z_ℓ = depth of mixed layer.

The relationships for σ_w/w_* given in Equation (2-129) were determined by Irwin from plotted data of Willis and Deardorff (1974) and Kaimal et al. (1976). For neutral and stable conditions Irwin recommends the relationships of Binkowski (1978) be used

$$\sigma_w/u_* = \left[\frac{\phi_m - Z/L}{1.2\ f_m}\right]^{1/3} \qquad (2\text{-}131)$$

where

u_* = surface friction velocity (m/s)
L = Monin-Obukov length (m)
Z = height aboveground (m)
$\phi_m = 1 + 5\ Z/L$, the nondimensional wind shear
$f_m = 0.4[1 + 3.39\ Z/L - 0.25^{\epsilon}\ (Z/L)^2] \qquad 0 < Z/L \leq 2.0$
$f_m = 0.4[6.78 + 2.39\ (Z/L-2)] \qquad Z/L > 2.0$

The determination of u_*, Z_ℓ, L, and w_* is given in Section 2.4 of this report.

The second option for σ_w is based on an approach given by MacCready, Baboolal and Lissaman (1974), which accounts for the influence of terrain roughness on σ_w. A background discussion on MacCready, Baboolal and Lissaman's approach is given in Section 2.5.10.3 of this report. The empirical equations of σ_w developed by MacCready, Baboolal and Lissaman are

for very stable conditions

$$\sigma_w = 0.123\ R_T^{0.42} U^{0.22} Z^{-0.17} \qquad (2\text{-}132)$$

for stable conditions

$$\sigma_w = 0.251\ R_T^{0.26} U^{0.05} Z^{-0.03} \qquad (2\text{-}133)$$

where

R_T = a measure of terrain roughness (m)
U = average wind speed (m/s)
Z = height aboveground (m).

MacCready, Baboolal and Lissaman did not present results for neutral and unstable conditions. If these relationships are available, they will be included in MELSAR at a later date. The interim scheme for determining σ_w for option 2 in MELSAR is: Equation (2-132) is used for very stable conditions, Equation (2-133) is used for stable and neutral conditions, and option 1 is used for unstable conditions. That is, Irwin's (1979) scheme described earlier is used for determining σ_w during unstable conditions. A plot of Equations (2-132) and (2-133) are given in Figure 2-25 for a height of 50 m and a wind speed of 5 m/s for the neutral case and 2.5 m/s for the very stable case.

FIGURE 2-25

PLOT OF σ_w VERSUS TERRAIN ROUGHNESS (R_T) FROM MACCREADY, BABOOLAL AND LISSAMAN'S (1974) EMPIRICAL RELATIONSHIPS ASSUMING A HEIGHT ABOVEGROUND OF 50 m AND A WIND SPEED OF 5 m/s FOR THE NEUTRAL CASE AND 2.5 m/s FOR THE VERY STABLE CASE

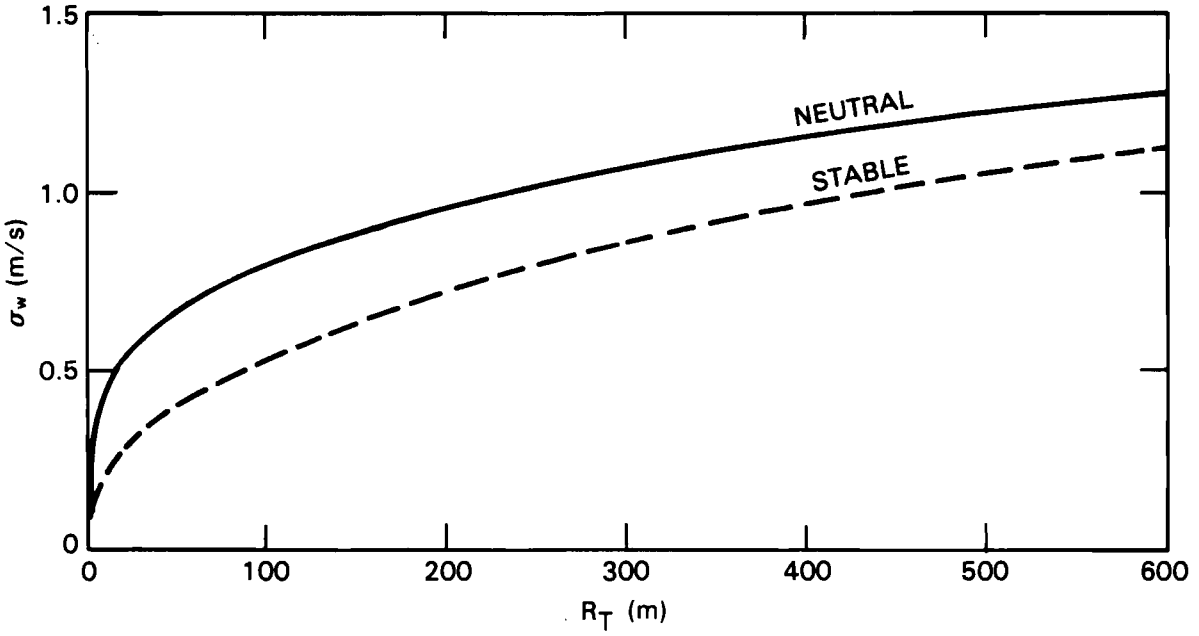

2.6 Averaging Process

POLUT creates a disk file of pollutant concentrations for one or two pollutants for all time steps of a simulation. The concentration at each receptor from each source is written out. These concentration values can then be operated on by the post-processor, POLPRC, to compute concentrations at various averaging times that can be compared with standards.

POLPRC computes moving average concentrations of pollutants at each receptor for up to three user-specified averaging times. The averaging times can range from 1 to 24 hr. The outputs are tables of highest and second highest pollutant concentrations for the duration of the simulation, at each receptor for each pollutant for each averaging time. The highest and second highest moving averages for the sum of all sources and the contribution of each source to the highest and second highest sum are computed. In addition, highest and second highest moving averages can be computed for each source individually. Tables of the time of occurrence of the highest and second highest values are also listed.

A moving average is simply an averaging process that progresses through the data by first computing an average using the number of hourly values required for the average and then computing a new average for each new hourly value encountered. For example, moving 3-hr averages would be computed by averaging the first three hourly values for the first average, the second through fourth values for the second average, the third through fifth values for the third average, and so on. Moving averages give a better estimate of peak average values, encountered over a duration of time, than block averaging.

Because all of the hourly concentrations resulting from a run of MELSAR are written to a disk file, any form of post-processing can be done by the user provided the software is available.

SECTION 3.0

USER'S GUIDE

Information and instructions for using MELSAR are provided in this section of the report. The reader should refer to Section 2.0 for technical details, and to Section 1.0 for a general description, applications, and limitations of MELSAR.

3.1 Introduction

MELSAR contains four main programs: TERRAIN, MET, POLUT, and POLPRC. It is written in FORTRAN 77 and is set up to run on a UNIVAC® 1108 computer. The code should be transferable to other systems and was developed on a VAX® 11/780 computer. This user's guide gives sufficient information for the user to set up and run MELSAR. A sample problem is carried through the guide from start to finish.

Section 3.2 provides the basis for the scoping, run setup, and operation of MELSAR. It gives an overview of MELSAR and identifies required inputs. If the user plans to make multiple runs of MELSAR or retain output files for later use, Section 3.2 also gives techniques for keeping track of the many input and output files. Finally, Section 3.2 describes the sample problem.

The four remaining sections in the user's guide give detailed instructions to the operator on input data format, job setup and execution, and diagnostic messages for using the four main programs of MELSAR. The sections are arranged as follows: Section 3.3 - TERRAIN program, Section 3.4 - MET program, Section 3.5 - POLUT program, and Section 3.6 - POLPRC.

Appendix B contains the UNIVAC® Job Control Language (JCL) files for compiling and mapping the four MELSAR programs. Appendix C gives the procedure for setting up the binary base terrain file.

®UNIVAC is a registered trademark of the Sperry Rand Corporation.
®VAX is a registered trademark of Digital Equipment Corporation, Maynard, Massachusetts.

3.2 Overall Scheme

To make a run of MELSAR the user must first define the problem, second determine and acquire the necessary inputs, and third set up the run and execute the required programs. This section gives an overview of this process and describes the sample problem.

3.2.1 Defining Application and Determining Inputs

MELSAR is designed to operate on a 500- by 450-km region covering western Colorado, eastern Utah, and southern Wyoming (refer to Figure 1-1 and the figures in Appendix A). This region is referred to as the GRAMA region in this user's guide. The MELSAR code can operate on any subpart of the GRAMA region, but the code has not been tested fully for this application. The coordinate system for the GRAMA region is a rectangular system and is described in Section 2.2. The user can specify input data in the GRAMA, UTM, or latitude-longitude coordinate systems. The GRAMA coordinate system can be laid out on a map using the latitude-longitude coordinates of the four corner points given in Table 2-2.

Once the modeling region is defined (either the whole GRAMA region or any subpart of it), the user can specify the required inputs. The modeling region is defined by specifying the origin in GRAMA coordinates and the length of each side in kilometers. For example, modeling the whole GRAMA region, the origin would be IXO = 0 km, IYO = 0 km, and the length of each side would be SLX = 500 km and SLY = 450 km.

The input data required by MELSAR are 1) gridded terrain data, 2) upper-air weather data, 3) surface weather data, 4) points to interpolate wind data to (primarily for boundary conditions), 5) gridded land-use categories, 6) source valley characteristics, 7) pollutant source inventory, and 8) receptor layout. All but the upper-air and surface weather data must be specified within the modeling region. Data from weather stations outside the modeling region can be used by MELSAR. The gridded terrain data are provided with MELSAR and do not have to be developed by the user. Also included with MELSAR are files of surface and upper-air weather data, wind interpolation points, and gridded land-use categories. These data files are described in Appendix D. Table 3-1 lists the required input data for MELSAR, and specifies certain constraints. The blank field at the end of the file names is used to keep track of the files and is explained in Section 3.2.4.

Depending on the modeling region chosen, the period of meteorology to be used, the sources to be modeled, and the receptor areas, the user may need to prepare new input data files for MELSAR. The procedures for preparing these files are given with the MET (Section 3.4) and POLUT (Section 3.5) operating instructions.

TABLE 3-1

INPUT DATA REQUIRED BY MELSAR

File Name	Description	Program	Format	General Use Files[a]	Files for Sample Problem[a]	Maximum Size or Constraints
TOPO	Base Terrain Data	TERRAIN	Unformatted	TOPO	TOPO	500 x 450 grid elements
UP_	Upper-Air Data	MET	Formatted	UP1 and UP2	UP2	10 stations, 600 soundings
SFC_	Surface Weather Data	MET	Formatted	SFC1 and SFC2	SFC2	15 stations, 10,800 records
WIP_	Wind Interpolation Points	MET	Formatted	WIP1 (whole domain)	WIP1	30 points
LANDU_	Land-Use Categories	MET	Formatted	LANDU1 (whole domain)	LANDU1	10 x 10 grid elements
VALLY_	Source Valley Characteristics	MET	Formatted		VALLY1	5 valleys, 10 segments/ valley
SOURC_	Source Inventory	POLUT	Formatted		SOURC1	5 point or area sources
RECPT_	Receptors	POLUT	Formatted		RECPT1	4 grids (25 x 25), 10 individual receptors

[a] Refer to Appendix D for details.

Once MELSAR has been run, output files from TERRAIN and MET are produced, in addition to the concentration files from POLUT. These output files, plus the concentration files, can be saved and used during other applications of MELSAR, thus saving the cost of regenerating these files. Table 3-2 lists the output files from MELSAR and their maximum sizes. Section 3.2.4 recommends a procedure for tracking these files for future use.

3.2.2 Program Interactions

MELSAR consists of four main programs named TERRAIN, MET, POLUT, and POLPRC. TERRAIN uses a base terrain file and produces files of spatially averaged terrain statistics for use by MET and POLUT. MET produces hourly winds, gridded mixing heights, stabilities, friction velocities, convective velocities, Monin-Obukov lengths, temperatures, pressures, and valley coupling coefficients, using upper-air and surface weather observations. POLUT uses the output files from MET and TERRAIN and produces pollutant concentrations, corrected to standard conditions, on a user-specified receptor network for each time step of a simulation. The concentration fields are used by POLPRC to compute moving-average concentrations of pollutants for up to three averaging times. The outputs from POLPRC are tables of highest and second highest pollutant concentrations at each receptor. Tables are produced for the sum of all sources along with the resulting contribution of each source to the sum. Also, highest and second highest concentration tables are generated for each receptor grid and set of individual receptors, considering each source individually. The interaction of the four main programs is given in Figure 1-2.

For the first application of MELSAR, all four programs must be executed. But for subsequent applications, the output files from TERRAIN or MET may be sufficient for running POLUT. This may be especially true when the user wants to make runs for additional sources using the same conditions. Figure 3-1 shows the interaction of the four main programs, the required run specification files, the input files, and the output files. It also shows that printed listings (PRINT$) result from a run of each program. These listings give summary results of each run to check that the program executed properly and to provide run documentation for later reference.

3.2.3 Sample Problem

Three hypothetical point sources, 'Source 1', 'Source 2', and 'Source 3' are located as shown in Figures 3-2 and 3-3. Source 3 is located in Clear Creek. Therefore, the characteristics of this valley will be required. The release heights are all at 60 m AGL with no plume rise. An SO_2 emission rate of 1000 g/s is assumed for each source. Two receptor grids and three individual receptors are located as shown in Figures 3-2 and 3-3. One grid contains 66 receptors covering a 20- by 40-krn portion of the

TABLE 3-2

NELSAR OUTPUT FILES

File Name	Description	Format	Program From	Program Used By	Maximum Size or Constraints
TERF_	Terrain Data for Froude Grid	Unformatted	TERRAIN	MET	30 records, 10 parameters/record
TERS_	Smoothed Terrain Data	Unformatted	TERRAIN	MET,POLUT	150 records, 50 parameters/record
FIGI_	Amplitude Functions	Unformatted	MET	POLUT	6,480 records[a], 66 parameters/record
BLPAR_	Boundary Layer Parameters	Unformatted	MET	POLUT	36,000 records[b], 11 parameters/record
MIXST_	Mixing Heights and Stabilities	Unformatted	MET	POLUT	14,400 records[c], 11 parameters/record
COEFF_	Valley Coupling Coefficient	Unformatted	MET	POLUT	3,600 records[d], 12 parameters/record
CONC_	Hourly Pollutant Concentrations	Unformatted	POLUT	POLPRC	363,600 records[e], 26 parameters/record

[a] 9 gamma surfaces/hr x 30 days x 24 hr/day
[b] 5 parameters/hr x 10 records/parameter x 30 days x 24 hr/day
[c] 2 parameters/hr x 10 records/parameter x 30 days x 24 hr/day
[d] 5 valleys/hr x 30 days x 24 hr/day
[e] 5 sources/hr x 101 records/source x 30 days x 24 hr/day (This must be multiplied by the puff release rate and the number of pollutants)

FIGURE 3-1

MELSAR INPUT AND OUTPUT FILES AND PROGRAM INTERACTIONS

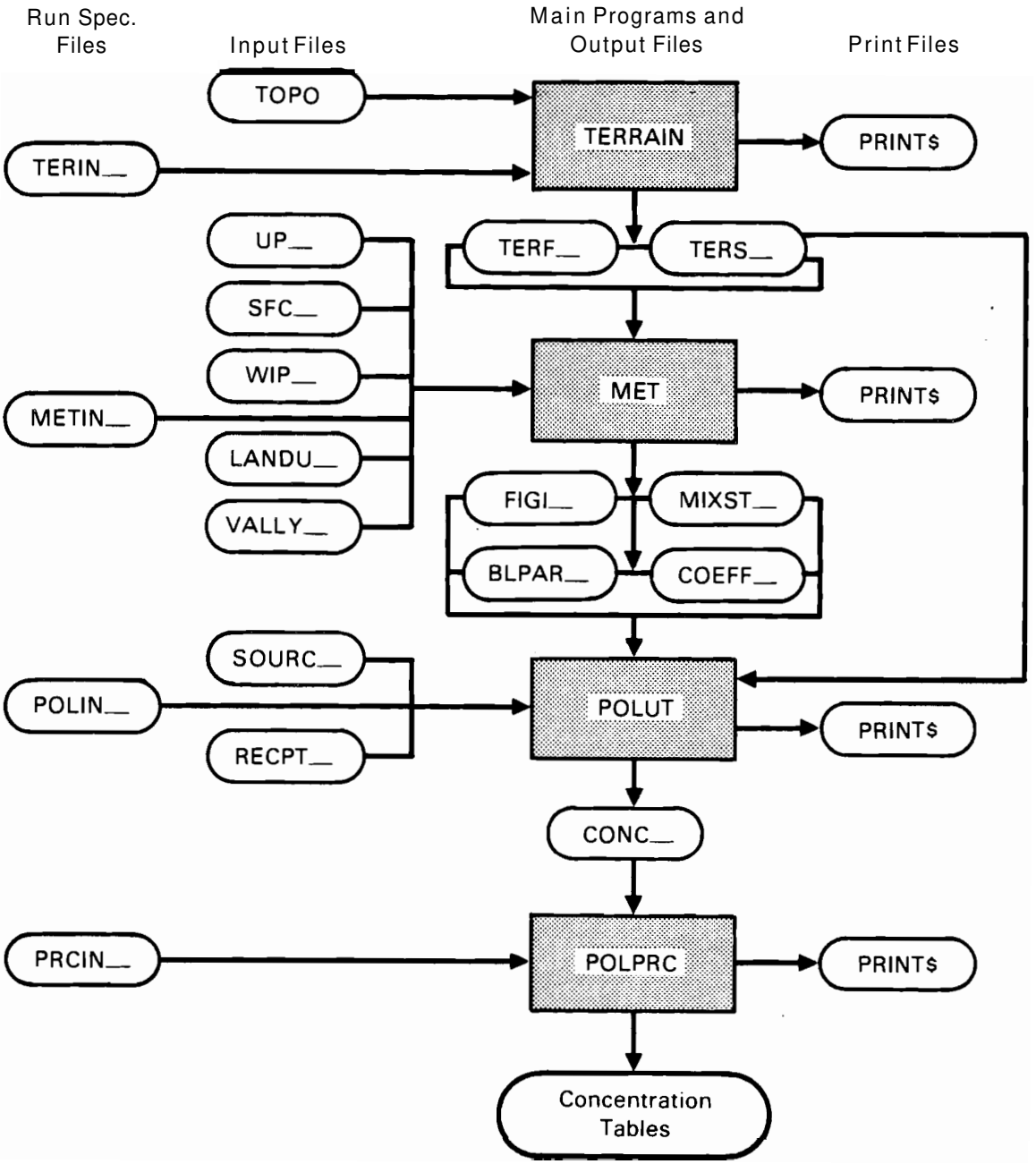

FIGURE 3-2

LOCATIONS OF POINT SOURCES AND RECEPTORS FOR THE SAMPLE PROBLEM

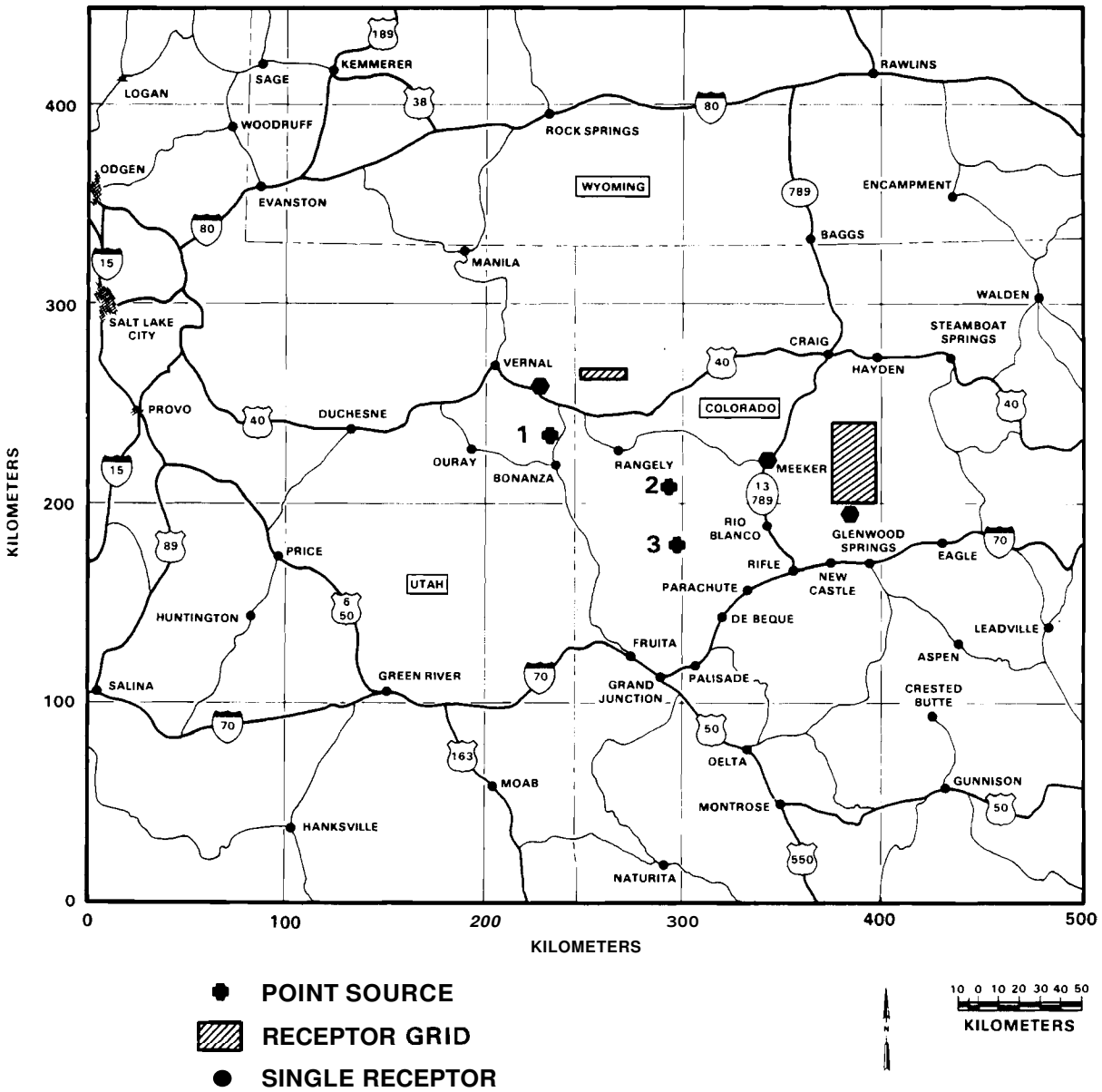

FIGURE 3-3

LOCATIONS OF POINT SOURCES AND RECEPTORS RELATIVE TO IMPORTANT IMPACT AREAS FOR THE SAMPLE PROBLEM

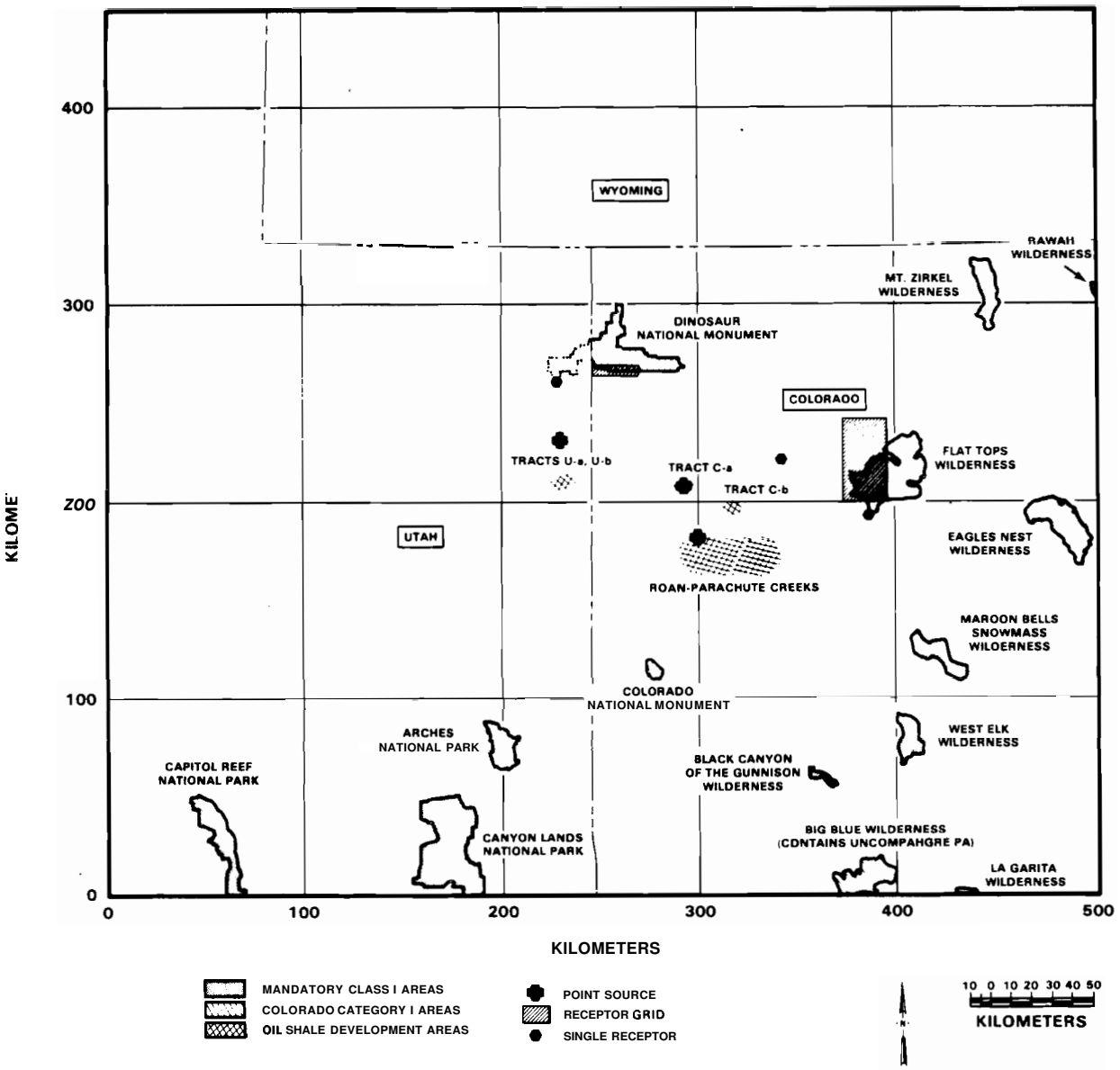

the Flattops Wilderness Area and the second grid contains 33 receptors covering a 20- by 4-km portion of the Dinosaur National Monument. Three individual receptors are located at the southern edge of the Flattops, at Meeker, Colorado, and at the Utah portion of the Dinosaur National Monument.

Pollutant concentrations are computed at each receptor for a 48-hr simulation period. The simulation period starts on July 11, 1978, at 0700 MST and ends July 13, 1978, at 0700 MST. Meteorological data from six upper-air stations and eight surface weather stations are used in the simulation. The locations of the meteorological stations are shown in Figure 3-4. The entire GRAMA region is used in the simulation.

The preparation of the run specification files, TERIN1, METIN1, POLIN1, and PRCIN1 are given in the following respective sections for each main program. The trailing blank field for each file name was filled with a '1' to denote sample problem. The input files used for the sample problem are TOPO, UP2, SFC2, WIP1, LANDU1, VALLY1, SOURC1, and RECPT1. They are described in Appendix D. All of the run specification files and input files necessary to run the sample problem are provided with MELSAR. The output files from TERRAIN, MET, and POLUT are named TERS1, TERF1, FIGI1, BLPAR1, MIXST1, COEFF1, and CONC1. The trailing blank field was assigned a '1', as with the run specification files. The summary listings from the execution of each program are given in Appendices H through K. Selected output concentration tables from POLPRC are given in Appendix L.

3.2.4 Multiple Runs and File Management

Inspection of Figure 3-1 shows four run specification files, eight input files, and seven output files are required for a run of MELSAR. In addition, once output files have been produced by runs of TERRAIN and MET, these files are available for use by POLUT for future runs. This section recommends an approach for keeping track of these many files required by the various components of MELSAR. The proper logging of the runs of MELSAR and the required files will ensure that documentation is available for future reference. Also, this will ensure that all of the run specification files, input data files, and output files will be available and retrievable for future runs of MELSAR.

The tools to help the user track these files are 1) the assignment of a run identification number unique to each run of TERRAIN, MET, POLUT, or POLPRC, 2) a simple file naming procedure, 3) summary sheets, kept up to date by the user, describing the input data files available, 4) file-log fo'rms filled in by the user, listing the names of the run specification files, input data files, and output files, for each run of TERRAIN, MET, POLUT, or POLPRC, 5) printed output summaries from each run of TERRAIN, MET, POLUT, or POLPRC, and 6) summary-of-runs forms for TERRAIN, MET, POLUT, and POLPRC, kept up to date by the user, listing each run made by run number.

FIGURE 3-4

LOCATIONS OF UPPER-AIR AND SURFACE WEATHER STATIONS
USED IN THE SAMPLE PROBLEM

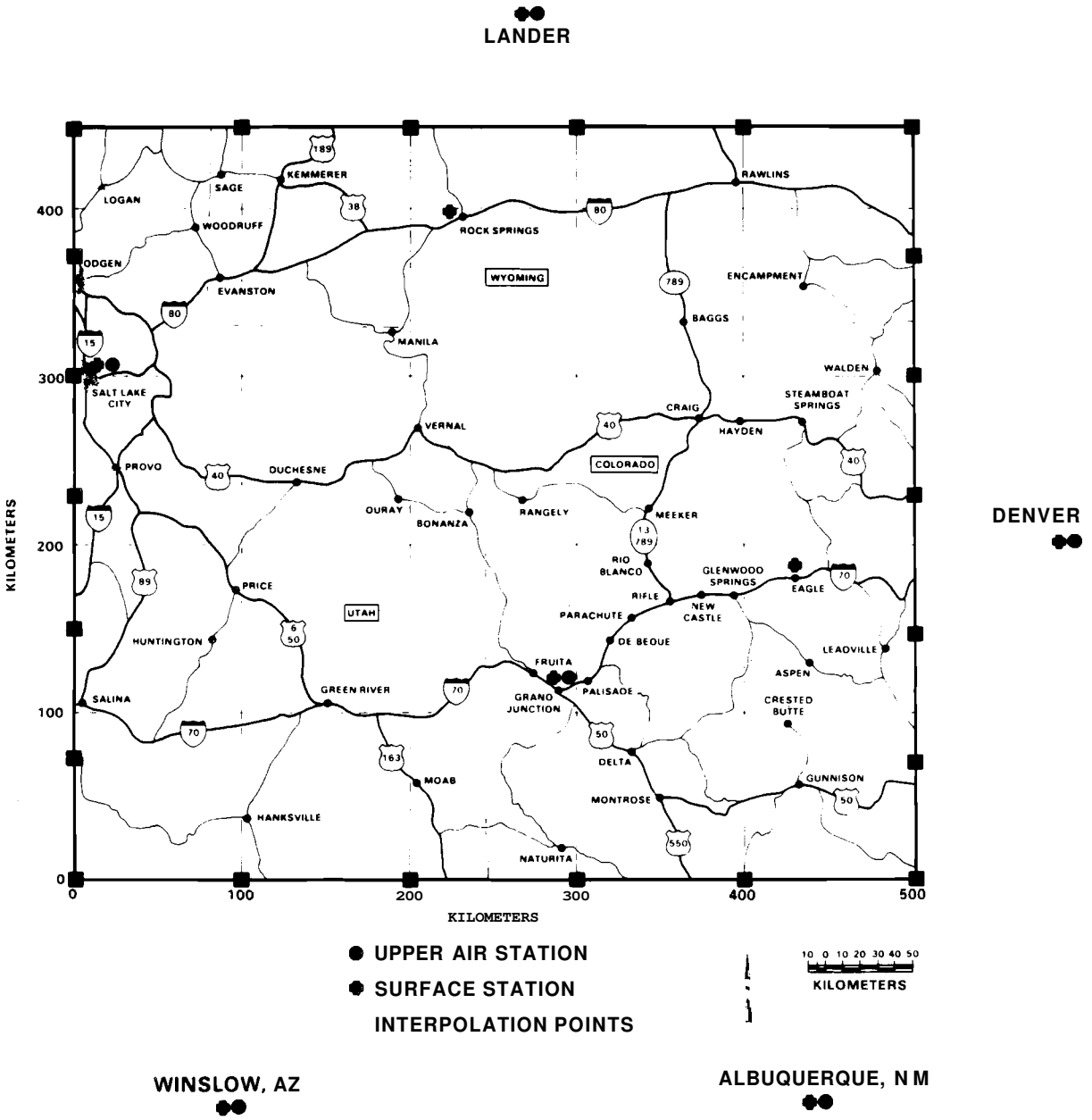

The cornerstone of the file tracking system is the run identification (ID) number. The file-log forms (item 4 above) and printed output summaries (item 5 above) from each run of TERRAIN, MET, POLUT, or POLPRC should be catalogued in a notebook by main program and run ID number. Therefore, when a particular run of interest is identified in the summary-of-runs form for TERRAIN, MET, POLUT, or POLPRC, the user can get detailed information about the run from items 4) and 5) above by just knowing the run ID number. A unique run ID number is specified in the run specification file of TERRAIN, MET, POLUT, or POLPRC as a 10-character alphanumeric string. A recommended numbering convention is to use the month, day, year, and hour at the time of a run. For example, a run of TERRAIN made on April 15, 1985, at noon would have a run ID number of ' 04158512 '.

The recommended file-naming convention for the run specification files and the output files is to fill the empty field at the end of the root file names given in Figure 3-1 with serial numbers starting with 1. This number would increase for each new run of TERRAIN, MET, or POLUT. For example, the run specification file and output files from the first run of MET would have names of METIN1, FIGI1, BLPAR1, MIXST1, and COEFF1.

The recommended file-naming convention for the input data files is the same as for the output files, except the number would increment for each new file of a particular type created. For example, two upper-air data files are provided with MELSAR, UP1 and UP2. If the user constructs a new upper air data set then he could name the file UP3, and log the information about the new file in the input data files summary sheets (item 3 above), which are given in Appendix D.

Provided in Appendix E are blank file-log (item 4 above) and summary-of-runs (item 6 above) forms. Appendix F shows these forms filled in for the sample problem, and Appendices H through K give the printed output summaries (item 5 above) for the sample problem.

3.3 TERRAIN Program

This section gives the UNIVAC® Job Control Language (JCL), run specifications, and input requirements for running TERRAIN. Inputs and resulting outputs for the sample problem are given. The user can refer to Section 2.3 for technical details of TERRAIN and Appendix O for a listing of the code.

3.3.1 Description

TERRAIN requires a run specification file, TERIN_, and one input file, TOPO, to operate, The input file is the base terrain file for the GRAMA modeling region. Two output files are produced by TERRAIN. One file contains smoothed terrain heights and averaged terrain roughness in the X-direction and Y-direction. The second file contains the terrain statistics used in the wind veering algorithm (Froude number based) of YET. Also

a run summary table is printed out for TERRAIN. Figure 3-1 shows the inputs and outputs for TERRAIN. The blank field at the end of file TERIN_, TERS_, and TERF is assigned a unique number for different runs. The field is set equal to—'1' for the sample problem. Section 3.2.4 discusses this in more detail.

TERRAIN requires approximately 250K words of memory to load on a UNIVAC® 1108 computer. It consists of one main program (AATER) and one subroutine; a total of approximately 350 lines of code with comments.

3.3.2 Job Control Language and Run Setup

The UNIVAC® JCL file, TERJCL, for running TERRAIN is given in Table 3-3. The first two lines in TERJCL show trailing periods. These indicate the need for additional general job information to be specified by the user. In addition, the /250/ in the first line indicates that a maximum of 250K words of memory will be required for the run. This file shows the input and output files needed for TERRAIN and the logical unit assignment for these files. The file names required for the sample problem are shown in the table. These files are provided with MELSAR in addition to file TERJCL.

TABLE 3-3

UNIVAC® JCL FILE, TERJCL, USED TO RUN TERRAIN

```
 1   @RUN TERAIN/250/.................
 2   @IDENT...................
 4   @ASG,A TERIN1.
 5   @USE 10,TERIN1.
 6   @ASG,A TOPO.
 7   @USE 11,TOPO.
 8   @ASG,UP TERS1.
 9   @USE 19. ,TERS1.
10   @ASG,UP TERF1.
11   @USE15. ,TERF1.
12   @XQT TERRAIN.AATER
13   @FIN
```

The run conditions for TERRAIN are specified in file TERIN_. The only run conditions required are the run identification, and the domain and grid size specifications. The contents of TERIN_ and the definition of each input element are given in Table 3-4. The range of values, variable type, and recommended values for each parameter are given in Table 3-5. The recommended values are for a run using the whole GRAMA region (refer to maps in Appendix A).

TERIN_ contains only three lines of entries where the entries are separated by commas (field-free format). Consequently this file can be easily created and modified using a UNIVAC® system editor.

Specifying the parameters in TERIN_ is straightforward once the domain size has been determined. That is, the domain origin (IXO, IYO) and the size in the X-direction (SLX) and Y-direction (SLY) have been defined. For the sample problem, the whole GRAMA region is being used, where IXO (and IXOF) is zero, IYO (and IYOF) is zero, SLX is 500 km, and SLY is 450 km. The number of grid cells in the X-direction for the smoothed terrain (NXC) is set at 50, the maximum number allowed. Therefore the cell size for the smoothed terrain (ICS) can be determined as ICS = SLX/NXC. For the sample problem, ICS is equal to 10 (500/50). The number of grid cells in the X-direction for the Froude grid (NXCF) is set at 10, the maximum number allowed. For the sample problem ICSF is equal to 50 (500110). ICS and ICSF must be greater than 1 km. The number of grid cells in the Y-direction can be determined as NYC = SLY/ICS, and NYCF = SLY/ICSF. For the sample problem NYC is 45 (450/10) and NYCF is 9 (450150).

The smoothing intervals IAI and IAIF must satisfy certain constraints. First IAI must be greater than ICS, and if ICS is an even integer number, then IAI must be even. If ICS is odd, then IAI must be an odd number. The same constraints must hold true for IAIF. For the sample problem IAI is 20 km and IAIF is 50 km. The user can refer to Section 2.3 for guidance in choosing appropriate smoothing intervals.

The run identification can be up to ten alphanumeric characters of the user's choice. It is recommended that the run identification contain the date and hour at the time of the run as discussed in Section 3.2.4. The run ID for the sample problem is ' 04158512 '. The parameter LEN is always set to 14 km. The run specification file, TERIN1, for the sample problem is given in Table 3-6.

3.3.3 Input Data Description

The only input data file required by TERRAIN is the base terrain file TOPO. File TOPO is an unformatted file containing 225,000 (500 x 450) elements. Each element is the average terrain elevation for a 1-km square. Section 2.3 gives the technical details of TOPO and a brief description is given in Appendix D. TOPO is provided with MELSAR, and Appendix C gives instructions for setting up TOPO to be used by TERRAIN.

TABLE 3-4

TERRAIN RUN SPECIFICATION FILE, TERIN_

File Contents and Format:

Line #	Contents
1	IDRUN
2	IXO,IYO,NXC,NYC,ICS,IAI,LEN
3	IXOF,IYOF,NXCF,NYCF,ICSF,IAIF

Parameter Definitions:

IDRUN = Run identification number

For Smoothed Terrain Grid -

IXO = X origin (km)
IYO = Y origin (km)
NXC = Number of grid cells in X-direction
NYC = Number of grid cells in Y-direction
ICS = Grid cell size (km)
IAI = Smoothing interval (km)
LEN = Length of segment in roughness computation (km)

For Froude Grid -

IXOF = X origin (km)
IYOF = Y origin (km)
NXCF = Number of grid cells in X-direction
NYCF = Number of grid cells in Y-direction
ICSF = Grid cell size (km)
IAIF = Smoothing interval (km)

3.3.4 Output Description

Two unformatted files result from TERRAIN. One file, TERS_, contains the 50 x 50 grid of smoothed terrain heights and terrain roughness. The other file, TERF_, contains the 10 x 10 grid of terrain statistics used in the wind veering algorithm (Froude number based). The user can refer to the main program (AATER) listing for the specific structure of these files. However, this information is not required by the user to run MELSAR. A print file also results from a run of TERRAIN. This file gives a summary of the specifications of the run. Appendix H lists the print file for the sample problem. The two output files from TERRAIN for the sample problem are TERS1 and TERF1.

TABLE 3-5

RANGE OF VALUES, VARIABLE TYPE, AND RECOMMENDED VALUES FOR EACH PARAMETER IN FILE TERIN_

Parameter	Variable Type	Range of Values	Recommended Value
IDRUN	CHARACTER	Up to 10 characters	
IXO	INTEGER	0 to 500 km	0
IYO	INTEGER	0 to 450 km	0
NXC	INTEGER	10 to 50	50
NYC	INTEGER	10 to 50	45
ICS	INTEGER	2 to 50 km	10
IAI	INTEGER	2 to 100 km	20
LEN	INTEGER	14	14
IXOF	INTEGER	0 to 500 km	0
IYOF	INTEGER	0 to 450 km	0
NXCF	INTEGER	10	10
NYCF	INTEGER	10	9
ICSF	INTEGER	2 to 50 km	50
IAIF	INTEGER	2 to 100 km	50

TABLE 3-6

TERRAIN RUN SPECIFICATION FILE, TERIN1, FOR THE SAMPLE PROBLEM

Line #	Contents
1	' 04158512 '
2	0,0,50,45,10,20,14
3	0,0,10,9,50,50

3.3.5 Diagnostic Messages

No diagnostic messages are included in TERRAIN. If the user gets any system error messages when executing TERRAIN, he should check to be sure the base terrain file TOPO is structured properly and the run specifications in file TERIN_ are declared properly.

3.4 MET Program

This section gives the UNIVAP JCL, run specifications, and input requirements for running MET. Inputs and resulting outputs for the sample problem are given. The user can refer to Section 2.4 for technical details of MET and Appendix P for a listing of the code.

3.4.1 Description

MET is a very flexible meteorological data processor. It is designed to receive upper-air and surface weather input data from many stations over different time periods and sampling intervals. It can handle missing data and was designed to handle any data that are available for a specified period of time. That is, observations from NWS stations, special studies or intensive field programs can be used.

MET requires a run specification file, METIN_, and seven input files, UP_, SFC_, WIP_, LANDU_, VALLY_, TERF_, and TERS_, to operate. The file UP_ contains the upper-air data, SFC contains the surface weather data, WIP_ contains the wind interpolation points on the boundaries of the domain, LANDU_ contains the gridded land-use categories from which surface roughness is determined, VALLY_ contains the characteristics of valley segments with sources in them, and TERF and TERS_ are terrain files from TERRAIN as described in Section 3.3.

Four output files are produced by MET, FIGI_, BLPAR_, MIXSP_, and COEFF_. The file FIGI_ contains the hourly amplitude functions which define the three-dimensional winds; BLPAR_ contains hourly gridded temperatures, pressures, friction velocities, convective velocities, and Monin-Obukov lengths; MIXST_ contains the hourly gridded mixing heights and PGT stability classes; and COEFF_ contains the hourly coupling coefficient for each valley segment. A run summary listing is printed out during a run of MET. Figure 3-1 shows the inputs and outputs for MET. The blank field at the end of METIN_, FIGI_, BLPAR_, MIXST_, and COEFF_ is assigned a unique number for different runs as described in Section 3.2.4.

MET requires approximately 70K words of memory to load on a UNIVAC® 1108 computer. It consists of one main program (AAMET) and 50 subroutines, a total of approxiniately 8000 lines of code with comments. One subroutine required by MET is an IMSL (International Mathematical and Statistical Libraries, Inc., Houston, Texas) system subroutine, LLSQF. This subroutine solves a set of equations using least-squares techniques. The UNIVAP JCL file listed in Appendix B for mapping MET contains LLSQF and the other system subroutines it requires. Appendix M contains tables detailing the subroutines interactions, common blocks, and parameter definitions in MET.

3.4.2 Job Control Language and Run Setup

The UNIVAC® JCL file, METJCL, for running MET is given in Table 3-7. This file shows the run specification file, input files, and output files needed for MET and the logical unit assignment for these files. The file names required for the sample problem are shown in the table. These files, in addition to file METJCL, are provided with MELSAR. Inspection of Table 3-7 shows that MET uses three temporary files (lines 15, 16 and 17)

TABLE 3-7

UNIVAC® JCL FILE, METJCL, USED TO RUN MET

```
 1  @RUNMET/100/.........................
 2  @IDENT.....................
 3  @ASG,A SFC2.
 4  @ASG,A UP2.
 5  @ASG,A WIP1.
 6  @ASG,A METIN1.
 7  @ASG,A TERF1.
 8  @ASG,A TERS1.
 9  @ASG,A LANDU1.
10  @ASG,A VALLY1.
11  @ASG,UP FIGI1.
12  @ASG,UP MIXST1.
13  @ASG,UP  BLPAR1.
14  @ASG,UP COEFF1.
15  @ASG,T UPWOUT.
16  @ASG,T UPTOUT.,///384/
17  @ASG,T SURWOUT.
18  @USE2,SFC2.
19  @USE 3,UP2.
20  @USE4,WIP1.
21  @USE8,UPWOUT.
22  @USE9,UPTOUT.
23  @USE 10,SURWOUT.
24  @USE12,FIGI1.
25  @USE14,METIN1.
26  @USE15,TERF1.
27  @USE17,MIXST1.
28  @USE19,TERS1.
29  @USE20,BLPAR1.
30  @USE25,LANDU1.
31  @USE26,VALLY1.
32  @USE27, COEFF1.
33  @XQT MET.AAMET
34  @FIN
```

during its execution. These are direct-access disk files and are transparent to the user as long as enough free disk space is available during a run. The trailing periods in the first two lines indicate additional UNIVAC® run information is required (e.g., account, user ID). In addition, the /100/ in the first line indicates that a maximum of 100K words of memory will be required for the run.

The run conditions for MET are specified in file METIN_. The contents of METIN_ and the definition of each input element are given in Table 3-8. The range of values, variable type, and recommended values for each parameter are given in Table 3-9. The recommended values are for a run using the whole GRAMA domain. The run specification file, METIN1, for the sample problem is given in Table 3-10.

METIN_ contains only seven lines of entries where the entries are separated by commas (field-free format). Consequently, this file can be easily created and modified using a UNIVAP system editor. The entries in METIN_ can be grouped into five categories: run initialization, domain, output grid, wind field, and other parameters. Specifying the entries in each category is discussed next.

3.4.2.1 Run Initialization

The run initialization entries are specified in lines one and two of METIN (refer to Table 3-8). IDRUN is set as discussed in Section 3.2.4. The simulation starting hour in IBEG, and ending hour in IEND, must be after sunrise and before sunset. If these conditions are not met by IBEG or IEND, MET will set the start hour to 2 hr after sunrise for a wrongly specified IBEG, and will set the ending hour to 2 hr before sunset for a wrongly specified IEND. The hour entries in MET must be specified as 01 to 24 (versus 00 to 23) where 24 is midnight. IBTZ is always set at 7 (Mountain Standard Time) for the GRAMA region. The USENAM field can be any 10 character alphanumeric string of the user's choice. The user's name is recommended.

The DETAIL logical variable, if specified .TRUE., directs MET to print out details of the run. This includes, in addition to the summary information, hourly input and output winds at the input points; hourly gridded mixing heights, stabilities, temperatures, pressures, friction velocities, convective velocities and Monin-Obukov lengths; and hourly valley coupling coefficients for each valley segment. The printed output is about three pages per simulation hour plus 12 summary pages. Therefore the sample problem (48 hours) would result in about 160 pages of printed output. If Froude number adjustments are applied to the wind field, the printed output is about 4 pages per simulation hour plus 13 summary pages. Consequently, the user should exercise caution when specifying DETAIL equal to .TRUE. for multiday simulations. The printed output for the sample run was 148 pages for DETAIL equal to .TRUE., and 7 pages for DETAIL equal to .FALSE..

TABLE 3-8

MET RUN SPECIFICATION FILE, METIN_

File Contents and Format:

Line #	Contents
1	IDRUN,IBEG,IEND,IBTZ,USENAM,DETAIL
2	NSTA,NSSTA,NVALE,NOSTA
3	IXO,IYO,SLX,SLY
4	ALAT,URLONG
5	NTEMAX,IHH,HH,NGAMA,(HTGAMA(K),K=1,NGAMA),FROU
6	IXOS,IYOS,NXCS,NYCS,ICSS
7	RAD,ZNOT,DS

Parameter Definitions:

IDRUN = Run identification number
IBEG = Simulation begin time in (MO DAY YR HR) in base time zone, (e.g., July 11, 1978 at 0800 is 07117808)
IEND = Simulation end time in base time zone
IBTZ = Base time zone, 5 (Eastern), 6 (Central), 7 (Mountain), 8 (Pacific)
USENAM = User name
DETAIL = Logical variable, if .TRUE., means print out detailed results of run
NSTA = Number of upper air stations
NSSTA = Number of surface weather stations
NVALE = Number of valleys with pollutant sources
NOSTA = Number of wind interpolation points
IXO = X-origin of modeling domain in GRAMA coordinates (km)
IYO = Y-origin of modeling domain in GRAMA coordinates (km)
SLX = Length in X-direction of modeling domain (km)
SLY = Length in Y-direction of modeling domain (km)
ALAT = Latitude of center of modeling region (deg)
URLONG = Longitude of center of modeling region (deg)
NTEMAX = Number of basis terms used in wind field fit
IHH = Defines form of top boundary to wind flow,
= 1 sets top boundary at a constant height above the terrain
= 2 sets top boundary at a constant mean-sea-level height
HH = Height of top boundary AGL or MSL, dpepending on whether IHH=1 or IHH=2, respectively (m)
NGAMA = Number of 'gamma' surfaces to compute winds on
HTGAMA = Array of heights of 'gamma' surfaces, values between 0.0 → 1.0
FROU = Logical variable, if .TRUE., then adjust wind field according to Froude number considerations
IXOS = X-origin of grid for yridded outputs (e.g., mixing heights), should be the same as IXO

TABLE 3-8

MET RUN SPECIFICATION FILE, METIN_ (Continued)

Parameter Definitions:

IYOS = Y-origin of grid for gridded outputs, should be equal to IYO
NXCS = Number of grid cells in X-direction for output grid
NYCS = Number of grid cells in Y-direction for output grid
ICSS = Grid cell size of output grid (km)
RAD = Distance greater than which 1/r2 weighted interpolation will not be performed (km)
ZNOT = Surface roughness (m), if equal to 999. then surface roughness will be determined from gridded land-use categories
DS = Seed for random number generator, which is used to vary wind directions input at whole 10 degree intervals.

NSTA is the number of upper-air stations in the upper air data input file UP_, NSSTA is the number of surface weather stations in file SFC_, NVALE is the number of valleys in file VALLY_, and NOSTA is the number of wind interpolation points in file WIP_.

3.4.2.2 Domain

The domain to be modeled can be the entire GRAMA region or any part of it. The parameters IXO, IYO, SLX, and SLY specify the domain. They are defined in Table 3-8. IXO and IYO specify the origin in GRAMA coordinates, and SLX and SLY specify the size of the domain in the X-direction and Y-direction, respectively. The units of IXO, IYO, SLX, and SLY are kilometers. The two input terrain files, TERS_ and TERF_ from TERRAIN, must match the domain specified in MET.

ALAT and URLONG specify the latitude and longitude, in degrees, of the center of the modeling domain. This coordinate is used in computing the time of sunrise and sunset for specifying the simulation starting hour and ending hour. Consequently, ALAT and URLONG specified to the nearest tenth of a degree is more than adequate.

3.4.2.3 Output Grid

Hourly mixing heights, stabilities, temperatures, pressures, friction velocities, convective velocities, and Monin-Obukov lengths are specified on the output grid. This grid is defined by IXOS, IYOS, NXCS, NYCS, and ICSS.

TABLE 3-9

RANGE OF VALUES, VARIABLE TYPE, AND RECOMMENDED VALUES FOR EACH PARAMETER IN FILE METIN_

Parameter	Variable Type	Range of Values	Recommended Value
IDRUN	CHARACTER	Up to 10 characters	
IBEG	INTEGER	8 digits (MMDDYYHH)	
IEND	INTEGER	8 digits (MMDDYYHH)	
IBTZ	INTEGER	5 to 8	7
USENAM	CHARACTER	Up to 10 characters	
DETAIL	LOGICAL	.TRUE. or .FALSE.	.FALSE.
NSTA	INTEGER	1 to 10	6 (using UP1 or UP2)
NSSTA	INTEGER	1 to 15	8 (using SFC1 or SFC2)
NVALE	INTEGER	1 to 5	
NOSTA	INTEGER	1 to 30	22 (using WIP1)
IXO	INTEGER	0 to 500 km	0
IYO	INTEGER	0 to 450 km	0
SLX	REAL	20. to 500. km	500.
SLY	REAL	20. to 450. km	450.
ALAT	REAL	38. to 42. deg	40.
URLONG	REAL	106. to 112. deg	109.
NTEMAX	INTEGER	10, 15 or 21	10
IHH	INTEGER	1 or 2	1
HH	REAL	100. to 6000. m (IHH=1)	1500.
		3500. to 6000. m (IHH=2)	4000.
NGAMA	INTEGER	3 to 9	5
FROU	LOGICAL	.TRUE. or .FALSE.	.FALSE.
IXOS	INTEGER	0 to 500 km	0
IYOS	INTEGER	0 to 450 km	0
NXCS	INTEGER	10	10
NYCS	INTEGER	10	9
ICSS	INTEGER	2 to 50 km	50
RAD	REAL	50. to 1000. km	500.
ZNOT	REAL	0.001 to 1.0 m (or 999.)	999.
DS	DOUBLE PREC	1.D0 to 2147483647.D0	1.D0

TABLE 3-10

MET RUN SPECIFICATION FILE, METIN1 FOR THE SAMPLE PROBLEM

Line No.	Contents
1	' 04158512 ',07117807,07137807,7,' MR JONES ',.FALSE.
2	6,8,1,22
3	0,0,500,450
4	40. ,109.
5	10,1,1500.,5, .0033,.067,.2, .533,1.,.FALSE.
6	0,0,10,9,50
7	500. ,999. ,1.D0

IXOS and IYOS specify the grid origin in GRAMA coordinates, NXCS and NYCS are the number of grid cells in the X and Y direction, and ICSS is the grid cell size in kilometers. IXOS and IYOS are set equal to IXO and IYO. Then dividing the longer of SLX or SLY by 10 will give ICSS. The number of grid cells in the longer dimension will be 10 and the number of grid cells in the shorter dimension will be SLX or SLY divided by ICSS. A constraint is that SLX and SLY must be multiples of ICSS. For the sample problem SLX is equal to 500 and SLY is equal to 450. Therefore, ICSS is equal to 50 (500/10), making NXCS equal to 10, and NYCS equal to 9 (450/50).

3.4.2.4 Wind Field

Winds are specified on up to nine 'gamma' surfaces that are conformal to the terrain and the upper boundary. The top gamma surface is the upper boundary to the flow and the lowest gamma surface should be set between 3 to 10 m above the ground. The upper boundary is specified with IHH and HH. For IHH equal to one, the upper boundary is terrain-following at HH meters above the ground. And for IHH equal to two, the upper boundary is at a constant mean-sea-level height of HH. When IHH is equal to two, HH must be higher than the highest terrain in the modeling region.

NGAMA specifies the number of gamma surfaces and the array HTGAMA specifies the gamma surface heights in the nondimensional vertical coordinate, gamma (refer to Figure 2-8). Gamma varies between zero and one, and, therefore, the gamma surface heights are specified between zero and one. The top gamma surface height should always be set equal to 1.0. The user may want to space the gamma surfaces closer together near the ground and farther apart up higher. For the sample problem, five gamma surfaces (NGAMA=5) were used and the upper boundary was defined as terrain-following (IHH=1) at 1500 m AGL (HH=1500). The gamma surfaces chosen were at 0.0033, 0.067, 0.2, 0.533, and 1.0, corresponding to 5, 100, 300, 800, and 1500 m AGL.

The logical variable FROU specifies whether or not the wind field should be modified using Froude number considerations. (The reader can refer to Section 2.4.1 for technical details). If set equal to .TRUE. then the winds are modified. The user should keep in mind that employing this option will increase the execution of MET.

3.4.2.5 Other Parameters

Three final parameters must be specified to run MET. RAD gives a separation distance in kilometers greater than which $1/r^2$ weighted interpolation will not be performed. This is used in the interpolation of upper-air data to the surface weather stations, and in the interpolation of data to the output grid. RAD should be large enough to be sure at least every point is covered by at least one upper-air station. A value of 500 km is recommended. ZNOT specifies the surface roughness if a constant value is desired over the region, or specifying ZNOT equal to 999. requests the determination of surface roughness from the gridded land-use categories. DS gives the seed for the random number generator, which adds variation to the wind direction for inputs in whole 10 degrees.

3.4.3 Input Data Description

Seven files are required as input by MET as shown in Figure 3-1. Two files, TERF and TERS_ are unformatted files from program TERRAIN. The preparation of these two files is described in Section 3.3. The remaining five files, UP_, SFC_, WIP_, LANDU_, and VALLY_ are formatted files prepared by the user. A set of these files are provided with MELSAR and are described in Appendix D and Table 3-1. The VALLY_ file provided with MELSAR, VALLY1, will not be of general use because it is just for Clear Creek. The user will have to prepare other VALLY_ files for the valleys with sources they are modeling. The name and description of any new files prepared should be entered into the list of available files given in Appendix D. Described next are instructions for the preparation and formatting of the UP_, SFC_, WIP_, LANDU_, and VALLY_ files. The input files used in the sample problem are UP2, SFC2, WIP1, LANDU1, VALLY1, TERF1, and TERS1.

3.4.3.1 Preparation of the Upper-Air Data File UP_

Two upper-air data files, UP1 and UP2, are provided with MELSAR. They are described in Appendix D and should be of general use to the user. File UP1 is a formatted file and contains upper-air data from six NWS radiosonde stations for the month of January 1978. File UP2 is for July 1978.

Detailed instructions for the preparation of new UP_ files is not given here. If the user has a data set that he would like to prepare for use with MELSAR, detailed instructions to do this are given in the first part of subroutine UPPER given in Appendix P. Either file UP1 or UP2 can be listed out to use as an example. To prepare an upper-air data file, the information required for each station is as follows: station identification number, name, location (either GRAMA, UTM, or latitude-longitude coordinates), elevation, time zone, total number of temperature soundings, and total number of wind soundings. For each sounding, the information required is as follows: station identification number, time of sounding, time zone that data are reported in (may be GMT), number of temperature observations (if any), and number of wind observations (if any). If a temperature sounding is indicated, then the data desired for each observation are height, pressure, temperature, and dew point or relative humidity. MELSAR can treat missing height or pressure data, and the user should refer to the first part of subroutine UPPER for more information about how to treat missing data. If a wind sounding is indicated then the data desired for each observation are height, wind direction, and wind speed. Missing heights in the wind sounding can be handled and wind speed can be input in either knots or meters per second.

3.4.3.2 Preparation of the Surface Weather Data File SFC_

Two surface weather data files, SFC1 and SFC2, are provided with MELSAR, They are described in Appendix D and should be of general use to the user. File SFC1 is a formatted file and contains surface weather data from eight NWS stations for the month of January 1978. File SFC2 is for July 1978.

Detailed instructions for the preparation of new SFC_ files are not given here. If the user has a data set that he would like to prepare for use by MELSAR, detailed instructions to do this are given in the first part of subroutine SRFC given in Appendix P. Either file SFC1 or SFC2 can be listed out to use as an example. To prepare a surface weather data file the information required for each station is as follows: station identification number, name, location, elevation, time zone, and number of observations. The desired information for each observation is as follows: station identification number, time of observation (in time zone of station), wind direction, wind speed, temperature, dew point, station pressure, and cloud cover. The data for any station do not have to be specified at any set time interval, nor do they need to be available during the entire simulation period. More details on data entry are given in subroutine SRFC.

3.4.3.3 Preparation of the Wind Interpolation Point File WIP_

The purpose of file WIP_ is to specify points in the modeling domain where upper-air wind data are to be interpolated. These interpolated upper-air wind soundings are then used as 'input' soundings, in addition to the

original soundings, to the flow model. These interpolation points are especially needed at the boundaries of the modeling region to keep the wind field from becoming unrealistic near the boundaries. The user may want to specify internal points to the domain if the distribution of input stations is very lopsided and the wind field looks unrealistic.

File WIP1 is provided with MELSAR and contains information on 22 points specified on the boundary of the entire GRAMA region. The 22 points consist of the four corner points, four points on each of the X-direction boundaries, and five points on each of the Y-direction boundaries. This file should be sufficient for any MELSAR runs made on the entire GRAMA region. For any smaller regions within the GRAMA region, the user will need to prepare additional WIP_ files.

WIP_ files are formatted files and contain a record for each point. Each record is read using the following FORTRAN READ statement:

```
      READ (4,35) IDO,NAMEO,XU,YU,ICODE
35 FORMAT (I6,1X,A10,2F10.3,I4)
```

where,

IDO = the point identification number, which can be any 6-digit integer of the users choice

NAMEO = a 10-character alphanumeric name assigned to the point (this field can be left blank)

XU = X-coordinate of point in GRAMA coordinates (km), UTM coordinates (km), or latitude-longitude coordinates (deg)

YU = Y-coordinate of point in GRAMA coordinates (km), UTM coordinates (km), or latitude-longitude coordinates (deg)

ICODE = code specifying coordinate system of XU and YU, (1 means latitude-longitude, 2 means UTM grid zone 12, 3 means UTM grid zone 13, and 4 means GRAMA).

The user can list out file WIP1 to use as an example in preparing any new WIP_ files.

3.4.3.4 Preparation of Gridded Land-Use Category File LANDU_

The gridded land-use category file, LANDU_, is currently used by MELSAR to specify the surface roughness (see Table 2-8). File LANDU1 is provided with MELSAR and should be of general use for applications covering the entire GRAMA region. A description of this file is given in Appendix D. For applications of MELSAR on portions of the GRAMA region, the user would need to prepare new LANDU_ files. An alternative to gridding new land-use categories would be to use the option in METIN_ (see Section 3.4.2.5), which

allows the user to specify surface roughness directly. This option assumes a constant surface roughness over the modeling region.

To develop a new LANDU_ file, the user would need to overlay up to a 10 by 10 grid onto a land-use map of the desired region. This grid would be a subset of the GRAMA coordinate system. Then land-use category numbers given in Table 2-8 would need to be assigned to each grid cell. The user would then need to input each row of land-use numbers, starting with the most southerly row, into a data file. This file would be a formatted file and each row would be read using a FORTRAN format statment of FORMAT(10I3). File LANDU1 could be listed out to use as an example.

3.4.3.5 Preparation of the Source Valley File VALLY_

This file contains the characteristics of each valley with a source located in it. The user will need to create VALLY_ files for different source inventories and different modeling domains. Once all the principal source valleys have been characterized, however, new VALLY_ files should not be required. The information on any new VALLY_ file created should be entered into the available-input-data form given in Appendix D. The VALLY1 file supplied with MELSAR can be listed out and used as an example for preparing other VALLY_ files. This file gives characteristics of one valley defined as eight valley segments from the head of Clear Creek down Roan Creek and the Colorado River to about 30 km below DeBeque, Colorado. The user can refer to Section 2.4.4 and 2.5.7 for technical details on the valley coupling process for which the valley information are needed.

The first step in creating a VALLY file is to determine which valleys in a modeling region will have a source—in them and whether or not the contaminants will remain trapped in the valleys through the night (the stack height plus reasonable plume rise is below the ridgetops). The next step is to identify the full length of the valleys to be characterized and the number of segments per valley. The criteria for doing this are given in Section 2.5.7.

VALLY_ is a formatted file and contains first a series of header records, one for each valley, followed by the characteristics for each valley segment. The data for one segment are included on one record and all the segments for each valley are grouped together. The segments for each valley must be listed in order going up-valley. Also the end point of the last segment must be down-valley from the source. The order of the segment groups is the same as the order of the header records. Each header record is read using the following FORTRAN READ statement:

```
      READ (26,360)  IDVAL,NAMVAL,NSEG,XU,YU,ICODE,VGAMAX,WSV,
                     ELVAL,DPVAL,ITZV
  360 FORMAT (I6,1X,A10,I3,2F10.3,I3,2F8.4,2F6.0,I3)
```

where,

IDVAL = valley identification number which can be up to a 6-digit number of the users choice

NAMVAL = a 10-character alphanumeric name for the valley

NSEG = number of segments for valley (not greater than 10)

XU = X-coordinate of valley center in GRAMA coordinates (km), UTM coordinates (km), or latitude-longitude coordinates (deg)

YU = Y-coordinate of valley center in GRAMA coordinates (km), UTM coordinates (km), or latitude-longitude coordinates (deg)

ICODE = code specifying coordinate system of XU and YU, (1 means latitude-longitude, 2 means UTM grid zone 12, 3 means UTM grid zone 13, and 4 means GRAMA).

VGAMAX = maximum potential temperature lapse rate expected in valley at sunrise (°K/m), a default value of 0.03 is recommended if data are not available

WSV = mean nocturnal down-valley wind speed in valley (m/s), a default value of 4 m/s is recommended if data are not available

ELVAL = average elevation of valley floor (m MSL)

DPVAL = average depth of valley (m)

ITZV = time zone valley is in, 5 (Eastern), 6 (Central), 7 (Mountain), 8 (Pacific); the time zone for the GRAMA region is 7.

Next the data are read for each valley segment, where all the segments for each valley are grouped together. Each record corresponds to a valley segment and is read with the following FORTRAN READ statement:

```
      READ (26,361)  IDV,IDSEG,XU,XU,ICODE,ELSEG,TOSEG,WSEG,AL1SEG,AL2SEG
  361 FORMAT (2I6,2F10.3,I3,5F6.0)
```

where,

IDV = valley identification number (same as IDVAL)

IDSEG = identification number of segment which can be up to a 6-digit number of the users choice

XU = X-coordinate of segment in GRAMA coordinates (km), UTM coordinates (km), or latitude-longitude coordinates (deg)

YU = Y-coordinate of segment in GRAMA coordinates (km), UTM coordinates (km), or latitude-longitude coordinates (deg)

ICODE = code specifying coordinate system of XU and YU, (1 means latitude-longitude, 2 means UTM grid zone 12, 3 means UTM grid zone 13, and 4 means GRAMA)

ELSEG = elevation of valley segment floor (m MSL)

TOSEG = elevation of ridgetops for vally segment (average of both sides of valley) (m MSL)

WSEG = width of valley floor for segment (m)

AL1SEG = slope angle of left (facing down-valley) sidewall (deg)

AL2SEG = slope angle of right (facing down-valley) sidewall (deg).

The VALLY_ file is read in subroutine COEFF. The listing in Appendix P can be referred to for more information.

3.4.4 Output Description

Four unformatted files result from MET as shown in Figure 3-1 and described in Table 3-2. File FIGI_ contains the hourly amplitude functions which describe the winds on each 'gamma' surface; BLPAR_ contains the hourly gridded temperatures, pressures, friction velocities, convective velocities and Monin-Obukov lengths; MIXST_ contains the hourly gridded mixing heights and PGT stability classes; and COEFF_ contains the hourly coupling coefficents for each valley segment. The user can refer to subroutines AMPLIT, BLPARS, MIXSTB, and COEFF, respectively, for the specific structure of these files. However, this information is not required to run MELSAR. A print file also results from a run of MET. This file gives a summary of the run, and if requested, provides detailed run results. Appendix I lists the summary print file for the sample problem. The four output files from MET for the sample problem are FIGI1, BLPAR1, MIXST1, and COEFF1.

3.4.5 Diagnostic Messages

Diagnostic messages from MET are given in Appendix G. This list includes suggestions to resolve the problem encountered.

3.5 POLUT Program

This section gives the UNIVAC® JCL, run specifications, and input requirements for running POLUT. Inputs and resulting outputs for the sample

problem are given. The user can refer to Section 2.5 for the technical details of POLUT and Appendix Q for a listing of the code.

3.5.1 Description

POLUT is a Lagrangian puff model where the pollutant distribution is described in a Gaussian fashion about the puff center of mass. The distribution in the vertical is modified by the treatment of multiple reflections from the ground and an upper mixing lid. The model is designed to be applied principally at source-to-receptor distances on the order of tens to hundreds of kilometers. However, the model is configured to treat any source-to-receptor distance. Ground-level concentrations for two pollutants can be computed for releases from up to five sources, either point or area sources. The area sources are treated as virtual point sources. Concentrations are computed on up to four 25- by 25-receptor grids and up to 10 individual receptors specified anywhere at ground level in the modeling domain. Currently POLUT is based on the conservative approach of assuming no pollutant removal or chemical transformations.

POLUT requires a run specification file, POLIN_, and seven input files, SOURC_, RECPT_, TERS_, FIGI_, BLPAR_, MIXST_, and COEFF_, to operate. SOURC_ contains the source characteristics data, RECPT_ contains the receptor specification information data, TERS_ is an output file from program TERRAIN and contains the smoothed terrain height and roughness data, and FIGI_, BLPAR_, MIXST_, and COEFF_ are output files from MET described in Section 3.4.

One output file, CONC_, is produced by POLUT. This file contains the concentrations for each time step (typically one hour), for each receptor, for each source, for each pollutant. This file is used by POLPRC to compute average concentrations. A run summary listing is printed out during a run of POLUT. Figure 3-1 shows the inputs and outputs for POLUT. The blank field at the end of the input file names for POLUT is assigned a unique number by the user for different runs as described in Section 3.2.4.

POLUT requires approximately 160K words of memory to load on a UNIVAC® 1108 computer. It consists of one main program (AAPOL) and 43 subroutines; a total of approximately 4300 lines of code with comments. Appendix N contains tables detailing the subroutine interactions, common blocks, and parameter definitions in POLUT.

3.5.2 Job Control Language and Run Setup

The UNIVAC® JCL file, POLJCL, for running POLUT is given in Table 3-11. This file shows the run specification file, input files, and output file needed for POLUT and the logical unit assignment for these files. The file

names required for the sample problem are shown in the table. Files POLIN1, SOURC1, and RECPT1, in addition to file POLJCL, are provided with MELSAR. The dotted fields in the first two lines of POLJCL indicate the need for additional information (e.g., user ID, password) to be supplied. In addition, the /180/ on the first line indicates that a maximum of 180K words of memory will be required for the run.

TABLE 3-11

UNIVAC® JCL FILE, POLJCL, USED TO RUN POLUT

```
 1   @RUN POLUT/180/.................
 2   @IDENT.................
 3   @ASG,A POLIN1.
 4   @ASG,A SOURC1.
 5   @ASG,A RECPT1.
 6   @ASG,A TERS1.
 7   @ASG,A FIGI1.
 8   @ASG,A BLPAR1.
 9   @ASG,A MIXST1.
10   @ASG,A COEFF1.
11   @ASG,UP CONC1.
12   @USE 13,POLIN1.
13   @USE 16,SOURC1.
14   @USE 15,RECPT1.
16   @USE 11,TERS1.
17   @USE12,FIGI1.
18   @USE 20,BLPAR1.
19   @USE 17,MIXST1.
20   @USE27,COEFF1.
21   @USE14,CONC1.
22   @XQT POLUT.AAPOL
23   @FIN
```

The run conditions for POLUT are specified in file POLIN_. The contents of POLIN_ and the definitions of each input element are given in Table 3-12. The range of values, variable type, and recommended values for each parameter are given in Table 3-13. The recommended values are for a run using the whole GRAMA domain. The run specification file, POLIN1, for the sample problem is given in Table 3-14.

POLIN_ contains only four lines of entries where the entries are separated by commas (field-free format). Consequently, this file can be easily created and modified using a UNIVAP system editor.

IDRUN is set as discussed in Section 3.2.4. The USENAM field can be any 10-character alphanumeric string of the user's choice. The user's name

TABLE 3-12

POLUT RUN SPECIFICATION FILE, POLIN_

File Contents and Format:

Line #	Contents
1	IDRUN,USENAM,IBTZ
2	IBEG,IEND,IPRR,LUFORM,WOFF,METHOD
3	IXO,IYO,SLX,SLY
4	(CT(I),I=1,6)

Parameter Definitions:

IDRUN	= Run identification number
USENAM	= User name
IBTZ	= Time zone, 5 (EST), 6 (CST), 7 (MST), 8 (PST)
IBEG	= Simulation begin time in (MMDDYYHH), (e.g., July 11, 1978 at 0800 is 07117808)
IEND	= Simulation end time
IPRR	= Puff release rate (1 to 6 puffs/hr)
LUFORM	= Logical variable, if .TRUE., means pollutants uniformly mixed through mixing layer at all times (provided pollutants emitted into mixing layer)
WOFF	= Logical variable, if .TRUE., means do not use vertical velocities from the flow model to compute vertical location of puff
METHOD	= Specifies one of two methods for computing σ_v and σ_w used in computing the horizontal and vertical diffusion coefficients, respectively. If METHOD = 2, compute using terrain roughness. If METHOD = 1, compute using empirical boundary layer relationships.
IXO	= X-origin of modeling domain in GRAMA coordinates (km)
IYO	= Y-origin of modeling domain in GRAMA coordinates (km)
SLX	= Length in X-direction of modeling domain (km)
SLY	= Length in Y-direction of modeling domain (km)
CT	= Array of the six terrain height adjustment coefficients described in Section 2.5.6.1. The first coefficient is for unstable conditions, and the last for stable conditions.

TABLE 3-13

RANGE OF VALUES, VARIABLE TYPE, AND RECOMMENDED VALUES FOR EACH PARAMETER IN FILE POLIN1

Parameter	Variable Type	Range of Values	Recommended Values
IDRUN	CHARACTER	Up to 10 characters	
USENAM	CHARACTER	Up to 10 character	
IBTZ	INTEGER	5 to 8	7
IBEG	INTEGER	8 digits (MMDDYYHH)	
IEND	INTEGER	8 digits (MMDDYYHH)	
IPRR	INTEGER	1 to 6	1
LUFORM	LOGICAL	.TRUE. or .FALSE.	.FALSE.
WOFF	LOGICAL	.TRUE. or .FALSE.	.TRUE.
METHOD	INTEGER	1 or 2	1
IXO	INTEGER	0 to 500 km	0
IYO	INTEGER	0 to 450 km	0
SLX	REAL	20. to 500. km	500.
SLY	REAL	20. to 450. km	450.
CT(6)	REAL ARRAY	0.1 to 1.0 per element	1.0

TABLE 3-14

POLUT RUN SPECIFICATION FILE, POLIN1, FOR THE SAMPLE PROBLEM

Line No.	Contents
1	' 04158512 ',' MR JONES ',7
2	07117807,07137807,1,.FALSE.,.TRUE. ,1
3	0,0,500.,450.
4	1.0,1.0,1.0,1.0,1.0,1.0

is recommended. The time zone, IBTZ, is set at 7 (Mountain Standard Time) for the GRAMA region. The simulation start time, IBEG, and ending time, IEND, must be within the IBEG to IEND period in MET for creating files FIGI_, BLPAR_, MIXST_, and COEFF_ used in a POLUT run.

The puff release rate, IPRR, can be set at 1 to 6 puffs/hr. This results in model time steps of 60, 30, 20, 15, 12, or 10 min. The appropriate choice of IPRR is based on the time resolution of the input meteorological data (into MET) or the spatial resolution of the input terrain data (into POLUT), whichever suggests the larger puff release rate (smaller time step). For example, the meteorological data are specified every hour for the sample problem, suggesting IPRR be set equal to one. If the meteorological data were available every 15 min, this would require IPRR to be equal to four. Terrain smoothing intervals are important in determining appropriate puff release rates because of the restriction that puffs not travel more than one terrain grid interval during a model time step. This is to ensure that a continuous plume is represented when 'tracking' puffs are divided as described in Section 2.5.7. The puff release rate considering terrain smoothing can be determined by

$$IPRR = U_{max}/IAI \qquad (3\text{-}1)$$

where

U_{max} = maximum wind speed expected during a simulation period (km/hr)

IAI = terrain smoothing interval (km).

IPRR is set to the nearest of 1, 2, 3, 4, 5, or 6 using the results from Equation (3-1). Table 3-15 gives recommended IPRR for various terrain smoothing intervals assuming a maximum wind speed of 20 km/hr. The user can specify puff release rates, for any smoothing interval, greater than that recommended in Table 3-15 (but not greater than 6).

TABLE 3-15

RECOMMENDED PUFF RELEASE RATE, IPRR, FOR VARIOUS TERRAIN SMOOTHING INTERVALS

Smoothing Interval (km)	Puff Release Rate
>3	6
>4	5
>5	4
>7	3
>10	2
>20	1

For the sample problem the terrain smoothing interval, IAI (see Table 3-4), is 20 km. From Table 3-15, the puff release rate suggested for this terrain smoothing interval is one. Consequently, considering both meteorological data and terrain smoothing, the puff release rate chosen for the sample problem would be one. As a second example, consider a subarea of the GRAMA region which is 200 km on a side. If the terrain smoothing interval were 8 km, the recommended puff release rate from Table 3-15 would be 3 puffs/hr. If the input meteorological data were specified every hour, this would impose IPRR equal to one. The IPRR actually used in the second example would be three, the higher of the suggested rate from meteorological and terrain considerations.

The LUFORM logical variable, if specified .TRUE., directs POLUT to treat every puff emitted into the mixed layer as having the pollutant uniformly distributed in the vertical. Otherwise, the vertical pollutant distribution is initially Gaussian with multiple reflections off the ground and mixing lid as the puff moves downwind. Section 2.5.1 gives some considerations for the choice of LUFORM.

The WOFF logical variable, if specified .TRUE., directs POLUT not to use the vertical velocities from MET in the puff transport. Instead, the approach described in Section 2.5.6 is used. It is recommended that the user always specify WOFF equal to .TRUE. unless the user can verify that the vertical velocities from MET are realistic. This aspect of the flow model in MET will require future evaluation.

METHOD can be set to either one or two, and specifies the method for computing the standard deviation of the horizontal wind component, σ_v, and the standard deviation of the vertical wind component, σ_w. These quantities are used to compute the horizontal and vertical diffusion coefficients, respectively. METHOD equal to one requests a method proposed by Irwin (1979) to be used, and METHOD equal to two requests empirical methods developed by MacCready, Baboolal, and Lissaman (1974) be used. These two methods are described in Section 2.5.10. The second method takes into account terrain roughness directly, in the computation of σ_v and σ_w for stable conditions.

The domain to be modeled can be the entire GRAMA region or any part of it. The parameters IXO, IYO, SLX, and SLY specify the domain. These are defined in Table 3-12. IXO and IYO specify the origin in GRAMA coordinates, and SLX and SLY specify the size of the domain in the X-direction and Y-direction, respectively. IXO, IYO, SLX, and SLY must be set equal to the values used in TERRAIN to produce file TERS_, which are equal to the values used in MET to produce files FIGL_, BLPAR_, MIXST_, and COEFF_.

The array, CT(6), specifies the height adjustment coefficient for each Pasquill-Gifford stability class starting with 'A' and finishing with 'F'. An example set of values is given in Table 2-11. If the user wants the puff center of mass to always follow the terrain at the final plume rise height, then the six elements in CT are set equal to one.

3.5.3 Input Data Description

Seven files are required as input by POLUT as shown in Figure 3-1. One file, TERS_, is an unformatted file from program TERRAIN, and four files, FIGI_, BLPAR_, MIXST_, and COEFF_, are unformatted files from program MET. The remaining two files, SOURC_ and RECPT_, are formatted files prepared by the user. A set of these two formatted files, SOURC1 and RECPT1, are provided with MELSAR and are described in Appendix D and Table 3-1. These two files will not be of general use because they specify the sources and receptors for the sample problem. The user will have to prepare other SOURC_ and RECPT_ files for specific model applications. The name and description of any new files prepared should be entered into the list of available files given in Appendix D. Given next are instructions for preparing and formatting the SOURC_ and RECPT_ files. The input files used in the sample problem are TERS1, FIGI1, BLPAR1, MIXST1, COEFF1, SOURC1, and RECPT1.

3.5.3.1 Preparation of the Source Data File SOURC_

SOURC_ contains the required input data for up to five sources. Four lines of entries are required for each source. The entries in each line are separated by commas (field-free format). The first line of the file gives the number of sources to be modeled, the number of pollutants and the pollutant names. Following this line are the groups of four lines for each source. The contents of SOURC_ and the definition of each input element are given in Table 3-16. The user can list out file SOURC1 to use as an example for preparing new SOURC_ files.

3.5.3.2 Preparation of the Receptor File, RECPT_

The receptor assignments for a run of POLUT are given in file RECPT_. POLUT can use up to four 25- by 25-receptor grids and 10 individual receptors. The entries in RECPT_ utilize a field-free format (the entries are separated by commas). In the first line of RECPT the number of receptor grids and number of individual receptors are specified. Following this line is one line for each receptor grid, followed by one line for each individual receptor. The contents of RECPT_ and the definition of each input element are given in Table 3-17. The user can list out file RECPT1 to use as an example for preparing new RECPT_ files.

3.5.4 Output Description

One unformatted file, CONC_, results from POLUT as shown in Figure 3-1 and described in Table 3-2. This file contains the resulting pollutant concentrations at each receptor for each modeling time step for each source

TABLE 3-16

POLLUTANT SOURCE INPUT DATA FILE, SOURC_

File Contents and Format:

Line #	Contents
1	NSOURC,NPLT,(PLTNAM(J),J=1,NPLT)
(Source 1)	
2	NAMES,XU,YU,ICOD,VALL
3	IDVALL,NAMVA (This line needed only if VALL=.TRUE.)
4	SIGIN,ZSH,VS,TS,RS
5	(EMIS(J),J=1,NPLT)
(Source 2)	
.	
(Source 5)	
18	
19	
20	
21	

Parameter Definitions:

NSOURC = Number of sources (up to 5)
NPLT = Number of pollutants (up to 2)
PLTNAM = Array of pollutants names (up to 2 names of not over 3 alphanumeric characters)
NAMES = Source name (not over 10 alphanumeric characters)
XU = X-coordinate of source in GRAMA coordinates (km), UTM coordinates (km), or latitude-longitude coordinates (deg)
YU = Y-coordinate of source in GRAMA coordinates (km), UTM coordinates (km), or latitude-longitude coordinates (deg)
ICOD = Code specifying coordinate system of XU and YU, (1 means latitude-longitude, 2 means UTM grid zone 12, 3 means UTM grid zone 13, and 4 means GRAMA)
VALL = Logical variable, if .TRUE., means source is located in a valley and valley coupling/decoupling will be used (the coupling coefficients for the source valley must be in file COEFF_)
IDVALL = Identification number of source valley (up to 6 numerals--same as specified in file COEFF_)
NAMVA = Source valley name (up to 10 alphanumeric characters--same as specified in file COEFF_)
SIGIN = Initial sigma-y (m), which must be assigned a value if an area source is being modeled; it must be specified zero for a point source (POLUT will compute an initial sigma-y for the point source)

TABLE 3-16

POLLUTANT SOURCE INPUT DATA FILE, SOURC_ (Continued)

Parameter Definitions:

ZSH = Stack height (m AGL) (set to zero if area source)
VS = Stack gas exit velocity (m/s) (set to zero if do not want plume rise or if an area source)
TS = Stack gas exit temperature (°K) (set to zero if area source)
RS = Stack exit diameter (m) (set to zero if area source)

TABLE 3-17

RECEPTOR SPECIFICATION FILE RECPT_

File Contents and Format:

Line #	Contents
1	NRGRID,NINDR
(Grid 1)	
2	NAMEG,XUG,NPTSX,YUG,NPTSY,RSPAC,ICOD
(Grid 2)	
⋮	
(Grid 4)	
5	
(Individual 1)	
6	NAMER,XUI,YUI,ICOD
(Individual 2)	
⋮	
(Individual 10)	
15	

Parameter Definitions:

NRGRID = Number of receptor grids (up to 4)
NINDR = Number of individual receptors (up to 10)
NAMEG = Name of receptor grid (up to 10 alphanumeric characters)

TABLE 3-17

RECEPTOR SPECIFICATION FILE RECPT_ (Continued)

Parameter Definitions:

XUG = X-coordinate of origin of receptor grid in GRAMA coordinate (km), UTM coordinates (km), or latitude-longitude coordinates (deg)
YUG = Y-coordinate of origin of receptor grid in GRAMA coordinates (km), UTM coordinates (km), or latitude-longitude coordinates (deg)
ICOD = Code specifying coordinate system of XUG and YUG, (1 means latitude-longitude, 2 means UTM grid zone 12, 3 means UTM grid zone 13, and 4 means GRAMA)
NPTSX = Number of receptor points in X-direction (up to 25)
NPTSY = Number of receptor points in Y-direction (up to 25)
RSPAC = Spacing between receptor points (km)
NAMER = Name of individual receptor (up to 10 characters)
XUI = X-coordinate of individual receptor in GRAMA coordinate (km), UTM cordinates (km), or latitude-longitude coordinates (deg)
YUI = Y-coordinate of individual receptor in GRAMA coordinates (km), UTM coordinates (km), or latitude-longitude coordinates (deg)
ICOD = Code specifying coordinate system of XUI and YUI, (1 means latitude-longitude, 2 means UTM grid zone 12, 3 means UTM grid zone 13, and 4 means GRAMA)

for each pollutant. Because of uncertainty in the concentrations near a source, concentrations are not computed within 5 km of a source. The concentrations are corrected to standard atmospheric conditions. This file is used as input by POLPRC to compute average concentrations. The user can refer to the main program AAPOL for the specific structure of this file. However, this information is not needed in order to run MELSAR. A print file also results from a run of POLUT. This file gives a summary of the run. Appendix J lists the summary print file for the sample problem. The output file from POLUT for the sample problem is CONC1.

3.5.5 Diagnostic Messages

Diagnostic messages from POLUT are given in Appendix G. This list includes suggestions for resolving the problem encountered.

3.6 POLPRC Program

This section gives the UNIVAP JCL, run specifications, and input requirements for running POLPRC. Inputs and resulting outputs for the sample problem are described. The user can refer to Section 2.5 for technical details of POLPRC and Appendix R for a listing of the code.

3.6.1 Description

POLPRC computes moving-average concentrations of pollutants at each receptor for up to three user-specified averaging times. The averaging times can range from 1 to 24 hr. Up to 20 sources can be processed at one time. The outputs are tables of highest and second highest pollutant concentrations for the duration of the simulation, at each receptor for each pollutant for each averaging time. The highest and second highest moving averages for the sum of all sources and the contribution of each source to the highest and second highest sum are computed. Highest and second highest moving averages can also be coniputed for each source individually. Tables of the time or occurrence of the highest and second highest values are also listed.

Up to five CONC_ files from POLUT can be processed at one time. However, the total number of sources from the five files cannot exceed 20. The only file POLPRC requires for operation besides the CONC_ files is the run specification file PRCIN_.

POLPRC requires approximately 90K words of memory to load on a UNIVAC® 1108 computer. It consists of one main program (AAPRC) and four subroutines, a total of approximately 1100 lines of code with comments.

3.6.2 Job Control Language and Run Setup

The UNIVAC® JCL file, PRCJCL, for running POLPRC is given in Table 3-18. This file shows the run specification file and the input file needed by POLPRC and the logical unit assignment for these files. The file names for the sample problem are shown in the table. File PRCIN1 is provided with MELSAR. Inspection of Table 3-18 shows that POLPRC uses six temporary files during its execution. These are direct-access disk files and are transparent to the user as long as enough free disk space is available during a run. Logical units 11 through 14 are reserved for additional CONC_ files as shown in Table 3-18. The dotted fields in the first two lines of PRCJCL indicate the need for additional information (e.g., user ID, password) required from the user. The /100/ in the first line of PRCJCL specifies the maximum amount of memory required for a run of POLPRC.

TABLE 3-18

UNIVAC® JCL FILE, PRCJCL, USED TO RUN POLPRC

```
                1    @RUNPOLPRC/100/.............
                2    @IDENT.................
                3    @ASG,A PRCIN1.
                4    @ASG,A CONC1.
                5    @USE9,PRCIN1.
                6    @USE10,CONC1.
                7    @ASG,T 15.
                8    @ASG,T 20.
                9    @ASG,T 21.
               10    @ASG,T 22.
               11    @ASG,T 23.
               12    @ASG,T 24.
               13    @ASG,T 25.
      (22)     14    @XQT POLPRC.AAPRC
      (23)     15    @FIN
(The remaining file assignments are made when additional CONC_ files
 are to be processed.  Up to four additional files can be processed.)
      (14)           @ASG,A CONC_.
      (15)           @ASG,A CONC_.
      (16)           @ASG,A CONC_.
      (17)           @ASG,A CONC_.
      (18)           @USE 11,CONC_.
      (19)           @USE 12,CONC_.
      (20)           @USE13,CONC_.
      (21)           @USE14,CONC_.
```

The run conditions for POLPC are specified in the file PRCIN_. The contents of PRCIN_ and the definitions of each input element are given in Table 3-19. The range of values, variable type, and recommended values for each parameter are given in Table 3-20. The recommended values are for a run using the whole GRAMA domain. The run specification file, PRCIN1, for the sample problem is given in Table 3-21.

PRCIN contains only four lines of entries where the entries are separated by commas (field-free format). Consequently, this file can be easily created and modified using a UNIVAC system editor.

IDRUN is set as discussed in Section 3.2.4. The USENAM field can be any 10-character alphanumeric string of the user's choice. The user's name is recommended. The time zone, IBTZ, is set at 7 (Mountain Standard Time), for the GRAMA region. The simulation start time, IBEG, and ending time, IEND, must correspond to the times in the input CONC_ files. The number of input concentration files, CONC_, from POLUT is specified as JFILES. Up to five files can be processed, but the combined number of sources cannot be

TABLE 3-19

POLPRC RUN SPECIFICATION FILE, PRCIN

File Contents and Format:

Line #	Contents
1	IDRUN,USENAM,IBTZ
2	IBEG,IEND,JFILES,NFLAG
3	IXO,IYO,SLX,SLY
4	NAVE,(IAVPER(J),J=1,NAVE)

Parameter Definitions:

IDRUN = Run identification number
USENAM = User name
IBTZ = Time zone, 5 (EST), 6 (CST), 7 (MST), 8 (PST)
IBEG = Simulation begin time in (MMDDYYHH) (e.g., July 11, 1978, at 0800 is 07117808)
IEND = Simulation end time
JFILES = Number of input CONC files
NFLAG = 1 means compute averages for individual sources in addition to sum of all sources; = 0 means compute averages for sum of all sources only
IXO = X-origin of modeling domain in GRAMA coordinates (km)
IYO = Y-origin of modeling domain in GRAMA coordinates (km)
SLX = Length in X-direction of modeling domain (km)
SLY = Length in Y-direction of modeling domain (km)
NAVE = Number of averaging periods
IAVPER = Array of averaging periods

over 20. In addition, each source in all input files must have identical beginning and ending times, identical number and types of pollutants, and identical receptors. If not, the program will stop execution and may then be restarted after all input files are compatible. ,

The field NFLAG tells POLPRC whether or not to compute highest and second highest output tables for each source individually in addition to the highest and second highest tables for the sum of all sources. If NFLAG is set equal to 1, then individual source tables are to be computed. If NFLAG is set equal to 0, then individual source tables are not to be computed.

One to three averaging periods can be processed during any single execution of POLPRC. NAVE specifies the number of averaging periods, and IAVPER specifies the desired averaging periods (IAVPER is a single array dimensioned by three). The averaging period can be any integer number between 1 to 24 hr, inclusive.

TABLE 3-20

RANGE OF VALUES, VARIABLE TYPES, AND RECOMMENDED VALUES FOR EACH PARAMETER IN FILE PRCIN_

Parameter	Variable Type	Range of Values	Recommended Value
IDRUN	CHARACTER	Up to 10 characters	
USENAM	CHARACTER	Up to 10 characters	
IBTZ	INTEGER	5 to 8	7
IBEG	INTEGER	8 digits (MMDDYYHH)	
IEND	INTEGER	8 digits (MMDDYYHH)	
JFILES	INTEGER	1 to 5	
NFLAG	INTEGER	0 to 1	
NAVE	INTEGER	1, 2, or 3	
IXO	INTEGER	0 to 500 km	0
IYO	INTEGER	0 to 450 km	0
SLX	REAL	20. to 500. km	500.
SLY	REAL	20. to 450 km	450.
IAVPER	INTEGER ARRAY	Three values from 1 to 24	3,8,24

TABLE 3-21

POLPRC RUN SPECIFICATION FILE, PRCIN1, FOR THE SAMPLE PROBLEM

Line No.	Contents
1	' 04158512 ', ' MR JONES ',7
2	07117807,07137807,1,0
3	0,0,500. ,450.
4	1,3

The domain to be modeled can be the entire GRAMA region or any part of it. The parameters IXO, IYO, SLX, and SLY specify the domain. IXO and IYO specify the origin in GRAMA coordinates, and SLX and SLY specify the size of the domain in the X-direction and Ydirection, respectively. IXO, IYO, SLX, and SLY must be set equal to the values used in POLUT to produce the CONC_ concentration files.

3.6.3 Input Data Description

The only input data files required by POLPRC are the output concentration files, CONC_, from POLUT. Up to five CONC_ files can be processed by POLPRC at any one time. However, the combined number of sources in the five files cannot be over 20. If POLUT were run for five sources at a time, then POLPRC could only use four of these CONC_ files at any one time. The sources in all CONC_ files used by POLPRC must have identical receptors, pollutants, domains, and starting and ending times. The POLUT runs should be logged in the summary-of-runs form (Section 3.2.4). This information should enable the user to be sure compatible CONC_ files are being assigned to POLPRC.

3.6.4 Output Description

As shown in Figure 3-1, two outputs result from a run of POLPRC. One (PRINT$) is a summary of the POLPRC run and the other is the set of highest and second highest concentration tables. The summary output listing for the sample problem is given in Appendix K, and the highest and second highest concentration tables for the sample problem are given in Appendix L.

Table 3-22 summarizes the output tables produced by POLPRC. The number of output tables increases very rapidly depending on the number of sources, pollutants, averaging times, and grids. The number of output tables from any run of POLPRC can be computed by

$$NTSUM = [2\ (2 + NS) \times NG + (1 + NS) \times NI] \times NA \times NP \qquad (3\text{-}2)$$

$$NTIND = (4 \times NG + NI) \times NS \times NA \times NP \qquad (3\text{-}3)$$

where

NTSUM = total number of tables for sums of all sources plus contribution of each source to the sum (maximum of 1182)
NTIND = total number of tables considering each source individually (maximum of 2040)
NS = number of sources (maximum of 20)
NP = number of pollutants (maximum of 2)
NA = number of averaging periods (maximum of 3)
NG = number of receptor grids (maximum of 4)
NI = 1 if have individual receptors,
= 0 if do not have individual receptors.

From Equations (3-2) and (3-3), if the maximum number for all parameters were used, a total of 3222 tables (pages) would be printed by POLPRC. The user should exercise caution when specifying the run conditions for POLPRC. Twenty-four output tables resulted from the same problem as listed in Appendix L.

TABLE 3-22

OUTPUT TABLES PRODUCED BY POLPRC

Sum of all Sources:

1 Highest Concentrations
2 Times of Highest Concentrations
3 Contribution of Each Source to Highest
4 Second Highest Concentrations
5 Times of Second Highest Concentrations
6 Contribution of Each Source to Second Highest

Individual Sources:

1 Highest Concentrations
2 Times of Highest Concentrations
3 Second Highest Concentrations
4 Times of Second Highest Concentrations

3.6.5 Diagnostic Messages

Diagnostic messages from POLPRC are given in Appendix G. This list includes suggestions for resolving the problem encountered.

SECTION 4.0

REFERENCES

Anderson, G. E., et al. Air Quality Impacts of Anticipated Development in Oil Shale Operations in Western Colorado and Eastern Utah. SAI No. 155-EF80-147, Systems Applications, Inc., San Rafael, California, August 1980.

Bader, D., and T. B. McKee. Dynamic Model Simulation of the Morning Boundary Layer Development in Deep Mountain Valleys. J. Climate and Appl. Meteor., 22(3):341-351, 1983.

Benkley, C. W., and A. Bass. Development of Mesoscale Air Quality Simulation Models. Volume 3. User's Guide to MESOPUFF Model. Environmental Research and Technology, Inc., Concord, Massachusetts, 1979.

Benkley, C. W., and L. L. Schulman. Estimating Hourly Mixing Depths from Historical Meteorological Data. J. Applied Meteor., 18:772-780, 1979.

Binkowski, F. S. A Simple Semi-Empirical Theory for Turbulence in the Atmospheric Surface Layer. Atmos. Eviron., 13(2):247-253, 1978.

Bjorklund, J. R., and J. F. Bowers. User's Instructions for the SHORTZ and LONGZ Computer Programs. EPA-903/9-82-004a, U.S. Environmental Protection Agency Region III, Philadelphia, Pennsylvania, 1982.

Brehm, M., and C. Freytag. Erosion of the Night-Time Thermal Circulation in an Alpine Valley. Arch. Met. Geophys. Biokl., Ser. B., 31:331-352, 1982.

Briggs, G. A. Chimney Plumes in Neutral and Stable Surroundings. Atmospheric Environment, 6(7):507-510, 1972.

Briggs, G. A. Plume Rise Predictions. In: Lectures on Air Pollution and Environmental Impact Analyses, American Meteorological Society, Boston, Massachusetts, 1975, pp. 59-111.

Cramer, H. E. Improved Techniques for Modeling the Dispersion of Tall Stack Plumes. In: Proc. 7th Int. Technical Meeting on Air Pollution Modeling and its Application. N.51, NATO/CCMS, 731-780. (NTIS PB 270 799), 1976.

Doran, J. C., T. W. Horst, and P. W. Nickola. Variations in Measured Values of Lateral Diffusion Parameters. J. Applied Meteor., 17(6):825-831, 1978.

Drake, R. L., and C. H. Huang. Mass-Consistent, Interpolated Wind Fields for Complex Terrain. Presented at Symposium on Intermediate Range Atmospheric Transport Processes and Technology Assessment, Gatlinburg, Tennessee, October 1-3, 1980.

Drake, R. L., C. H. Huang, and W. E. Davis. Green River Ambient Model Assessment Program - Progress Report for the Regional and Mesoscale Flow Modeling Components. PNL-3988, Pacific Northwest Laboratory, Richland, Washington, 1981.

Draxler, R. R. Determination of Atmospheric Diffusion Parameters. Atmospheric Environment, 10:99-105, 1976.

Duncan, D. C., and V. E. Swanson. Organic-Rich Shale of the United States and World Land Areas. U.S.G.S. Cir. 523, U.S. Government Printing Office, Washington, D.C., 1965.

Egan, B. A., R. D'Errico, and C. Vaudo. Estimating Air Quality Levels in Regions of High Terrain Under Stable Atmospheric Conditions. In: Proceedings of Fourth Symposium on Turbulence, Diffusion, and Air Pollution, American Meteorological Society, January 15-18, 1979, Reno, Nevada, pp. 177-181.

Gifford, F. A. Horizontal Diffusion in the Atmosphere: A Lagrangian-Dynamical Theory. Atmospheric Environment, 16(3):505-512, 1982.

Hales, J. M., D. C. Powell, and T. D. Fox. STRAM- An Air Pollution Model Incorporating Non-linear Chemistry, Variable Trajectories, and Plume Segment Diffusion. EPA450/3-77-012, U.S. Environmental Protection Agency, Research Triangle Park, North Carolina, 1977.

Hanna, S. R., G. A. Briggs, J. Deardorff, B. A. Egan, F. A. Gifford, and F. Pasquill. AMS Workshop on Stability Classification Schemes and Sigma Curves-Summary of Recommendations. Bull. Am Meteor. Soc., 58(12):305-1309, 1977.

Hanna, S. R., G. A. Briggs, and R. P. Hosker, Jr. Handbook on Atmospheric Diffusion. DOE-TIC-11223, Technical Information Center, U.S. Department of Energy, Washington, D.C., 1982.

Heffter, J. L. The Variation of Horizontal Diffusion Parameters with Time for Travel Periods of One Hour or Longer. Journal of Applied Meteorology, 4:153-156, 1965.

Hinds, W. T., and P. W. Nickola. The Mountain Iron Diffusion Program: Phase I, South Vandenberg: Vol. I, BNWL-572, Pacific Northwest Laboratories, Richland, Washington, 1967, p 220.

Irwin, J. S. Estimating Plume Dispersion- A Recommended Generalized Scheme. In: Proceedings of Fourth Symposium on Turbulence, Diffusion, and Air Pollution, American Meteorological Society, January 15-18, 1979, Reno, Nevada, 1979.

Irwin, J. S. Estimating Plume Dispersion-A Comparison of Several Sigma Schemes. Journal of Climate and Applied Meteorology, 22:92-114, 1983.

Kaimal, J. C., J. C. Wyngaard, D. A. Haugen, O. R. Cote, and Y. Izumi. Turbulence Structure in the Convective Boundary Layer. J. Atmos. Sci., 33:2152-2169, 1976.

Kronenberger, L., et al. The Impact of the Clean Air Act on Oil Shale Development: API Oil Shale Case Study Group Report. American Petroleum Institute, Washington, D.C., 1981.

Latimer, D. A., and J. R. Doyle. Prevention of Significant Deterioration Policy Implications for Projected Oil Shale Development. Draft Final Report. U.S. Environmental Protection Agency, Washington, D.C., 1981.

MacCready, P. B., Jr., L. B. Baboolal, and P. B. S. Lissaman. Diffusion and Turbulence Aloft Over Complex Terrain. Presented at AMS Symposium on Atmospheric Diffusion and Air Pollution, Santa Barbara, California, September 9-13, 1974.

Maul, P. R. Atmospheric Transport of Sulfur Compound Pollutants, Central Electricity Generating Bureau MID/SSD/80/0026/R, Nottingham, England, 1980.

Panofsky, H. A., H. Tennekes, D. H. Lenschow, and J. C. Wyngaard. The characteristics of Turbulent Velocity Components in the Surface Layer Under Convective Conditions. Boundary-Layer Meteor., 11:355-361, 1977.

Pasquill, F. Atmospheric Dispersion Parameters in Gaussian Plume Modeling, Part II. Possible Requirements for Change in the Turner Workbook Values. EPA-60014-76-030b. U.S. Environmental Protection Agency, Research Triangle Park, North Carolina, 1976, 53 pp.

PEDCO. Colorado's Climate, Meteorology and Air Quality. PEDCO Environmental, Inc., Cincinnati, Ohio. Prepared for U.S. Dept. of Interior, Bureau of Land Management, Denver, CO, 1981.

Ramsdell, J. V., S. R. Hanna, and H. E. Cramer. Turbulent Diffusion Coefficients Within and Above the Urban Domain. Prepared for the U.S. Army, White Sands Missile Range, New Mexico, Pacific Northwest Laboratory, Richland, Washington, 1982.

Ramsdell, J. V., G. F. Athey, and C. S. Glantz. MESOI Version 2.0: An Interactive Mesoscale Lagrangian Puff Dispersion Model with Deposition and Decay. NUREG/CR-3344, U.S. Nuclear Regulatory Commission, Washington, D.C., 1983.

Richardus, P., and R. K. Adler. Map Projections. North-Holland Publishing Company, Amsterdam, 1972.

Schulman, L. L., and J. S. Scire. Buoyant Line and Point Source Dispersion Model Users Guide. PB81-164642, National Technical Information Service, Springfield, Virginia, 1980.

Scire, J. S., F. W. Lurmann, A. Bass, and S. R. Hanna. Development of the MESOPUFF II Dispersion Model, Environmental Research and Technology, Inc., Concord, Massachusetts, 1984.

Sheih, C. M., M. L. Wesely, and B. B. Hicks. Estimated Dry Deposition Velocities of Sulfur Over the Eastern United States and Surrounding Regions. Atmos. Environ. 13(10):1361-1368, 1979.

Slade, D. H., ed. Meteorology and Atomic Energy. National Technical Information Service, Springfield, Virginia, 1968.

Snyder, W. H. Towing Tank Studies in Support of Field Experiments at Cinder Cone Butte, Idaho. Phase III: Verification of Formula for Prediction of Dividing Streamline Height. U.S. Environmental Protection Agency, Research Triangle Park, North Carolina, 1980.

Turner, D. B. Workbook of Atmospheric Dispersion Estimates. AP-26, U.S. Environmental Protection Agency, Research Triangle Park, North Carolina, 1970.

U.S. Army. Universal Transverse Mercator Grid. TM5-241-8, Department of the Army, Washington, D.C., 1973.

Venkatram, A. Estimation of Turbulence Velocity Scales in the Stable and the Unstable Boundary Layer for Dispersion Applications. In: Eleventh NATO-CCSM International Technical Meeting on Air Pollution Modeling and Its Application, pp. 54-56, 1980a.

Venkatram, A. Estimating the Monin-Obukhov Length in the Stable Boundary Layer for Dispersion Calculations, Boundary-Layer Meteorology 19:481-485, 1980b.

Vergeiner, I. Eine Energetische Theorie der Hangwinde." Ann. Meteor., NF19:189-191, 1982.

Wang, I. T., and P. C. Chen. Estimations of Heat and Momentum Fluxes Near the Ground. Proc. 2nd Joint Conf. on Applications of Air Pollu. Meteorology, New Orleans, LA, pp. 764-769, March 24-27, 1980.

Whiteman, C. D. Breakup of Temperature Inversions in Colorado Mountain Valleys. Ph.D. Dissertation, Colorado State University, pp. 250. Available from University Microfilms, Ann Arbor, Michigan, or as Atmospheric Science Paper No. 328 from Department of Atmospheric Science, Colorado State University, Fort Collins, Colorado, 1980.

Whiteman, C. D. Breakup of Temperature Inversions in Deep Mountain Valleys: Part I. Observations. J. Applied Meteorology, 21:270-289, 1982.

Whiteman, C. D., and T. B. McKee. Breakup of Temperature Inversion in Deep Mountain Valleys: Part II, Thermodynamic Model. J. Applied Meteor., 21:290-302, 1982.

Whiteman, C. D., and K. J. Allwine. VALMET - A Valley Air Pollution Model. PNL-4728 Rev. 1. Pacific Northwest Laboratory, Richland, Washington, 1985.

Willis, G. E., and J. W. Deardorff. A Laboratory Model of the Unstable Planetary Boundary Layer. J. Atmos. Sci., 31(5):1297-1307, 1974.

Zannetti, P. An Improved Puff Algoritm for Plume Dispersion Simulation. J. Applied Meteor., 20:1203-1211, 1981.

DISTRIBUTION

No. of Copies

OFFSITE

5 Alan H. Huber
U.S. EPA/ESRL, MD-80
Meteorology and Assessment Division
Research Triangle Park, NC 27711

Peter Finkelstein
U.S. EPA/ESRL, MD-80
Meteorology and Assessment Division
Research Triangle Park, NC 27711

Frank Schiermeier
U.S. EPA/ESRL, MD-80
Meteorology and Assessment Division
Research Triangle Park, NC 27711

Rich Fisher
EPA Region VIII Meteorologist
U.S. Forest Service
Rocky Mountain Forest and Range Experiment Station
240 W. Prospect St.
Fort Collins, CO 80521

Bill Keith
U.S. EPA/ORD/OADENQA
Energy Air Division, RD-680
Washington, D.C. 20460

2 DOE Technical Information Center

No. of Copies

ONSITE

73 Pacific Northwest Laboratory

K. J. Allwine (60)
D. W. Dragnich
P. C. Hays
N. S. Laulainen
J. V. Ramsdell
C. D. Whiteman
R. W. Woodruff
Publishing Coordination (2)
Technical Information (5)

DOE Richland Operations Office

H. E. Ransom